Predicting Minimum Control Speed on the Ground (VMCG) and Minimum Control Airspeed (VMCA) of Engine Inoperative Flight Using Aerodynamic Database and Propulsion Database Generators

by

Eric Michael Hadder

A Thesis Presented in Partial Fulfillment
of the Requirements for the Degree
Master of Science

Approved November 2016 by the
Graduate Supervisory Committee:

Timothy Takahashi, Chair
Marc Mignolet
Daniel White

ARIZONA STATE UNIVERSITY

December 2016

ABSTRACT

There are many computer aided engineering tools and software used by aerospace engineers to design and predict specific parameters of an airplane. These tools help a design engineer predict and calculate such parameters such as lift, drag, pitching moment, takeoff range, maximum takeoff weight, maximum flight range and much more. However, there are very limited ways to predict and calculate the minimum control speeds of an airplane in engine inoperative flight. There are simple solutions, as well as complicated solutions, yet there is neither standard technique nor consistency throughout the aerospace industry. To further complicate this subject, airplane designers have the option of using an Automatic Thrust Control System (ATCS), which directly alters the minimum control speeds of an airplane.

This work addresses this issue with a tool used to predict and calculate the Minimum Control Speed on the Ground (VMCG) as well as the Minimum Control Airspeed (VMCA) of any existing or design-stage airplane. With simple line art of an airplane, a program called VORLAX is used to generate an aerodynamic database used to calculate the stability derivatives of an airplane. Using another program called Numerical Propulsion System Simulation (NPSS), a propulsion database is generated to use with the aerodynamic database to calculate both VMCG and VMCA.

This tool was tested using two airplanes, the Airbus A320 and the Lockheed Martin C130J-30 Super Hercules. The A320 does not use an Automatic Thrust Control System (ATCS), whereas the C130J-30 does use an ATCS. The tool was able to properly

calculate and match known values of VMCG and VMCA for both of the airplanes. The fact that this tool was able to calculate the known values of VMCG and VMCA for both airplanes means that this tool would be able to predict the VMCG and VMCA of an airplane in the preliminary stages of design. This would allow design engineers the ability to use an Automatic Thrust Control System (ATCS) as part of the design of an airplane and still have the ability to predict the VMCG and VMCA of the airplane.

DEDICATION

In loving memory of my beautiful and supportive mother.

ACKNOWLEDGMENTS

This thesis derives from work funded by DragonFly Aeronautics LLC under Contract No. FP00006911.

TABLE OF CONTENTS

Page

LIST OF TABLES

Table Page

Table Page

Table Page

LIST OF FIGURES

Figure Page

Figure Page

Figure Page

Figure Page

Chapter 1: Introduction

As a form of travel, airplanes are becoming more and more economically efficient and safe. A driver of a car needs only to obtain a driver's license. After receiving this license, a driver does not need to go through any continual education, drug tests, or performance tests. Even though a traveler may be an extremely defensive and good driver, there are many other drivers that are reckless and dangerous. On the other hand, a pilot must go through rigorous tests, continual education as well as medical and drug tests to maintain his or her pilot's licenses. Additionally, every Instruments Flight Rules (IFR) flight must be approved through Air Traffic Control, a government service provided by ground-based controllers to help direct the flow of air traffic and avoid collisions. The airplane itself must also be certified and maintained for it to be approved for flight.

For an airplane to be certified to fly it must go through many inspections and tests that are mandated by the United States government. These tests and regulations are found in the Code of Federal Regulations (CFR). The Code of Federal Regulations (CFR) is a codification of all of the regulations and administrative laws mandated by the Federal Government. These regulations cover a broad range of subject matter: there are factors of safety that ensure that each individual part of the airplane structure is multiple times stronger than the worst case load bearing scenario. The materials used have been designed to be strong, replaceable, durable, corrosion resistant, etc.

If for any reason there is a failure in the material or parts, there are redundancies designed to protect the airplane and its passengers. Some of these redundancies are

backup systems of the same function, meaning there may be a second computer for each automated part of the airplane that will override the original if there is a system error, or damage sustained to the computer.

Another main redundancy is that every airplane is designed to be able to take-off and land in the case that an engine fails or malfunctions. When an engine fails, it can no longer develop thrust to propel the airplane. When this occurs, aerodynamic control surfaces need to be able to control the airplane with significantly less thrust than normal; the thrust of the remaining engines is asymmetric. When the airplane flies with an engine inoperative, there are redundancies in the design of the rudder, ailerons, elevators, and flap settings, which allow for the pilot to still control and fly the airplane. These redundancies are a bit more complicated than a backup computer for these redundancies depend on the outside temperature, altitude of the airplane, and flight specific weight of the airplane. Therefore to be able to control the airplane the pilot must get the aircraft to a critical, minimal, controllable speed that the control surfaces can generate enough forces and moments to control the airplane.

The forces and moments needed to control the airplane are directly influenced by the remaining operating engines. Engines have the ability to regulate the amount of thrust they produce; therefore the engine power setting of the operating engines will directly influence the aerodynamic characteristics of an airplane. Furthmore, these engine power setting influences are much greater at low airspeeds than they are at high airspeeds[1]. The

engine power settings will therefore need to be taken into account when trying to isolate the minimum control speed.

The minimum control speed of an aircraft with an engine inoperative is an important parameter that determines how an aircraft can maneuver in the event of an engine failure. We define the minimum control speed to be the lowest speed in which the airplane flies in trim. An airplane is trimmed when all of the forces (lift, drag and side force) and moments (pitching, rolling and yawing) are in balance; thus equal to 0. Figure **1** is a diagram illustrated by NASA[2] showing an airplane that is trimmed in pitching moment, meaning that the pitching moment about the center of gravity (cg) is equal to 0.

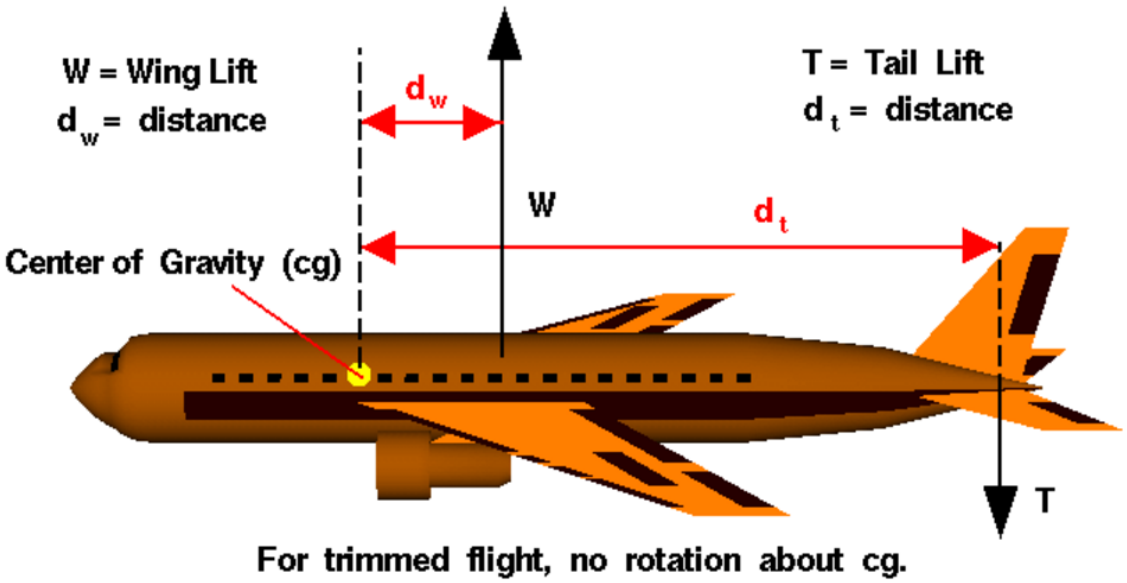

Figure 1. Diagram of a Trimmed Airplane

The minimum ground control speed (VMCG) is the lowest possible ground speed where asymmetric forces and moments arising from propulsion may be countered by the aerodynamic forces and moments developed from control surfaces. In this case, the

aircraft is still on the ground. It is partially supported by its landing gear. Therefore at this point we do not need to consider that aerodynamic lift must weight. In addition the angle of attack (α) of the airplane is governed by the configuration of the landing gear. The asymmetric forces are generated by an uneven number of engines on one side opposed to the other side. For example, if the airplane only has two engines, and the left side engine fails, then there will now by asymmetric force generated by the right engine. Now let us say there are four engines and the furthest outboard engine fails on the left side, then the left and right inboard engines would still develop symmetrical forces, however the outboard right engine would generate asymmetric forces. At zero airspeed, the control surfaces on the airplane do not generate any aerodynamic forces or moments on the airplane. As airspeed increases, the control surfaces interact with the flow velocity of air to generate aerodynamic forces; these forces in conjunction with the location of the control surfaces on the airplane develop moments. As the airspeed increases, the aerodynamic forces and moments increase, therefore there will be a speed at which the aerodynamic forces and moments counter the asymmetric forces aroused by propulsion. This speed is referred to as the minimum ground control speed (VMCG). This is a theoretical explanation of VMCG, later we will look at all the governing equations and showing an example of how VMCG is calculated.

Now that we have a way to calculate the minimal speed required to be able to control the airplane while it is still on the ground. However, we need to address the case of flight. When an aircraft is in flight, the lift generated must be greater than or equal to the weight of the airplane. The minimum air control speed (VMCA) is the speed at which

the control surfaces can trim the aircraft with a critical engine inoperative. When an airplane is in flight and a critical engine is fails, the airplane goes into engine inoperative flight conditions to be able to maintain trimmed flight. During engine inoperative flight conditions the airplane may pitch and bank, thus adjusting to the moments created by the asymmetric propulsion force. Also the control surfaces deflect to develop the appropriate aerodynamic forces and moments to maintain trimmed flight. Just like in calculating VMCG there is a certain speed at which the control surfaces, in adjusted by pitch and bank angles, develop aerodynamic forces and moments that counter the asymmetric propulsion force. This speed is the minimum air control speed (VMCA).

These speeds are important when mapping out a flight plan, to plan for the unfortunate scenario where an engine or multiple engines are inoperative. Starting on the ground, if an airplane is on a runway and an engine gives out early, the pilot may be able to stop the airplane in time before the end of the runway, however if this is not the case then the pilot must take-off to avoid crashing the airplane at the end of the runway. This window of decision making is shortened if the airplane is on a short runway. If the even that the engine fails and the airplane is in engine inoperative conditions and the pilot determines that they must take-off, then the calculations for the VMCG will blend into the calculations for the VMCA. It is extremely important for a pilot to know the bridge between these two speeds. If these speeds are relatively close to one another, the flight plan will merge from the VMCG to the VMCA. On the other hand if there is a major gap between these speeds then the flight plan should take this into account and adjust for it accordingly. Therefore there is a need to know these speeds and especially for the ability

to calculate these speeds prior to the event of an engine failure. The flight plan becomes even more complicated if when there are geographical limitations surrounding the specific airport. These limitations include no-fly zones or mountains. Being able to calculate the VMCA and subsequently turn speeds will allow for a flight plan that will not crash the airplane into the surrounding topology.

A clear understanding of engine inoperative trim is necessary when developing a contingency plan because it is the limiting factor on what maneuvers the pilot may perform. If there are a few maneuvers that the pilot wishes to preform, and only one maintains engine inoperative trim then the pilot is limited to the one maneuver and must know how to use this maneuver is a variety of ways to accomplish the end flight goal.

What is the point of calculating values for VMCA, if a pilot does not know (is not given instruction) how to achieve these trim conditions? Therefore not only is it important to calculate the VMCA, but to also record the flight conditions to achieve the VMCA. Conditions such as bank angle, rudder deflection, and aileron deflection. Tracking the flight conditions for each engine inoperative trim condition will allow us to see similarities as well as limiting factors to be able to best develop a flight plan to provide the pilot with a general rule of thumb or reaction to engine inoperative scenarios. These flight conditions may also vary as the altitude, temperature, and weight or the airplane changes.

The transition from one flight condition to another must be seamless to allow for steady and controllable flight. If one flight condition calls for an aileron deflection of -5 degrees then the next one transitioned to calls for 3 degrees then back to a -6 degrees, there will be a difficultly in the actual execution of these transitions, and may cause unsteady flight. Therefore when calculating the VMCA's of different specific parameters, the recording of flight conditions may lead to powerful trends and general conditions that may be applied to any general engine inoperative flight scenario.

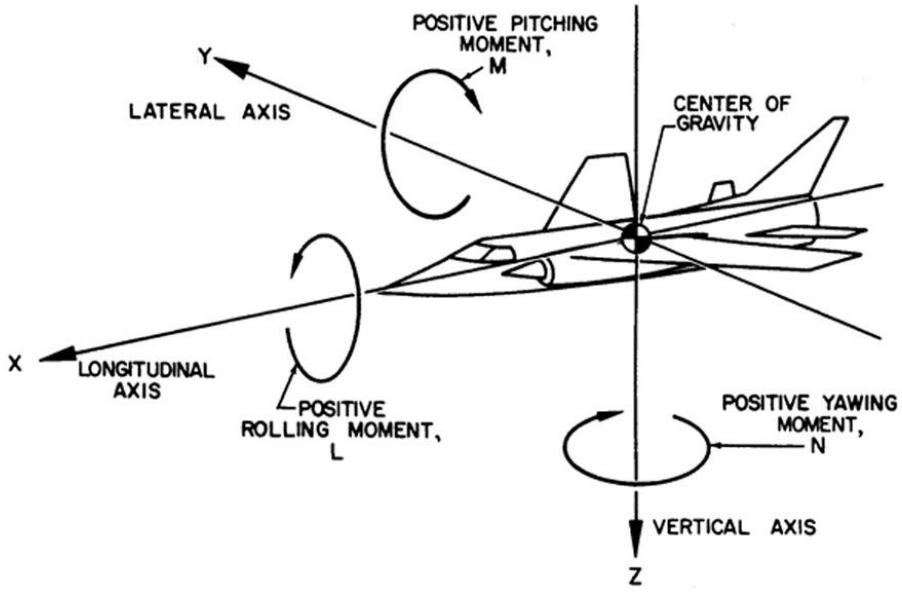

Figure 2. Demonstration of *x*, *y* and *z* Axes, as Well as the Pitching, Yawing and Rolling Moments[3]

While many aircraft manufacturers publish a single value for VMCA for use in all circumstances, reality is more complex. There are many factors that go into calculating this minimum control speed (VMCA or VMCG). To calculate VMCA and VMCG the airplane must be engine inoperative trimmed. Not only must the airplane be trimmed as described in Figure 1, but it must also be trimmed in all three axes. This means there

must be a balance of force in the *x*, *y*, and *z* direction, as well as a balance of pitching, yawing, and rolling moments (see Figure 2). These trim conditions vary on geometry of the aircraft, weight, external winds, control surface deflections, altitude, angle of attack (α), and outside temperature. Not only are all of these factors affecting the airplane, there are also some artificial limits to the engine inoperative flight plan such as stated in the Code of Federal Regulation (CFR) 14 § 25.149 Minimum control speed. One major limitation imposed by this regulation states, "V_{MC} is the calibrated airspeed at which, when the critical engine is suddenly made inoperative, it is possible to maintain control of the airplane with that engine still inoperative and maintain straight flight with an angle of bank of not more than 5 degrees."[4] This limitation is greater than it sounds due to the fact that under normal flight conditions the airplane may bank as far as 30 degrees. However this is the regulation thus suggesting a flight pattern or plan that would include anything beyond a bank angle of 5 degrees would not be "to code", thus 5 degrees bank angle is an artificial limitation that bound the algorithm to conform to CFR regulations.

In this work, we have come up with a way of using first principles aerodynamics and propulsion codes to accurately estimate minimum control speed. There are two major tools used to predict and generate the aerodynamic and propulsive database used to estimate VMCA and VMCG, VORLAX and NPSS. VORLAX is an old NASA sponsored computational fluid dynamic code that can calculate the aerodynamic force and moment coefficients used in the minimal control speed equations. To obtain the asymmetric propulsion force component of the minimal control speed equations, NPSS is used to generate five-column engine data (thrust and fuel flow as a function of speed,

altitude and throttle setting). Both VORLAX and NPSS will be explained more in depth later on in this work.

In this work, we will calculate the VMCA and VMCG dependency arising from more sophisticated parameters such as outside temperature, external winds, altitude, airplane weight, flap settings, angle of attack (α), and individual control surface deflections. Every airplane has its own geometry, control surface sizing, engine sizing, center of gravity location and other unique characteristics, therefore all of these unique qualities should play its role in calculating VMCG and VMCA. By building a database of these results, we can predict how a future airplane may behave, and thus enhance the development and design process of an airplane.

We can calculate the minimal control speed, taking into account all the listed variables above, as well as the trim conditions for each speed; meaning at what bank angle, elevator deflection, aileron deflection, rudder deflection, flaps setting, and angle of attack (α). There are also certain CFR regulations that dictate how a pilot may react in an engine inoperative situation. Title 14 CFR § 25.121 describes take-off and climb regulation in an engine inoperative situation. The pilot, and flight path, must reflect the regulations imposed in this section of the CFR, thus limiting how VMCG and VMCA may be calculated. Therefore, the algorithms have been bounded by these regulations to ensure that the trim cases meet regulations as well as bounds limiting the individual aircrafts geometry and maximum angles of deflection of control surfaces.

By recording these parameters at the various speeds may allow us to develop a standard to reacting to an engine inoperative circumstance. As mentioned earlier, there are many different types and designs of airplanes, ranging in size, power, shape and maneuverability. However, amongst the diversity there may be some common ground that we can observe and understand to help pilots react to engine inoperative flight. There may also be some standards of reaction that only apply to some categories of airplanes and not others. An airline could use this algorithm on all of the airplanes in their fleet, and discover standards for their fleet.

To do this for every airplane would not be over complicated or expensive. This algorithm only requires an accurate line art of the airplane as well as engine data at various temperatures. For this work we highlight two different airplanes; the Airbus A320, and the Lockheed Martin C130J-30 Super Hercules. For the A320 we used published line art from the book "Jane's All the World's Aircraft"[5]. For the C130J-30 we simply used a poster found in a web search[6]. For both the A320 and the C130J-30 we used NPSS generated 5-colum engine data, which will be explained in the next section.

Chapter 2: Method

As previously stated there are three major tools used for these algorithms.

1. The coding used for these algorithms is Visual Basic for Applications (VBA), using Microsoft EXCEL as the platform. Microsoft EXCEL has sheets that are already divided into cells that make for easy data input and data collection. These cells may be formatted, named, and even linked to other cells to help in data processing. Under the hood of EXCEL, in the developer tools, there is a user interface that runs off of VBA. VBA is a dynamic coding language that allows the user to not only interact with the sheets and cells of EXCEL itself, but also create data, export data, import data, and even used other programs and applications.

2. VORLAX is a vortex lattice computational fluid dynamics application developed by Lockheed for NASA in 1977. By inputting various parameters of an airplane, VORLAX will simulate flight and output various performance parameters of the inputted airplane for use of understanding the dynamics and characteristics of the inputted airplane. NASA produced a manual[7] that fully explains the usage of VORLAX. This manual explains all of the equations and calculations that VORLAX produces. This tool is used mainly to generate a database of six particular parameters namely: Lift coefficient (CL), Drag coefficient (CD), Lateral force coefficient (CY), Pitching moment coefficient (CPM), Rolling moment coefficient (CRM), and Yawing moment coefficient (CYM) all at various angles of attack (α). These are the values that will be used in the algorithm to generate the stability derivatives needed to satisfy the trim equations. There are

two of the variables that are outputted by VORLAX that we will change the name of to more closely follow the common nomenclature. VORLAX outputs the rolling moment coefficient as CRM, however looking at Figure 2 we will call this variable Cl. VORLAX also calls the yawing moment coefficient as CYM, once again Figure 2 leads us to name this variable Cn.

3. Another tool developed by NASA that is used in this algorithm is the Numerical Propulsion System Simulation (NPSS)[8]. NPSS is a programming framework used to model the mechanical, fluid and thermodynamic processes within an engine. The program is able to represent physical components of an engine such as inlets, various compressors, combustion chamber, turbines and exit nozzles. The program then loops through Mach numbers of the subsonic regime, altitudes ranging from 0 to 50,000ft and numerous power codes PLA. Then the NPSS program is able to analyze the properties of the specified inputs through the looped parameters to generate 5-column formatted data[9] (Figure 3). The 5 columns consist of Mach number, altitude, PLA, Thrust generated, and Thrust Specific Fuel Consumption (TSFC). The Mach number, altitude and PLA will determine the thrust used as the aforementioned asymmetrical propulsion force.

```
PROP
*BPR 5.0 / OPR 33:1 / TIT=2500F / FPR- 1.6 - TURBOFAN
* 25000 LB STATIC THRUST AT SEA-LEVEL
*39.5    -in fan diameter
NPLA
5
NMACH
10
NALT
11
* MACH  ALT     PLA     THRUST  TSFC
DATA
0       0       0.85    1075.679413     0.60553656
0       0       0.9     6111.155121     0.2834298
0       0       0.96    15277.82669     0.2887542
0       0       0.98    18333.52648     0.29703348
0       0       1       27000.00000     0.32896692
0       5000    0.85    1641.419599     0.40294908
0       5000    0.9     6111.216233     0.27192348
0       5000    0.96    14857.86811     0.2892348
0       5000    0.98    18332.73203     0.30161916
0       5000    1       24097.01798     0.3313116
0       10000   0.85    3055.583672     0.28677132
0       10000   0.9     6111.075676     0.263385
0       10000   0.96    14383.52025     0.29121984
0       10000   0.98    18332.54869     0.31253688
0       10000   1       18600.76729     0.31427028
0       15000   0.85    3055.565338     0.27040716
0       15000   0.9     6111.155121     0.25877232
0       15000   0.96    13946.69488     0.29734452
0       15000   0.98    16456.0574      0.31676724
0       15000   1       16456.0574      0.31676724
0       20000   0.85    3055.644783     0.25663608
0       20000   0.9     6111.216233     0.25834464
0       20000   0.96    13170.45596     0.30663792
0       20000   0.98    14418.23161     0.32067468
0       20000   1       14418.23161     0.32067468
0       25000   0.85    3055.577561     0.24627996
0       25000   0.9     6111.155121     0.25993872
0       25000   0.96    11874.76885     0.31616244
0       25000   0.98    12464.06754     0.32682852
0       25000   1       12464.06754     0.32682852
0       30000   0.85    3055.57145      0.24007212
0       30000   0.9     6111.057343     0.263061
0       30000   0.96    10467.18649     0.3342006
0       30000   0.98    10539.1759      0.33626448
0       30000   1       10539.1759      0.33626448
```

Figure 3. 5-column Data

```
0       50000   0.9     3233.308285     0.27988848
0       50000   0.96    4381.343775     0.34735932
0       50000   0.98    4381.343775     0.34735932
0       50000   1       4381.343775     0.34735932
0.1     0       0.85    629.8278691     1.03000572
0.1     0       0.9     5865.095572     0.34314624
0.1     0       0.96    13212.19515     0.33412176
0.1     0       0.98    18333.89315     0.3446442
0.1     0       1       24266.17476     0.36689652
0.1     5000    0.85    1103.344613     0.59649804
0.1     5000    0.9     6111.14901      0.32577012
0.1     5000    0.96    12953.63218     0.33098328
0.1     5000    0.98    18129.04723     0.34820172
0.1     5000    1       21751.25109     0.3680694
0.1     10000   0.85    2967.479149     0.35059824
0.1     10000   0.9     6111.14901      0.31501656
0.1     10000   0.96    12666.77455     0.32973048
0.1     10000   0.98    16718.95929     0.35050752
0.1     10000   1       16718.95929     0.35050752
0.1     15000   0.85    3055.577561     0.32602176
0.1     15000   0.9     6111.155121     0.30872232
0.1     15000   0.96    12402.34487     0.33305364
0.1     15000   0.98    14856.64588     0.35183592
0.1     15000   1       14856.64588     0.35183592
0.1     20000   0.85    3055.577561     0.3080376
0.1     20000   0.9     6111.155121     0.30521448
0.1     20000   0.96    11850.81312     0.34061148
0.1     20000   0.98    13072.98304     0.35470872
0.1     20000   1       13072.98304     0.35470872
0.1     25000   0.85    3055.516449     0.29457972
0.1     25000   0.9     6110.965676     0.3026106
0.1     25000   0.96    10760.03305     0.34907112
0.1     25000   0.98    11349.08729     0.36011196
0.1     25000   1       11349.08729     0.36011196
0.1     30000   0.85    3055.553116     0.28658988
0.1     30000   0.9     5952.393423     0.30307392
0.1     30000   0.96    9540.796487     0.36647964
0.1     30000   0.98    9631.547141     0.3692196
0.1     30000   1       9631.547141     0.3692196
0.1     35000   0.85    3055.577561     0.28238328
0.1     35000   0.9     5771.55212      0.30962844
0.1     35000   0.96    8140.36418      0.3776976
0.1     35000   0.98    8140.36418      0.3776976
0.1     35000   1       8140.36418      0.3776976
0.1     40000   0.85    2788.960085     0.28338012
0.1     40000   0.9     4699.349954     0.3112182
0.1     40000   0.96    6501.413488     0.37968156
```

Figure 4. Continuation of Figure 3

Chapter 3: Aerodynamic Database Generator

Figure 5 is a flowchart that shows how the overall sketch-to-VMC process operates.

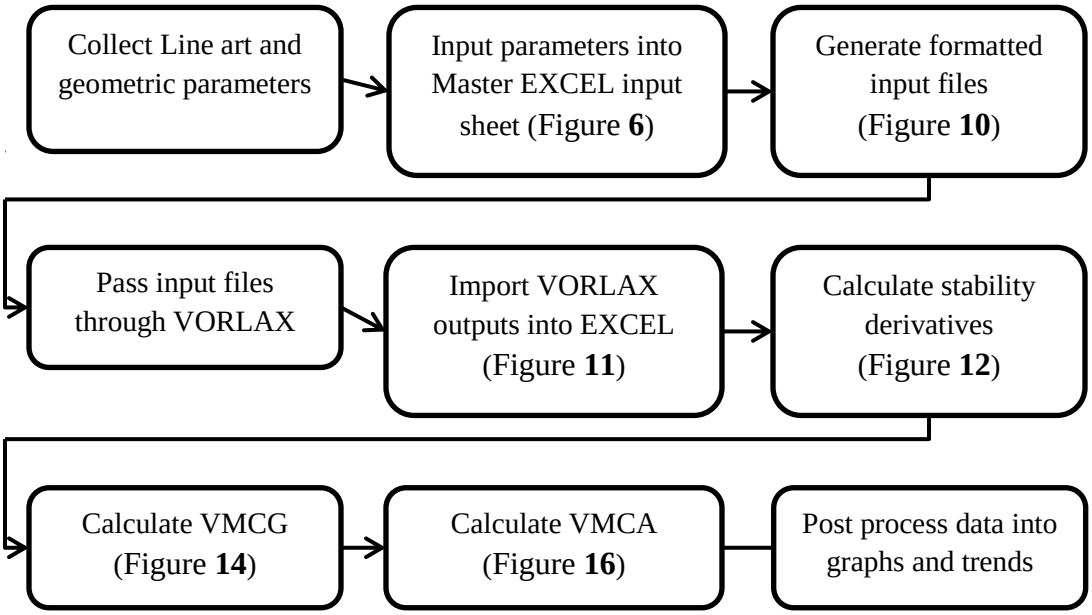

Figure 5. Flowchart of Main Algorithm

For each individual airplane, first we collect the line art and geometric parameters, and enter these into the first sheet of the master EXCEL book (Figure 6). The line art of the airplane is sub-divided into “panels” that are essentially glued together to represent (in a flat panel vortex lattice model) the aerodynamics of the aircraft.

There are also key parameters that are unique to each aircraft that are also inputted into VORLAX to generate the aircraft performance variables. These inputs include Mach numbers, angles of attack (α), Sideslip Angle (β), Reference Area (Sref),

Reference Chord (CBAR), Longitudinal Center of Gravity (XBAR), Vertical Center of Gravity (ZBAR), and Reference Span (WSPAN).

For example, with a C130J-30 there are 14 panels that constitute the line art of the aircraft (Figure 6, Figure 8 and Figure 7). For the panels that represent the control surfaces such as the ailerons, elevators, and the rudder, the panels are defined with the maximum angle of deflection respectively. The final view of the aircraft would be one were the rudder, elevators, and ailerons are at full deflected, as well as any flap panels for the specified flaps setting (Figure 9).

Once the inputs and geometric parameters are accurate and match the desired airplane design and shape, the VBA code then generates five different input files to be passed into VORLAX. VORLAX is an application that is coded in FORTRAN, therefore the input files must be very specific on spacing as well as where text may and may not be. Figure 10 is an example of what the input file must look like. Figure 10 is only a small portion of what the entire input file looks like, for the entire input file includes all of the panels that were defined in the master EXCEL input sheet (Figure 6 and Figure 7).

In order to generate these very specific input files, there was a lot of coding done to ensure spacing and location of all of the values and text of the input files. The intent of running VORLAX is to be able to get a baseline of how the airplane flies as well as how the control surfaces affect this baseline.

As mentioned earlier there will be five different input files that are generated to be passed through VORLAX. The five different files will be referred to as **Baseline**, **Sideslip**, **Aileron**, **Rudder** and **Elevator**. These five files will be discussed in deeper detail below.

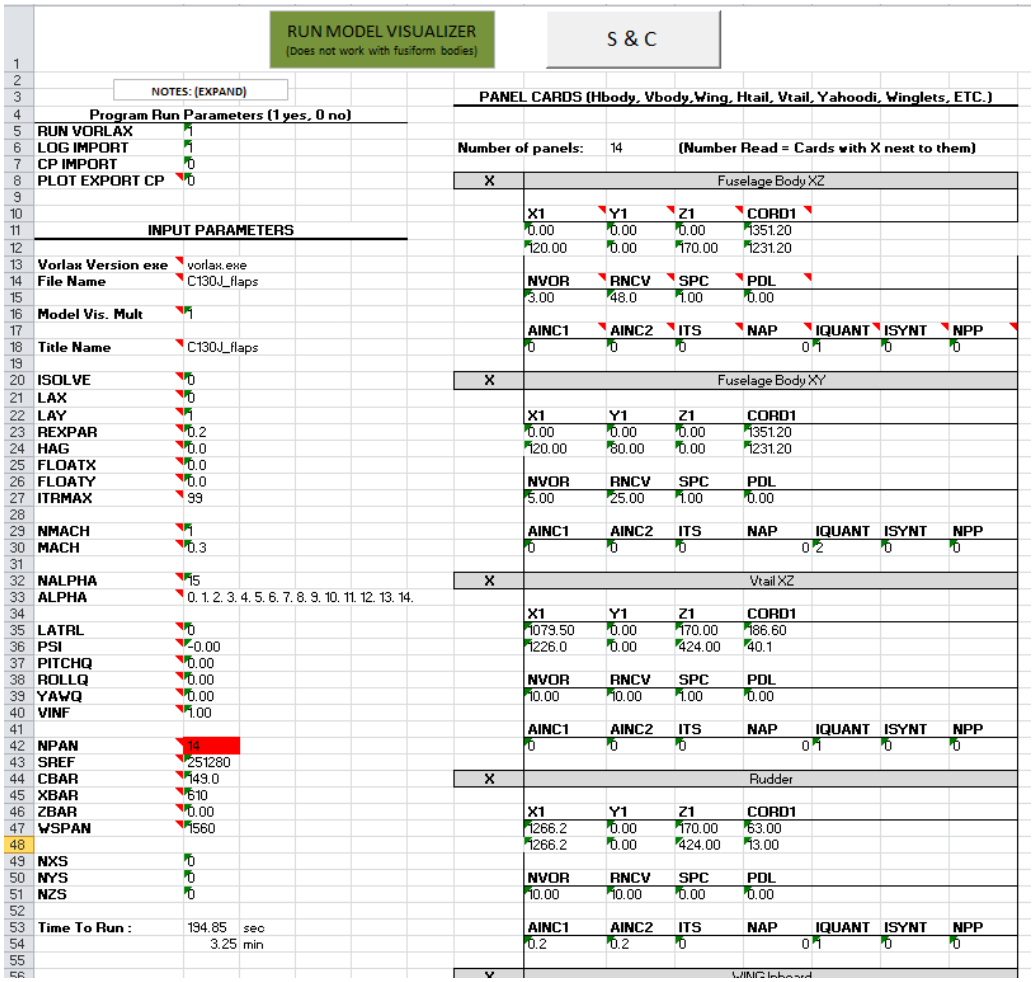

RUN MODEL VISUALIZER
(Does not work with fusiform bodies)

S & C

NOTES: (EXPAND)

Program Run Parameters (1 yes, 0 no)

RUN VORLAX	1
LOG IMPORT	1
CP IMPORT	0
PLOT EXPORT CP	0

INPUT PARAMETERS

Vorlax Version exe	vorlax.exe
File Name	C130J_flaps
Model Vis. Mult	1
Title Name	C130J_flaps
ISOLVE	0
LAX	0
LAY	1
REXPAR	0.2
HAG	0.0
FLOATX	0.0
FLOATY	0.0
ITRMAX	99
NMACH	1
MACH	0.3
NALPHA	15
ALPHA	0. 1. 2. 3. 4. 5. 6. 7. 8. 9. 10. 11. 12. 13. 14.
LATRL	0
PSI	-0.00
PITCHQ	0.00
ROLLQ	0.00
YAWQ	0.00
VINF	1.00
NPAN	14
SREF	251280
CBAR	149.0
XBAR	610
ZBAR	0.00
WSPAN	560
NXS	0
NYS	0
NZS	0
Time To Run :	194.85 sec
	3.25 min

PANEL CARDS (Hbody, Vbody,Wing, Htail, Vtail, Yahoodi, Winglets, ETC.)

Number of panels: 14 (Number Read = Cards with X next to them)

X	Fuselage Body XZ			
	X1	Y1	Z1	CORD1
	0.00	0.00	0.00	351.20
	120.00	0.00	170.00	231.20
	NVOR	RNCV	SPC	PDL
	3.00	48.0	1.00	0.00
	AINC1	AINC2	ITS	NAP / IQUANT / ISYNT / NPP
	0	0	0	0 / 1 / 0 / 0
X	Fuselage Body XY			
	X1	Y1	Z1	CORD1
	0.00	0.00	0.00	351.20
	120.00	80.00	0.00	231.20
	NVOR	RNCV	SPC	PDL
	5.00	25.00	1.00	0.00
	AINC1	AINC2	ITS	NAP / IQUANT / ISYNT / NPP
	0	0	0	0 / 2 / 0 / 0
X	Vtail XZ			
	X1	Y1	Z1	CORD1
	1079.50	0.00	170.00	186.60
	1226.0	0.00	424.00	40.1
	NVOR	RNCV	SPC	PDL
	10.00	10.00	1.00	0.00
	AINC1	AINC2	ITS	NAP / IQUANT / ISYNT / NPP
	0	0	0	0 / 1 / 0 / 0
X	Rudder			
	X1	Y1	Z1	CORD1
	1266.2	0.00	170.00	63.00
	1266.2	0.00	424.00	13.00
	NVOR	RNCV	SPC	PDL
	10.00	10.00	0.00	0.00
	AINC1	AINC2	ITS	NAP / IQUANT / ISYNT / NPP
	0.2	0.2	0	0 / 1 / 0 / 0
X	WING Inboard			

Figure 6. Master EXCEL Input Example Using C130J-30 Inputs

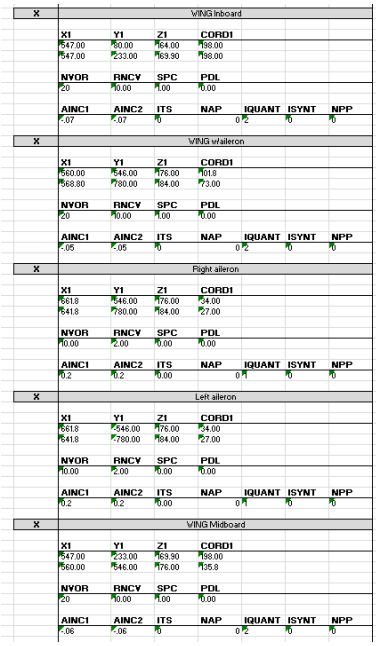

WING Inboard

X1	Y1	Z1	CORD1
547.00	60.00	64.00	98.00
547.00	233.00	63.90	98.00

NYOR	RNCV	SPC	PDL
20	0.00	1.00	0.00

AINC1	AINC2	ITS	NAP	IQUANT	ISYNT	NPP
-.07	-.07	0	0	2	0	0

WING w/aileron

X1	Y1	Z1	CORD1
560.00	546.00	76.00	91.8
568.80	780.00	84.00	73.00

NYOR	RNCV	SPC	PDL
20	0.00	1.00	0.00

AINC1	AINC2	ITS	NAP	IQUANT	ISYNT	NPP
-.05	-.05	0	0	2	0	0

Flight aileron

X1	Y1	Z1	CORD1
581.8	546.00	76.00	54.00
541.8	780.00	84.00	27.00

NYOR	RNCV	SPC	PDL
0.00	2.00	0.00	0.00

AINC1	AINC2	ITS	NAP	IQUANT	ISYNT	NPP
0.2	0.2	0.00	0	1	0	0

Left aileron

X1	Y1	Z1	CORD1
581.8	546.00	76.00	54.00
541.8	780.00	84.00	27.00

NYOR	RNCV	SPC	PDL
0.00	2.00	0.00	0.00

AINC1	AINC2	ITS	NAP	IQUANT	ISYNT	NPP
0.2	0.2	0.00	0	1	0	0

WING Midboard

X1	Y1	Z1	CORD1
547.00	233.00	63.90	98.00
560.00	546.00	76.00	95.8

NYOR	RNCV	SPC	PDL
20	0.00	1.00	0.00

AINC1	AINC2	ITS	NAP	IQUANT	ISYNT	NPP
-.06	-.06	0	0	2	0	0

Figure 8. Continuation of Figure 6

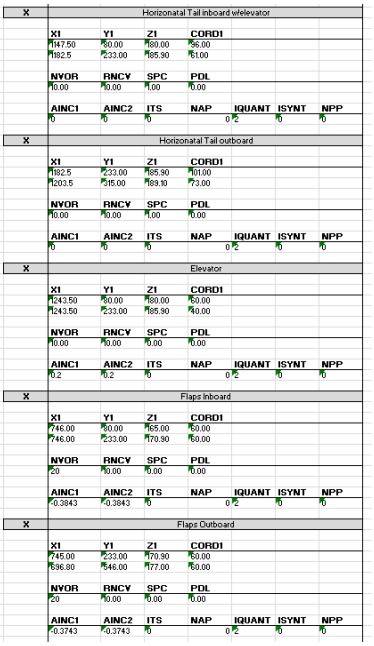

Horizonatal Tail inboard w/elevator

X1	Y1	Z1	CORD1
147.50	60.00	80.00	96.00
182.5	233.00	85.90	61.00

NYOR	RNCV	SPC	PDL
10.00	0.00	1.00	0.00

AINC1	AINC2	ITS	NAP	IQUANT	ISYNT	NPP
0	0	0	0	2	0	0

Horizonatal Tail outboard

X1	Y1	Z1	CORD1
182.5	233.00	85.90	91.00
203.5	515.00	89.10	73.00

NYOR	RNCV	SPC	PDL
10.00	0.00	1.00	0.00

AINC1	AINC2	ITS	NAP	IQUANT	ISYNT	NPP
0	0	0	0	2	0	0

Elevator

X1	Y1	Z1	CORD1
243.50	60.00	80.00	60.00
243.50	233.00	85.90	40.00

NYOR	RNCV	SPC	PDL
10.00	0.00	0.00	0.00

AINC1	AINC2	ITS	NAP	IQUANT	ISYNT	NPP
0.2	0.2	0	0	2	0	0

Flaps Inboard

X1	Y1	Z1	CORD1
746.00	60.00	65.00	59.00
746.00	233.00	70.90	59.00

NYOR	RNCV	SPC	PDL
20	0.00	0.00	0.00

AINC1	AINC2	ITS	NAP	IQUANT	ISYNT	NPP
-0.3843	-0.3843	0	0	2	0	0

Flaps Outboard

X1	Y1	Z1	CORD1
745.00	233.00	70.90	60.00
696.80	546.00	77.00	60.00

NYOR	RNCV	SPC	PDL
20	0.00	0.00	0.00

AINC1	AINC2	ITS	NAP	IQUANT	ISYNT	NPP
-0.3743	-0.3743	0	0	2	0	0

Figure 7. Continuation of Figure 6

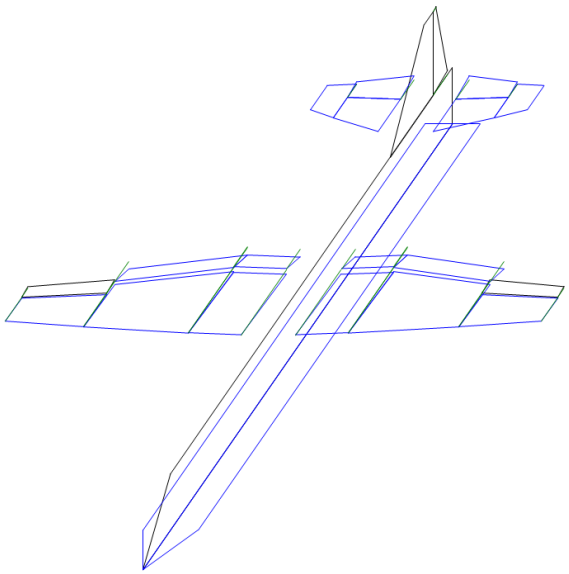

Figure 9. Oblique View of "panels" Glued Together with Control Surfaces at Maximum Deflection

The first input file generated represents the longitudinal **Baseline** aerodynamic properties. This is the case where the aircraft flies at zero sideslip angle and all control surface deflections are set to neutral (zero). This is done by overriding whatever the sideslip angle (β) is in the master EXCEL input sheet to zero degrees. Then the code finds the panels that represent the ailerons, rudder and elevators and manually straightens them to a deflection of zero degrees (AINC=0). This input file is generated with the title of **Baseline**, meaning it is just the baseline of aircraft performance parameters of the aircraft. Although there is no sideslip angle or deflection of the control surfaces, the flaps are still represented as extended and deflected to the appropriate flaps setting. The intent of this first VORLAX input file is to generate performance parameters of the airplane in takeoff flaps settings, thus the flaps still need to be represented in the baseline outputs to paint a clear picture of how the airplane behaves in this flight configuration. From this run, we compute CL vs α, Cm vs α and CD vs α.

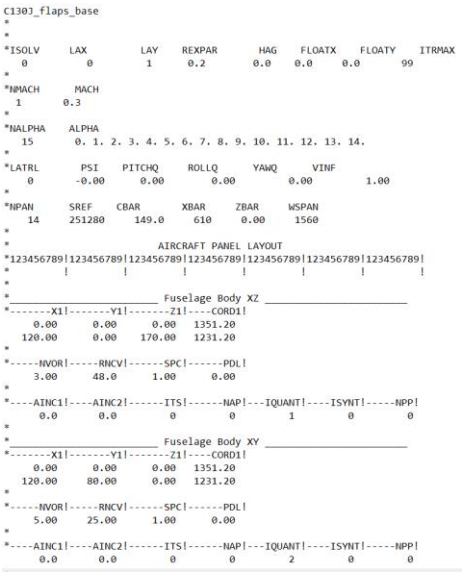

```
C130J_flaps_base
*
*
*ISOLV     LAX         LAY    REXPAR       HAG    FLOATX    FLOATY    ITRMAX
   0          0          1      0.2       0.0    0.0     0.0        99
*
*NMACH      MACH
  1       0.3
*
*NALPHA     ALPHA
   15       0. 1. 2. 3. 4. 5. 6. 7. 8. 9. 10. 11. 12. 13. 14.
*
*LATRL       PSI    PITCHQ      ROLLQ       YAWQ       VINF
    0       -0.00      0.00        0.00          0.00          1.00
*
*NPAN      SREF     CBAR       XBAR      ZBAR      WSPAN
    14     251280     149.0      610     0.00     1560
*
*                          AIRCRAFT PANEL LAYOUT
*123456789|123456789|123456789|123456789|123456789|123456789|123456789|123456789|
*         |         |         |         |         |         |         |         |
*
*_____________________ Fuselage Body XZ _____________________
*-------X1|-------Y1|-------Z1|----CORD1|
     0.00      0.00      0.00   1351.20
   120.00      0.00    170.00   1231.20
*
*-----NVOR|-----RNCV|------SPC|------PDL|
     3.00      48.0      1.00      0.00
*
*----AINC1|----AINC2|------ITS|------NAP|---IQUANT|----ISYNT|-----NPP|
      0.0       0.0         0         0         1         0         0
*
*_____________________ Fuselage Body XY _____________________
*-------X1|-------Y1|-------Z1|----CORD1|
     0.00      0.00      0.00   1351.20
   120.00     80.00      0.00   1231.20
*
*-----NVOR|-----RNCV|------SPC|------PDL|
     5.00     25.00      1.00      0.00
*
*----AINC1|----AINC2|------ITS|------NAP|---IQUANT|----ISYNT|-----NPP|
      0.0       0.0         0         0         2         0         0
```

Figure 10. Formatted Input File for VORLAX Using C130J-30 Inputs

The second input file generated by the VBA code is the **Sideslip** case. Then intent of this VORLAX input file is to be able to compare the outputs with the Baseline configuration to see how sideslip winds affect the airplanes performance; it provides the basis to develop linearized β dependent aerodynamic derivatives. This input file has a forces the sideslip angle to one degrees, however all three of the control surface need to remain at zero degrees of deflections. Thus, like in the **Baseline** configuration, the code forces the deflection angle of the ailerons, rudder and elevators to zero degrees. From this run, we compute δCY/δ β vs α, δCn/δβ vs α and δCl/δ β vs α.

Now that the **Baseline** and **Sideslip** input files have been generated, we need to see how the control surfaces affect the airplane, thus the third input file that is generated has the intent on isolating the effects of the ailerons on the airplane performance. The third input file, titled **Aileron**, is generated the same way as the first two via the code that generates these VORLAX input files. The sideslip angle is forced to zero degrees, same as the **Baseline** configuration, the rudder and elevator panels are also forced to zero degrees of deflection, however whatever is inputted in the master EXCEL input sheet as the maximum angle of deflection for the aileron panels will be the angle of deflection for the ailerons in this input file. From this run, we compute δCY/δθaileron vs α, δCn/δθaileron vs α and δCl/δθdaileron vs α.

The fourth input file is titled **Rudder**, with the intentions of isolating the rudder effects on the airplane performance parameters. Just as in the **Baseline** and **Aileron** configurations, the sideslip angle is forced to zero degrees. The aileron and elevator

panels are also found via the search algorithm and set to zero degrees deflection. When the rudder panel is isolated and generated in the input file, the angle of deflection that is inputted in the master EXCEL sheet is what will be generated in the VORLAX input file. From this run, we compute $\delta CY/\delta\theta rudder$ vs α, $\delta Cn/\delta\theta rudder$ vs α and $\delta Cl/\delta\theta rudder$ vs α.

The fifth and final VORLAX input file that is generated is the one intended on isolating the effects of the elevator on the airplane. Thus this final file, titled **Elevator**, has a sideslip angle of zero degrees. The aileron and rudder panels are forced to a deflection of zero degrees, and the elevator panels are generated exactly as they are defined in the master EXCEL sheet, thus representing an airplane that has only the elevators that are influencing the performance parameters of the airplane. From this run, we compute $\delta CL/\delta\theta elevator$ vs α, $\delta CD/\delta\theta elevator$ vs α and $\delta Cm/\delta\theta elevator$ vs α.

It is important to remember that as in the **Baseline** configuration, all of the other four input files represent the airplane in takeoff flaps configuration, thus the panels that represented the inboard and outboard flaps are extended and angled to the specified takeoff settings. For the case of the C130J-30 takeoff flaps setting, which is represented in all of the example figure, the angle of the flaps is eighteen degrees. For eighteen degrees to be represented accurately, this angle must be added to any deflection angle of the wing. For example the inboard wing has a deflection of about four degrees; therefore the inboard flaps have a deflection of twenty-two degrees to allow the flaps to be represented at eighteen degrees.

Moving on to the fourth section of Figure 5, all five of the VORLAX input files are passed through the VORLAX program in sequence, one at a time. Each individual execution of the VORLAX program generates an output file. This output file is called the log file, and has more information in it than is needed to calculate VMCG and VMCA. Due to the fact that all of this information is not needed, the code then parses this information into another output file that is specific for the needs of calculating VMCG and VMCA. This information includes Lift coefficient (CL), Drag coefficient (CD), Lateral force coefficient (CY), Pitching moment coefficient (Cm) (designated CPM in the VORLAX output file), Rolling moment coefficient (Cl) (designated CRM in the VORLAX output file), and Yawing moment coefficient (Cn) (designated CYM in the VORLAX output file).

Figure 11 shows exactly what information is parsed form the log file and then imported into another EXCEL sheet. The **Baseline** VORLAX file was passed through VORLAX and the values seen in Figure 11 as the parsed values needed for solving VMCG and VMCA. As seen in Figure 11 there is only one Mach number used and fifteen different angles of attack (α) with corresponding performance parameters of CL, CD, CY, CPM, CRM and CYM. It is noted that there is no CY, CRM or CYM values; this makes sense because there are not control surfaces deflected nor is there any sideslip angle. This is a good way of gut checking the outputs of the Base file.

	A	B	C	D	E	F	G	H	I	J	K	L	M	N	O	P	Q	R	S	T	U
1	*C130J_flaps_base																				
2	*MACH	ALFA	PSI	PITCHR	ROLLR	YAWR		HAG	SREF	CBAR	WSPAN	XBAR	ZBAR		CL	CD	CY	CPM	CRM	CYM	
3	0.3	0	0	0	0	0		0	3E+05	149	1560	610	0		0.538	0.0539	0	0.1422	0	0	
4	0.3	1	0	0	0	0		0	3E+05	149	1560	610	0		0.6133	0.0605	0	0.1351	0	0	
5	0.3	2	0	0	0	0		0	3E+05	149	1560	610	0		0.6881	0.0678	0	0.1259	0	0	
6	0.3	3	0	0	0	0		0	3E+05	149	1560	610	0		0.7624	0.0759	0	0.1145	0	0	
7	0.3	4	0	0	0	0		0	3E+05	149	1560	610	0		0.8362	0.0847	0	0.1009	0	0	
8	0.3	5	0	0	0	0		0	3E+05	149	1560	610	0		0.9096	0.094	0	0.0852	0	0	
9	0.3	6	0	0	0	0		0	3E+05	149	1560	610	0		0.9821	0.1041	0	0.0674	0	0	
10	0.3	7	0	0	0	0		0	3E+05	149	1560	610	0		1.0539	0.115	0	0.0476	0	0	
11	0.3	8	0	0	0	0		0	3E+05	149	1560	610	0		1.1248	0.1264	0	0.0257	0	0	
12	0.3	9	0	0	0	0		0	3E+05	149	1560	610	0		1.195	0.1385	0	0.0018	0	0	
13	0.3	10	0	0	0	0		0	3E+05	149	1560	610	0		1.2643	0.1512	0	-0.0241	0	0	
14	0.3	11	0	0	0	0		0	3E+05	149	1560	610	0		1.3327	0.1644	0	-0.052	0	0	
15	0.3	12	0	0	0	0		0	3E+05	149	1560	610	0		1.4001	0.1781	0	-0.0818	0	0	
16	0.3	13	0	0	0	0		0	3E+05	149	1560	610	0		1.4666	0.1923	0	-0.1134	0	0	
17	0.3	14	0	0	0	0		0	3E+05	149	1560	610	0		1.5321	0.2071	0	-0.1469	0	0	
18																					

Figure 11. Imported Vorlax Output into EXCEL Using C130J-30 Inputs

The code then parses and grabs this information for the **Sideslip**, **Aileron**, **Rudder** and **Elevator** VORLAX output files. Now that all of this information is generated, there is a database that can be used to interpolate any information desired within the scope of the inputs.

The next step in the process is to determine the stability derivatives in terms of sideslip angle, aileron deflection, rudder deflection and elevator deflection. At this point an assumption is made to be able to calculate these stability derivatives. The assumption is that the effects of sideslip angle and the control surfaces are linear. By making this assumption, we are able to compare the output values at every angle of attack (α) for each performance parameter and derive the stability derivatives, then interpolate these values when solving for VMCG and VMCA. One of the major discoveries of this work, which will be elaborated on later, is the observation that this linearization of the stability derivatives for each individual angle of attack (α) still produces an accurate estimation of VMCG and VMCA.

For example the Sideslip configuration had a sideslip angle of one degree, if we assume the stability derivatives of δCn/δβ, δCl/δβ and δCY/δβ to be linear, then each of the stability derivatives of δCn/δβ, δCl/δβ and δCY/δβ may be calculated by Equations 1, 2 and 3 respectively at each angle of attack (α). If there is a sideslip angle of three degrees, then the effects would just be three times these stability derivatives, due to the linearization of these stability derivatives.

$$\frac{\partial Cn}{\partial \beta} = \frac{Cn_{Sideslip} - Cn_{Base}}{\beta_{Sideslip} - \beta_{Base}} \quad [1]$$

$$\frac{\partial Cl}{\partial \beta} = \frac{Cl_{Sideslip} - Cl_{Base}}{\beta_{Sideslip} - \beta_{Base}} \quad [2]$$

$$\frac{\partial CY}{\partial \beta} = \frac{CY_{Sideslip} - CY_{Base}}{\beta_{Sideslip} - \beta_{Base}} \quad [3]$$

The next step in the process is to calculate the stability derivatives due to the aileron effects. To do this the same linearization assumption is applied to the comparison of the **Baseline** and **Aileron** output configuration files. The stability derivatives of δCn/δθaileron, δCl/δθaileron and δCY/δθaileron are calculated via Equations 4, 5 and 6 at each angle of attack (α).

$$\frac{\partial Cn}{\partial \theta aileron} = \frac{Cn_{Aileron} - Cn_{Base}}{\theta aileron_{Aileron} - \theta aileron_{Base}} \quad [4]$$

$$\frac{\partial Cl}{\partial \theta aileron} = \frac{Cl_{Aileron} - Cl_{Base}}{\theta aileron_{Aileron} - \theta aileron_{Base}} \quad [5]$$

$$\frac{\partial CY}{\partial \theta aileron} = \frac{CY_{Aileron} - CY_{Base}}{\theta aileron_{Aileron} - \theta aileron_{Base}} \quad [6]$$

Just as for the sideslip and aileron effects, the rudder effects are calculated in the same manner. Once again the linearization assumption is applied to the calculation of the stability derivatives due to the rudder. The stability derivatives of δCn/δθrudder, δCl/δθrudder and δCY/δθrudder are calculated via Equations 7, 8 and 9 at each angle of attack (α).

$$\frac{\partial Cn}{\partial \theta rudder} = \frac{Cn_{Rudder} - Cn_{Base}}{\theta rudder_{Rudder} - \theta rudder_{Base}} \quad [7]$$

$$\frac{\partial Cl}{\partial \theta rudder} = \frac{Cl_{Rudder} - Cl_{Base}}{\theta rudder_{Rudder} - \theta rudder_{Base}} \quad [8]$$

$$\frac{\partial CY}{\partial \theta rudder} = \frac{CY_{Rudder} - CY_{Base}}{\theta rudder_{Rudder} - \theta rudder_{Base}} \quad [9]$$

Finally the stability derivatives of δCn/δθelevator, δCl/δθelevator and δCY/δθelevator are found. Just as with all of the other comparisons the linearization of the stability derivatives is assumed in the calculations. These stability derivatives are calculated using Equations 10, 11 and 12 at each angle of attack (α).

$$\frac{\partial Cn}{\partial \theta elevator} = \frac{Cn_{Elevator} - Cn_{Base}}{\theta elevator_{Elevator} - \theta elevator_{Base}} \quad [10]$$

$$\frac{\partial Cn}{\partial \theta elevator} = \frac{Cn_{Elevator} - Cn_{Base}}{\theta elevator_{Elevator} - \theta elevator_{Base}} \quad [11]$$

$$\frac{\partial Cn}{\partial \theta elevator} = \frac{Cn_{Elevator} - Cn_{Base}}{\theta elevator_{Elevator} - \theta elevator_{Base}} \quad [12]$$

Now that all of the needed stability derivatives have been obtained, the code generates a table of these values to use in future parts of the algorithm (Figure 12). It is

important to remember that although the linearization assumption was made for the stability derivatives, the Mach number and angle of attack (α) dependencies were not linearized.

Each Equation 1 through 12 is solved at each angle of attack (α) from zero to fourteen degrees. As seen in Figure 12, the database generated for the stability derivatives is angle of attack (α) dependent. Just like for the Mach number, once an angle of attack (α) is interpolated, then the stability derivative values will also be interpolated within a single degree of angle of attack (α) to account for the non-linearity dependency of angle of attack (α).

angle of attack	dCn/dbeta	dCl/dbeta	dCY/dbeta	dCn/drudder	dCl/drudder	dCY/drudder	dCn/daileron	dCl/daileron	dCY/daileron	dCn/delevator	dCl/delevator	dCY/delevator
0	0.00309	-0.00338	-0.02053	-0.002334	0.000908	0.006041	0.000050	0.004134	3.421E-04	0	0	0
1	0.00312	-0.00343	-0.02071	-0.002349	0.000867	0.006040	0.000009	0.004133	3.421E-04	0	0	0
2	0.00316	-0.00346	-0.02092	-0.002362	0.000825	0.006034	-0.000033	0.004130	3.421E-04	0	0	0
3	0.00319	-0.0035	-0.02117	-0.002373	0.000782	0.006025	-0.000074	0.004124	3.412E-04	0	0	0
4	0.00323	-0.00354	-0.02144	-0.002382	0.000739	0.006012	-0.000115	0.004115	3.403E-04	0	0	0
5	0.00327	-0.00357	-0.02175	-0.002388	0.000696	0.005996	-0.000156	0.004104	3.395E-04	0	0	0
6	0.00331	-0.00359	-0.02209	-0.002391	0.000651	0.005976	-0.000196	0.004091	3.386E-04	0	0	0
7	0.00335	-0.00362	-0.02247	-0.002393	0.000607	0.005952	-0.000236	0.004074	3.368E-04	0	0	0
8	0.00339	-0.00363	-0.02287	-0.002393	0.000563	0.005925	-0.000276	0.004055	3.360E-04	0	0	0
9	0.00343	-0.00365	-0.0233	-0.002390	0.000518	0.005895	-0.000315	0.004034	3.342E-04	0	0	0
10	0.00348	-0.00366	-0.02376	-0.002385	0.000474	0.005862	-0.000353	0.004010	3.325E-04	0	0	0
11	0.00353	-0.00367	-0.02425	-0.002378	0.000429	0.005824	-0.000390	0.003984	3.299E-04	0	0	0
12	0.00357	-0.00367	-0.02477	-0.002369	0.000385	0.005784	-0.000427	0.003955	3.281E-04	-8.7266E-07	0	0
13	0.00362	-0.00367	-0.02532	-0.002358	0.000340	0.005740	-0.000463	0.003924	3.255E-04	-8.7266E-07	0	0
14	0.00367	-0.00366	-0.02589	-0.002345	0.000297	0.005694	-0.000497	0.003892	3.229E-04	-8.7266E-07	0	0

Figure 12. Recorded Stability Derivatives in EXCEL Using C130J-30 Inputs

This generated database has the benefit and pro of searching for and accounting for some non-linear characteristics of aircraft aerodynamics. However, this database linearizes all stability derivatives and therefore is not as comprehensive as what you might obtain from an extensive wind tunnel test program. In a wind tunnel, we would test the airplane model with a range of Mach numbers, angle of attack (α) and sideslip including getting data at several sideslip angles simultaneously with several different

control surface deflections. We might isolate each control surface as max up, half up, neutral, half down, and full down, for each control surface. However wind tunnel data in not perfect either; it needs to be adjusted for Reynolds number effects or "crud drag" arising from excrescences and other imperfections of the skin along the actual airplane.

Once again, the assumption of linearization of the stability derivatives due to the control surfaces is found to be acceptable due to the interpolation and algorithm used in finding the minimal control airspeeds. If the time was spent in writing more input files and running them through VORLAX at different deflections of the control surfaces to generate a deeper aerodynamics database, the final solution would not be affected significantly for the amount of time and computing power required to do so.

Now that a comprehensive aerodynamic database is generated, we can use numerical methods to find the flight configurations needed to satisfy the trim conditions necessary for minimal control speeds of VMCG and VMCA. As defined earlier, trim conditions are when the forces and moments on the airplane in powered flight are neutralized in every axis.

At this point, all of the aerodynamic forces and moments are generated in a database, and are ready to be used in balancing the asymmetric propulsion force. Using the NPSS generated five-column data; the algorithm will use interpolation of the nonlinear data between two significantly small numbers to account for the non-linearity

dependency of Mach number. This will then allow us to have a database of aerodynamics and a database of propulsion data to be able to solve for VMCG and VMCA.

Chapter 4: Computing Minimum Control Speed on the Ground (VMCG)

Minimum control speed on the ground (VMCG) is calculated when the airplane is still on the ground rolling on its landing gear. This knowledge simplifies the calculation of VMCG in several different ways. First off, the lift generated by the airplane does not have to equal or be higher than the weight of the airplane, because some fraction of the airplanes weight is supported by the landing gear. This in conjunction with the fact that Federal Aviation Administration (FAA) rules do not permit any credit for nose wheel steering[10], thus the calculation of VMCG is non-dependent on weight.

Another simplification of solving for VMCG is that the aerodynamic pitching moments and rolling moments need not to be neutralized. The landing gear supports and counters any non-zero aerodynamic moments acting on the airplane. At the same time, the landing gear prohibits the aircraft from rolling left-to-right. The last significant simplification is that the angle of attack (α) of the airplane is zero degrees, due to the fact that the airplane is still on the ground, thus meaning there is no need to interpolate between angles of attack (α).

These simplifications mean that VMCG is found when the yawing moment due to the control surfaces is greater or equal to the yawing moment induced by the asymmetric propulsion force of the engine. The ailerons provide a very small amount of yawing moment; however that small amount of yawing moment comes with a large rolling moment. Therefore, for the purposes of balancing the yawing moments, the yawing

moment due to the control surfaces will be generated solely by the rudder, and hence will refer to this moment as the yawing moment due to the rudder (YMrudder).

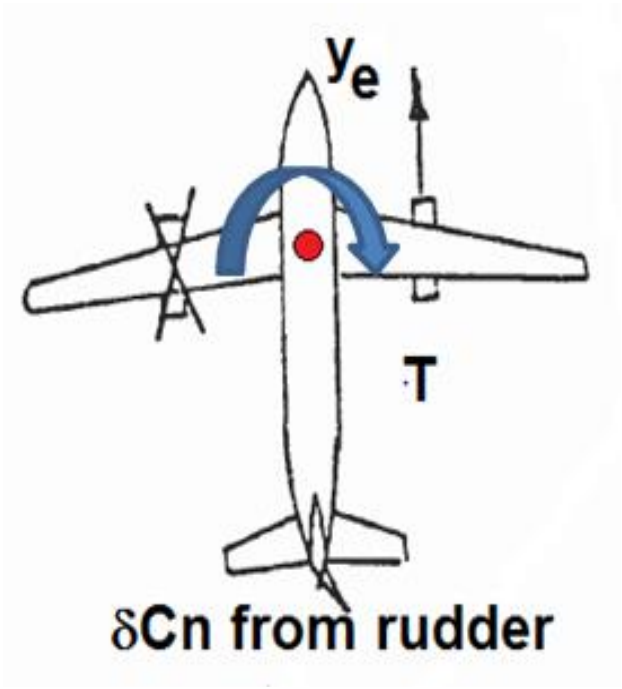

Figure 13. Force Balance for Simplified VMCG Computation[11]

Figure 13 is a free body diagram of the simplified forces and moments acting on the airplane when calculating for VMCG. This free body diagram will later be used to generate the equation needed to solve for the VMCG.

Figure 14 is a local flowchart of how the algorithm determines VMCG. The algorithm solves for the VMCG values at various temperature and altitudes, so that we may find trends and discover how an airplane behaves when an engine is inoperative. This algorithm closely follows the logic of the code used to solve for VMCG.

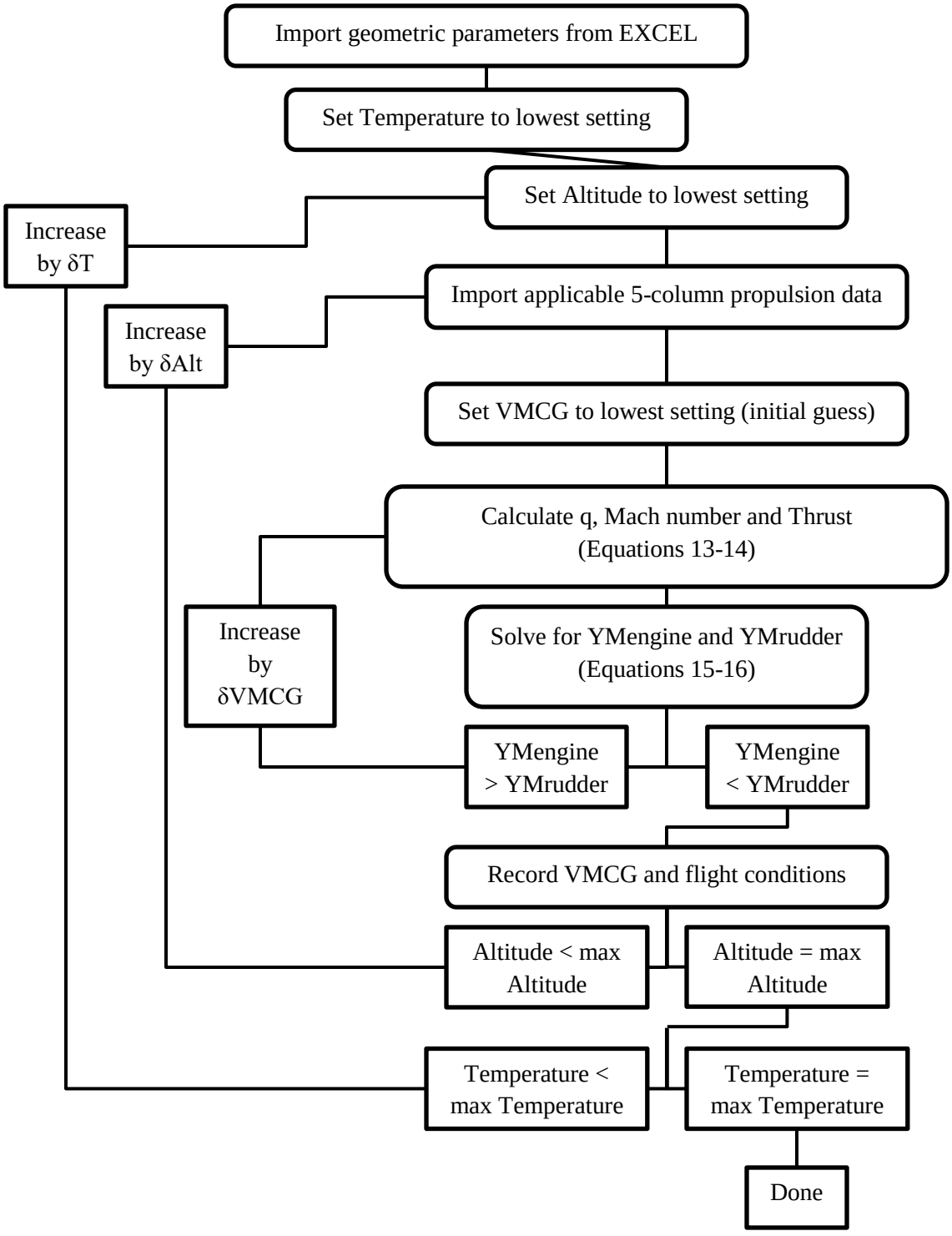

Figure 14. Flowchart of Solving for VMCG

For the case of the C130J-30 there are five different 5-column engine data files that are used at temperatures of -5°C, 5°C, 15°C, 25°C and 35°C, thus the δT referred to in Figure 14 is equal to 10°C. This particular experiment was run from an altitude of 0 ft up to various altitudes for comparison to real data. For computational savings, the initial guess of VMCG was set to 50 Knots, with increments δVMCG of 1 Knot. Therefore, the first time the algorithm calculates q, CL, Mach number, Thrust, moment due to engine (YMengine) and yawing moment due to rudder (YMrudder) it does so at a temperature of -5°C and an altitude of 0 ft.

The dynamic pressure (q) is the kinetic energy per unit volume of fluid, in this case air. The dynamic pressure (q) is found by taking the guessed value of VMCG (or VMCA) and applying Equation 13.

$$q = \left(\frac{(VMCG \text{ or } VMCA)}{660.8}\right)^2 * 1481 \qquad [13]$$

Mach number squared times dynamic pressure (qm) is a standard variable found in the Standard Atmospheric Table (STDATM). Therefore given altitude and temperature, the value of qm may be looked up via the SAT; for the algorithm, there is a 1976 standard atmosphere subroutine[12] developed by Prof. W.H. Mason at Virginia Tech is used to find qm. Once the qm value is known, the Mach number (M) may be found by Equation 14.

$$M = \sqrt{\frac{q}{qm}} \qquad [14]$$

Now that the Mach number is known and the altitude is selected, the asymmetric Thrust can be found by interpolating the 5-column engine data generated by the NPSS program. After interpolating Thrust the yawing moment due to the engine YMengine can be calculated by Equation 15.

$$YM_{engine} = \frac{y_e * Thrust}{q * S_{ref} * b} \quad [15]$$

Were (y_e) is the distance between the centerline of the airplane and the location of the engine, (S_{ref}) being the reference area, and (b) being the reference wingspan.

The free body diagram of the airplane on the ground, with its simplifications is seen in Figure 13. From this free body diagram, the yawing moment due to the rudder is found by Equation 16.

$$YM_{rudder} = \frac{\partial Cn}{\partial \theta rudder}(\alpha = 0°) * \theta rudder_{Max} \quad [16]$$

If the case were the YMengine is greater than YMrudder, then the algorithm increases VMCG by δVMCG and calculates dynamic pressure (q), lift coefficient (CL), Mach number, Thrust, (YMengine) and (YMrudder) again. The algorithm will continue to follow this pattern until the condition of YMrudder is greater than YMengine. The reason why we are looking for this condition is because this tells us that there is enough aerodynamic yawing moment due to the rudder to be able to counter the opposing yawing moment developed by the asymmectric propulsion force.

Once this condition is met, namely the condition where YMrudder is greater to or equal to YMengine, then the algoithm records the VMCG in the EXCEL book for post processing purposes. Then the algorithm increases the altitude by δAlt and cycles through until the maximum specified altitude is reached, recording the VMCG at every δAlt. Finally the algorithm increases the temperature by δT and restarts the process at an altitude of 0 ft. The algorithm stops after finding the VMCG at every combination of temperature and altitude. Now that VMCG has been calculated and recorded as a function of both temperature and altitude, the algorithm moves on to finding VMCA as a function of temperature, altitude and weight.

Chapter 5: Computing Minimum Control Airspeed (VMCA)

While VMCG is found when the landing gear is in contact with the ground, thus allowing us to make simplifications to the trim condition calculations. On the other hand VMCA is found at the flight condition where the landing gear is fully retracted and the airplane is 400 ft above the ground[13]. The airplane must be in full trim flight even with an engine inoperative to calculate VMCA.

In the case of VMCA the lift generated by the airplane must equal the weight of the airplane. The rolling moment, yawing moment and side force induced by the asymmetric propulsion thrust must be countered and balanced by the control surfaces. As another method of countering the asymmetric propulsion force induced by the engine, the pilot is also allowed up to five degrees of bank angle (φ) as well as increasing or decreasing the angle of attack (α), further complicating the calculation of VMCA. This means that there are less equations than unknowns, thus this problem will be solved using a "guess and check" brute force algorithm, much like in VMCG but with more variables.

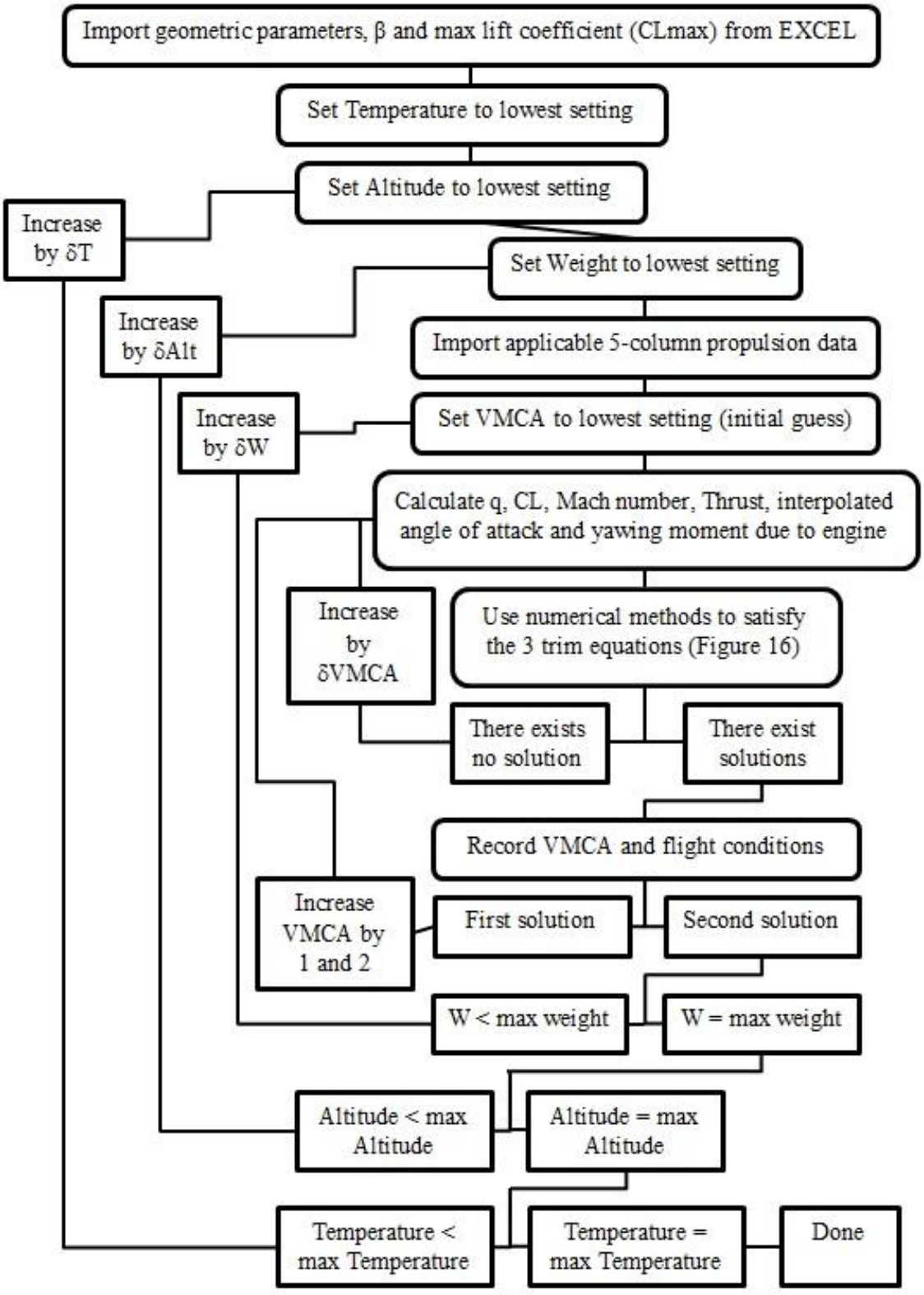

Figure 15. Flowchart of Solving for VMCA

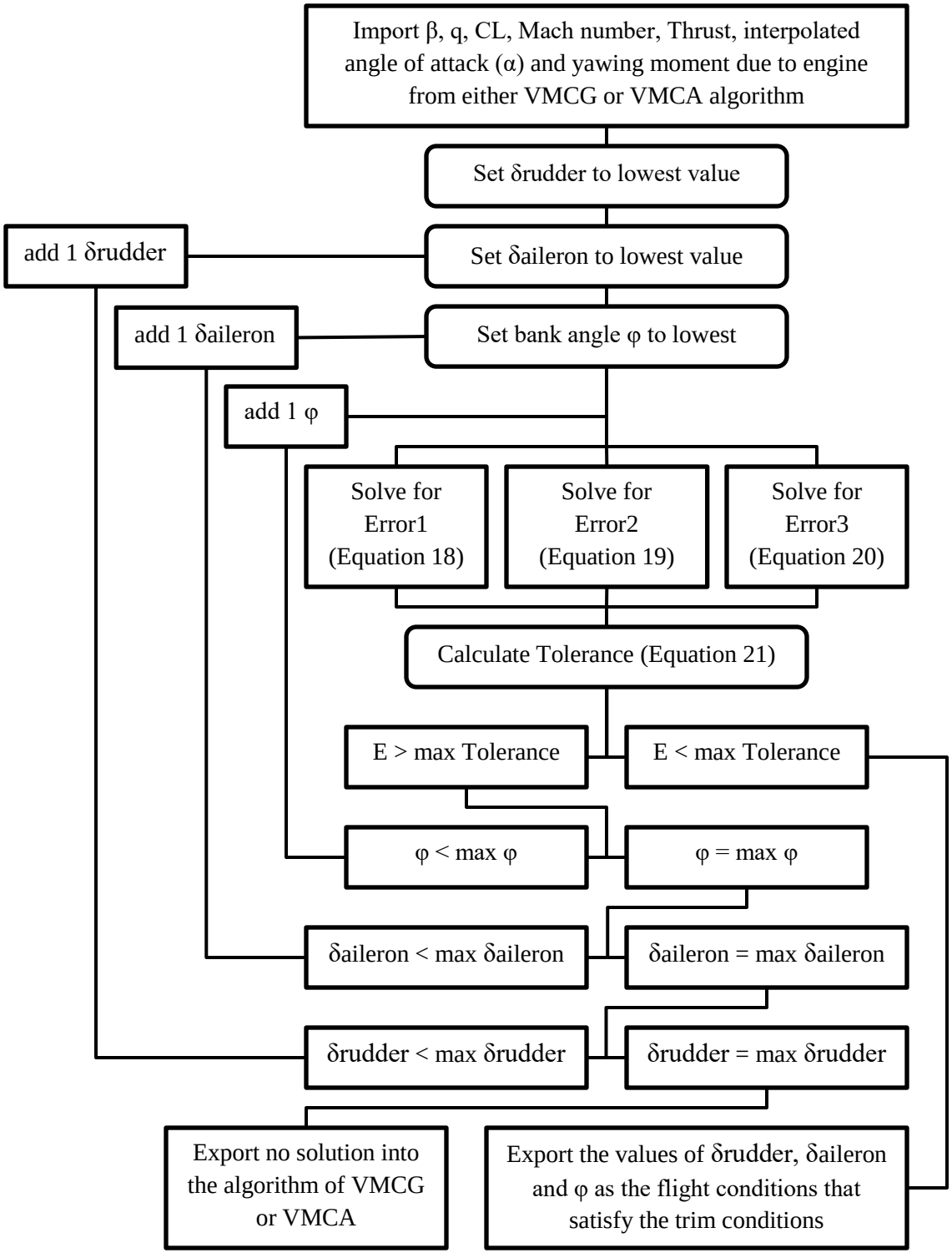

Figure 16. Algorithm Used to Satisfy the Three Trim Equations

When calculating VMCG, the thrust generated by the operative engine must be the full Thrust available, this same constraint is in effect when calculating VMCA, therefore the Thrust is dependent on the temperature and altitude. Figure 15 is a flowchart on how the algorithm solves for VMCA at the varying parameters of temperature, altitude, weight, rudder deflection, aileron deflection and bank angle. Figure 15 passes information into Figure 16 which is another algorithm to just solve for the specific flight conditions needed to satisfy trim flight.

To solve for VMCA, first the code imports the geometric parameters of the airplane as well as the sideslip angle and maximum coefficient of lift (CL_{max}). Then it sets the temperature to the lowest setting of -5°C, altitude to the lowest setting of 0 ft and weight to the lowest setting of 75,600 lbm. 75,600 lbm is just over the Operational Empty Weight (OEW) of the C130J-30. Then the algorithm imports the appropriate NPSS 5-column engine data. Next it sets VMCA to the lowest setting, chosen to be 50 Knots.

Unlike VMCG, VMCA is weight dependent, thus we need to ensure that the lift being generated by the airplane is equal to the weight of the airplane. We can check this by calculating the coefficient of lift (CL). The coefficient of lift (CL) is found by Equation 17.

$$CL = \frac{Weight}{q * Sref} \quad [17]$$

Then the algorithm solves for dynamic pressure (q) (Equation 13) and the coefficient of lift (CL) (Equation 17) before moving on to solve for the other parameters, this is because if the airplane cannot generate enough lift to overcome the weight of the airplane then there is no point in solving for the other trim conditions of the airplane. If the CL calculated is less than the CL_{max} that was generated by VORLAX at the maximum angle of attack (α), then the algorithm increases the VMCA by an increment δVMCA of 1 Knot, until CL is greater than or equal to CL_{max}.

Once the lowest VMCA that correlates to a sufficient CL is found, the algorithm goes on to interpolate the angle of attack (α) at which the airplane is flight to maintain the trim condition. The reason why we are not just assuming that CL is at maximum angle of attack (α) is because this may not always be the case. As we will discuss later on in the results section of this paper, at low weights, altitude, and cold temperatures the maximum angle of attack (α) does not produce a fulling trimmed solution. Although the airplane may be generating enough lift, there is also stall of the wings and diminished control power of the control surfaces that occur at high angles of attack (α). Therefore a CL may be produced at different combinations of airspeeds and angles of attack (α). Each stability derivative is dependent on the angle of attack (α), and consequently must be tracked to find the appropriate angle of attack (α) dependent stability derivative.

Once the angle of attack (α) has been interpolated, the algorithm then solves for the Mach number (Equation 14) and interpolates the asymmetric Thrust generated by the

counter operative engine. Just like VMCG, the algorithm also calculates the YMengine using Equation 15.

Now that all of these parameters for this specific guess of VMCA have been calculated or interpolated, the algorithm passes this information into Figure 16 to numerically solve for any flight conditions that will satisfy the three trim equations, namely Equations 18, 19 and 20.

In order for the airplane to be trimmed it must counter and balance the asymmetric force produced by the engine. There are three trim equations that are developed to satisfy the condition of balancing forces and moments that are represented in the free body diagrams (Figure 17, Figure 18 and Figure 19).

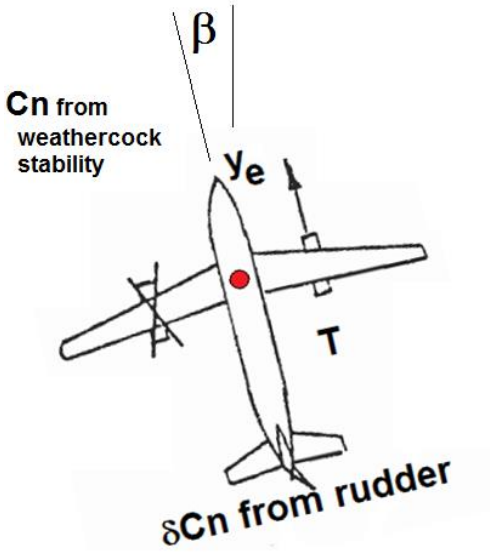

Figure 17. Force and Yawing Moment Balance for Calculating VMCA[14]

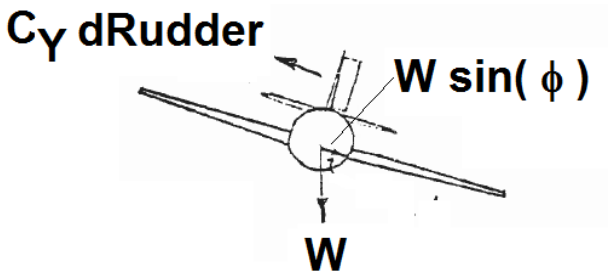

Figure 18. Side Force Balance for Calculating VMCA[14]

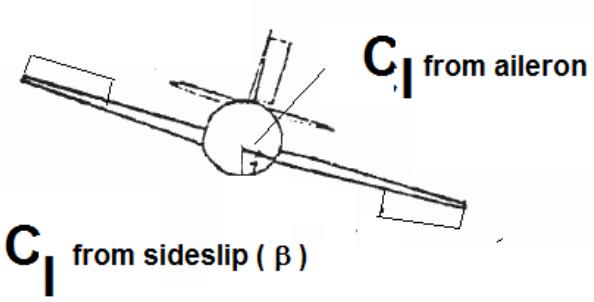

Figure 19. Rolling Moment Balance for Calculating VMCA[14]

Looking at the free body diagram represented in Figure 17, the equation developed to balance the yawning moments is seen in Equation 18.

$$Error1 = \frac{\partial Cn}{\partial \beta}(\alpha) * \beta + \frac{\partial Cn}{\partial \theta rudder}(\alpha) * \theta rudder + \frac{\partial Cn}{\partial \theta aileron}(\alpha) * \theta aileron - YM_{engine} \quad [18]$$

Looking at the free body diagram represented in Figure 18, the equation developed to balance the side forces is seen in Equation 19.

$$Error2 = \frac{\partial CY}{\partial \beta}(\alpha) * \beta + \frac{\partial CY}{\partial \theta rudder}(\alpha) * \theta rudder + \frac{\partial CY}{\partial \theta aileron}(\alpha) * \theta aileron + \sin(\varphi) * \frac{Weight}{q * S_{ref}} \quad [19]$$

Looking at the free body diagram represented in Figure 19, the equation developed to balance the rolling moments is seen in Equation 20.

$$Error3 = \frac{\partial Cl}{\partial \beta}(\alpha) * \beta + \frac{\partial Cl}{\partial \theta rudder}(\alpha) * \theta rudder + \frac{\partial CY}{\partial \theta aileron}(\alpha) * \theta aileron \quad [20]$$

The left hand sides of all three of these equations are named *Error1*, *Error2* and *Error3* respectively because these equations are being solved numerically, hence will never equal exactly zero. Therefore an artificial threshold of accuracy constrains these three trim equations. This artificial constraint is defined as the *Tolerance* and is calculated by Equation 21. The airplane is considered trimmed if the *Tolerance* is under the tolerance threshold of 0.0001.

$$Tolerance = Error1^2 + Error2^2 + Error3^2 \quad [21]$$

If *Tolerance* is greater than the threshold of 0.0001 then Figure 16 shows that "no solution" will be passed back into Figure 15. This means that the algorithm will then increase the guessed VMCA by an increment δVMCA of 1. Then the algorithm will recalculate the dynamic pressure (q), coefficient of lift (CL), Mach number (M), interpolated Thrust, interpolated angle of attack (α) and yawing moment due to the operative engine YMengine.

After these new calculated parameters have been found, the algorithm passes them back into Figure 16. This process of increasing the VMCA by δVMCA will continue until there is a solution that can be found to satisfy the three trim equations Equation 18, 19 and 20 in such a way that the Tolerance calculated in Equation 21 is under the preset threshold of 0.0001. At the point that there is a flight configuration that satisfies this condition, Figure 16 will pass the "there exists a solution" to the main VMCA algorithm of Figure 15.

Once a solution exists, the algorithm will record all of the possible flight configurations that satisfy the three trim equations and the tolerance equation. To observe any trends or develop a better understanding on the flight conditions required to fly trimmed, the algorithm then increases the VMCA by 1 and 2 to record all of the flight conditions just past the minimal controllable airspeed. These trends will be discussed later on in the results section.

After recording all of the flight conditions of VMCA and VMCA plus 1 and 2, the algorithm then increases the weight of the airplane an increment δW of 5,000 pounds. Due to the fact that VMCA is dependent on weight, it is important to not just calculate VMCA at the lowest weight, but to see how this speed varies as the weight varies. At this new weight the algorithm loops through all that has been done at the lowest setting of weight, namely calculates VMCA, and records all of the flight conditions for VMCA and VMCA plus 1 and 2.

As in the algorithm of VMCG, VMCA is dependent on altitude. However unlike VMCG, VMCA is to be calculated at all flight conditions, thus the increment δAlt used in the calculation of VMCA is 2,000 ft. At this new altitude the algorithm loops through all that has been done at the lowest setting of altitude, namely loops through all weights, calculates VMCA, and records all of the flight conditions for VMCA and VMCA plus 1 and 2.

The final parameter that VMCA is dependent on is the outside temperature. Therefor after the algorithm loops through all of the different altitudes, the algorithm increases the temperature by an increment δT of 10°C, just as it does for VMCG. At this new temperature the algorithm loops through all that has been done at the lowest setting of temperature. This includes looping through all the weights then altitudes to find VMCA and records all of the flight conditions for VMCA and VMCA plus 1 and 2.

Once all of the weights, altitudes and temperatures have been looped through, and all of the flight conditions have been recorded for VMCA and VMCA plus 1 and 2, the post processing section can begin. This post processing section is used to calibrate the algorithm and compare to known values of VMCG and VMCA of various airplanes. The next section will demonstrate the accuracy of this algorithm for both the Airbus A320 and the Super Hercules C130J-30.

Chapter 6: Calibration of Test Cases

To check and make sure that the algorithm is working, we ran the algorithm to simulate the Airbus A320 as well as the Lockheed C130J-30. First we will discuss the calibration of the algorithm to the Airbus A320.

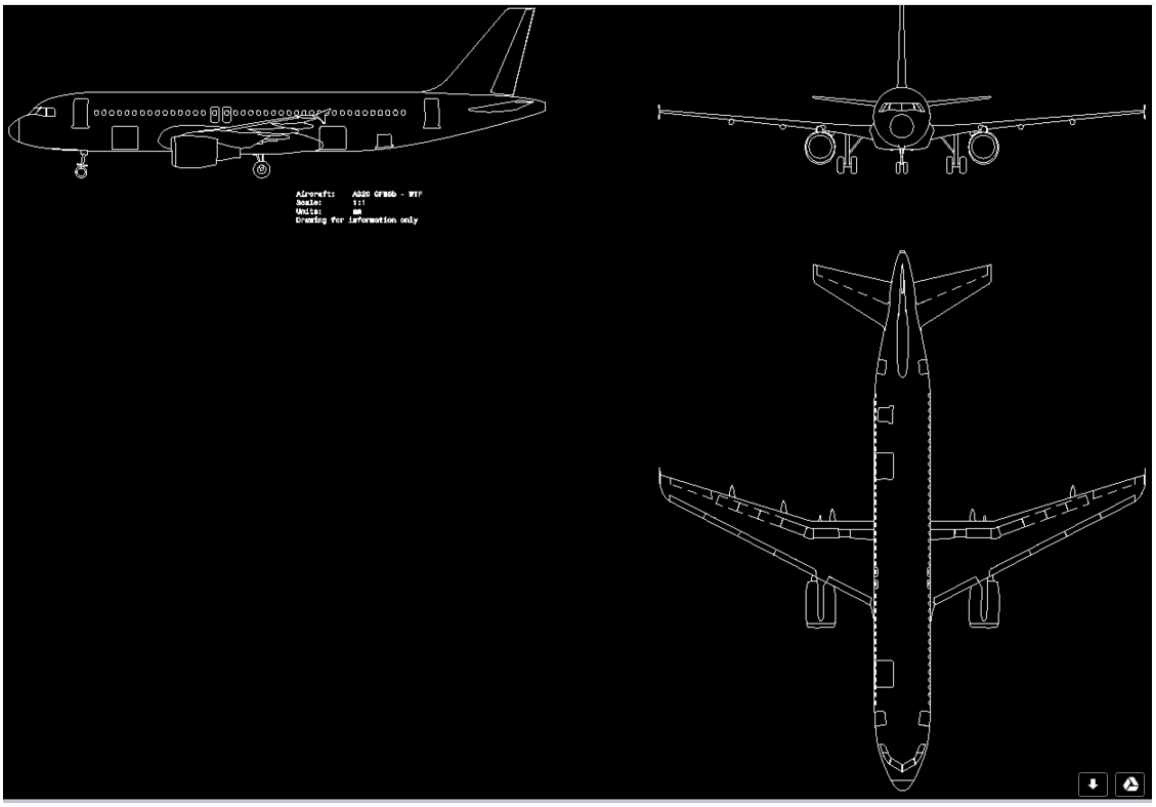

Figure 20. Line Art of Airbus A320[15]

As Figure 5 suggests, the first thing we did was gather line art and geometric values for the Airbus A320. Figure 20 is some line art found from "*Jane's All the World's Aircraft*". From this line art and easily accessible information found on the internet about

the A320[16], the inputs used for the Airbus A320 that were inputted into the master EXCEL Inputs sheet (Figure 6) are:

Asymmetric Engine location (ye) = 16 ft

Reference Wing Area (S_{ref}) = 190080 in^2

Reference Chord (CBAR) = 132 in

Longitudinal Center of Gravity (XBAR) = 680 in

Vertical Center of Gravity (ZBAR) = 0

Reference Span (WSPAN) = 1343 in

15 geometrical panels glued together to represent the line art (Figure 21).

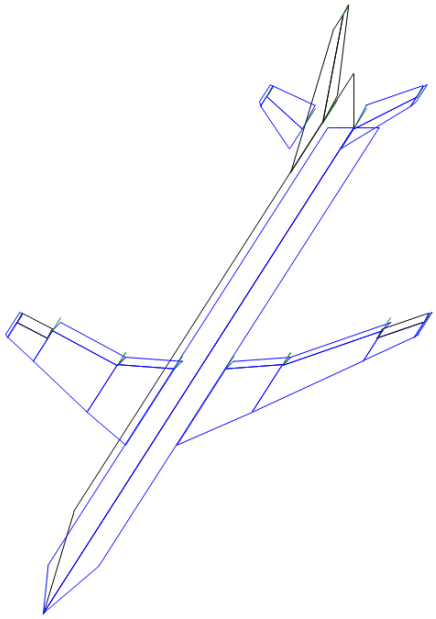

Figure 21. Isometric View of the A320 Represented by 15 Geometric Panels

After the algorithm generates the five individual input files, the algorithm passes them through VORLAX to obtain the basic performance parameters, as well as the stability derivatives. Airplane performance can be represented in many ways; we have

chosen to represent them by three different plots, namely CL vs α (Figure 22), CD vs CL (Figure 23) and Cm vs CL (Figure 24).

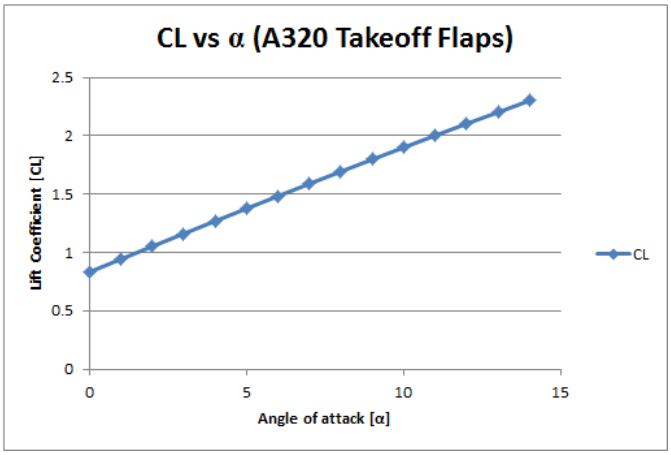

Figure 22. Coefficient of Lift (CL) Vs Angle of Attack (α) for A320 (Takeoff Flaps)

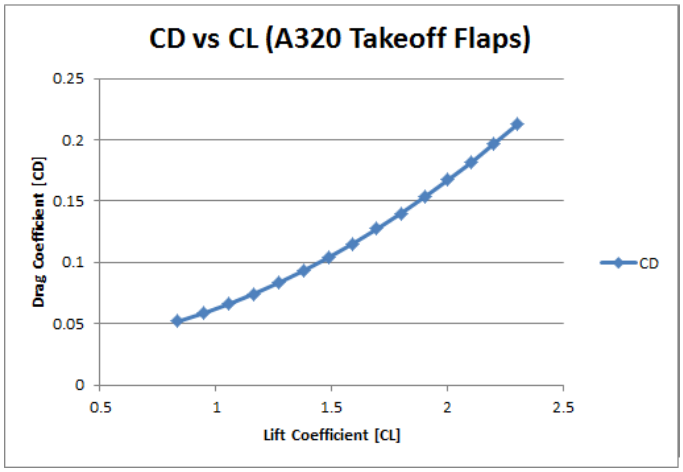

Figure 23 Coefficient of Drag (CD) Vs Coefficient of Lift (CL) for A320 (Takeoff Flaps)

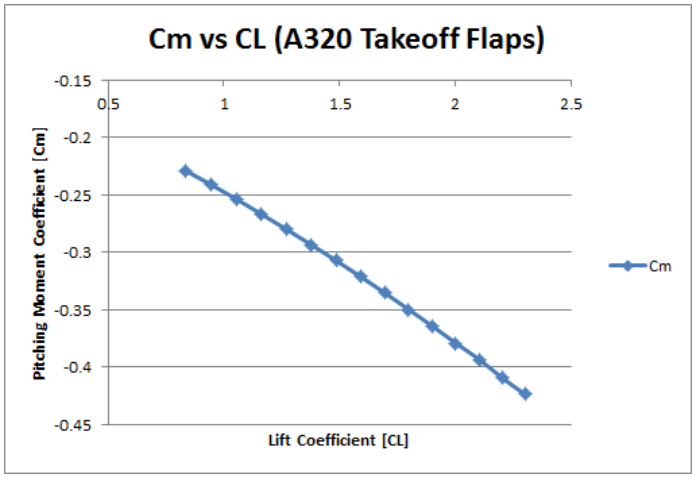

Figure 24. Pitching Moment Coefficient (Cm) Vs Coefficient of Lift (CL) for A320 (Takeoff Flaps)

Additionally to the performance plots above, we have also plotted the stability derivatives as a function of angle of attack (α). We found that the elevator actually gives no contribution to the trim equations developed earlier (Equations 18-20), thus the plots of the elevator stability derivatives will not be represented here, for it is extraneous information that does not help us in solving for VMCG or VMCA, nor calibrating the algorithm. Therefore the stability derivatives presented here are: $\delta Cn/\delta\beta$ vs α (Figure 25), $\delta Cl/\delta\beta$ vs α (Figure 26), $\delta CY/\delta\beta$ vs α (Figure 27), $\delta Cn/\delta\theta$aileron vs α (Figure 28), $\delta Cl/\delta\theta$aileron vs α (Figure 29), $\delta CY/\delta\theta$daileron vs α (Figure 30), $\delta Cn/\delta\theta$rudder vs α (Figure 31), $\delta Cl/\delta\theta$rudder vs α (Figure 32) and $\delta CY/\delta\theta$rudder vs α (Figure 33).

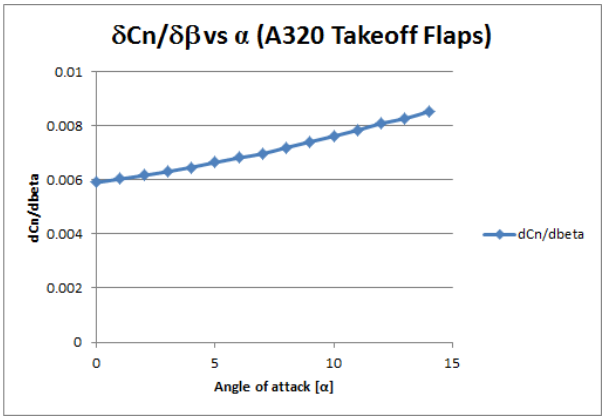

Figure 25. δCn/δβ Vs Angle of Attack (α) for A320

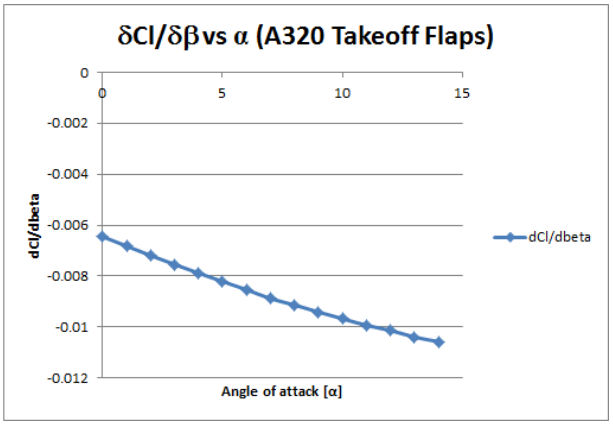

Figure 26. δCl/δβ Vs Angle of Attack (α) for A320

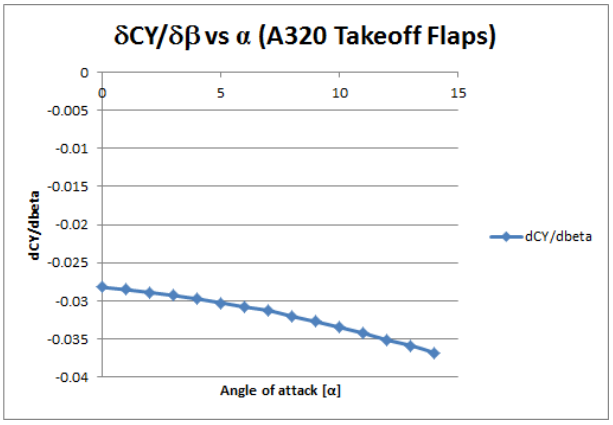

Figure 27. δCY/δβ Vs Angle of Attack (α) for A320

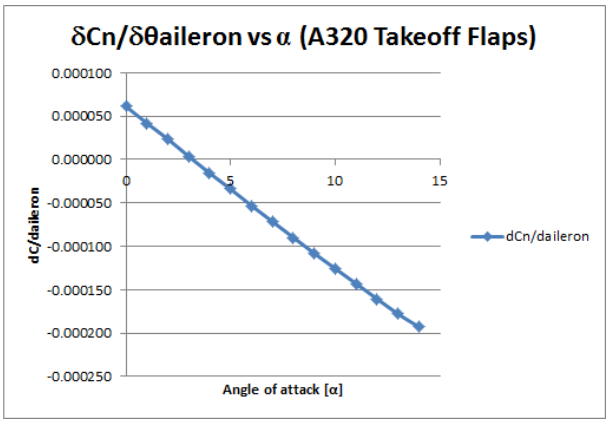

Figure 28. δCn/δθaileron Vs Angle of Attack (α) for A320

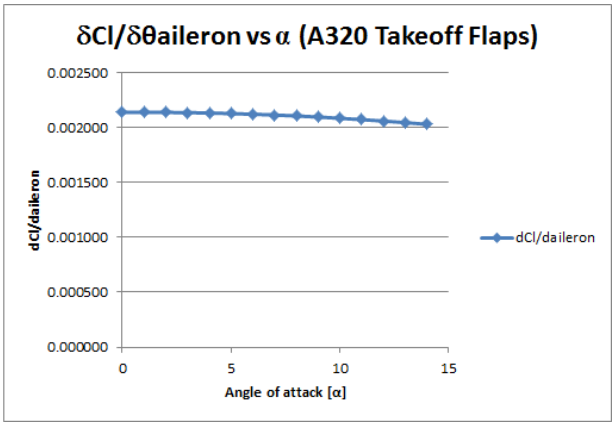

Figure 29. δCl/δθaileron Vs Angle of Attack (α) for A320

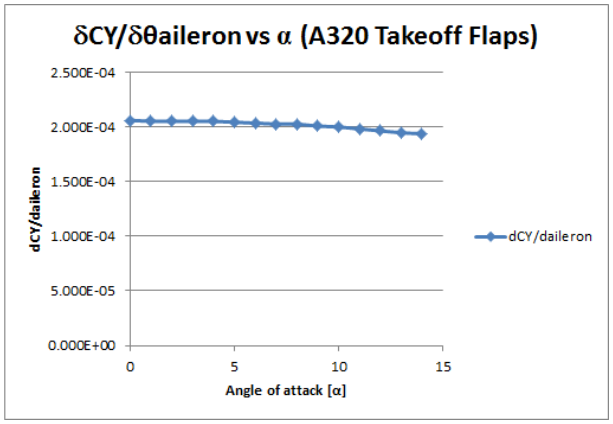

Figure 30. δCY/δθaileron Vs Angle of Attack (α) for A320

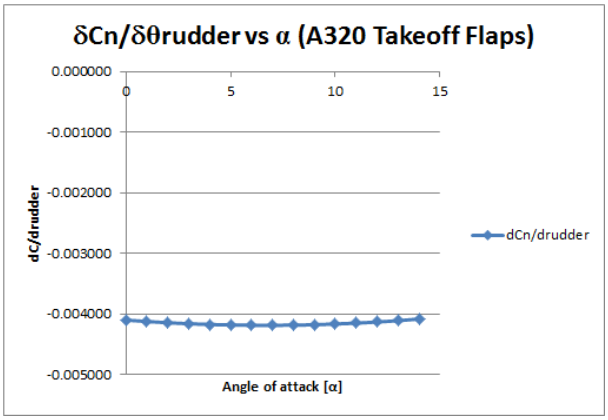

Figure 31. δCn/δθrudder Vs Angle of Attack (α) for A320

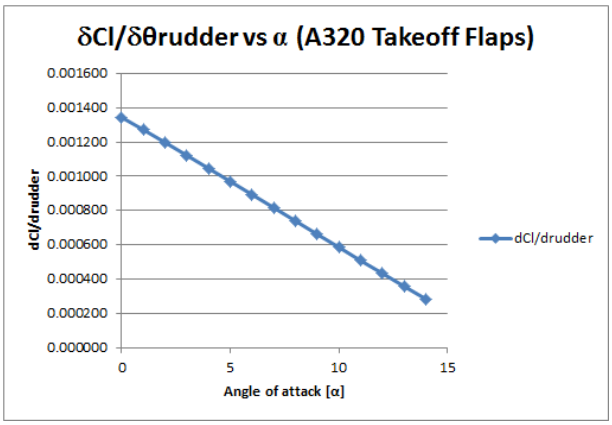

Figure 32. δCl/δθrudder Vs Angle of Attack (α) for A320

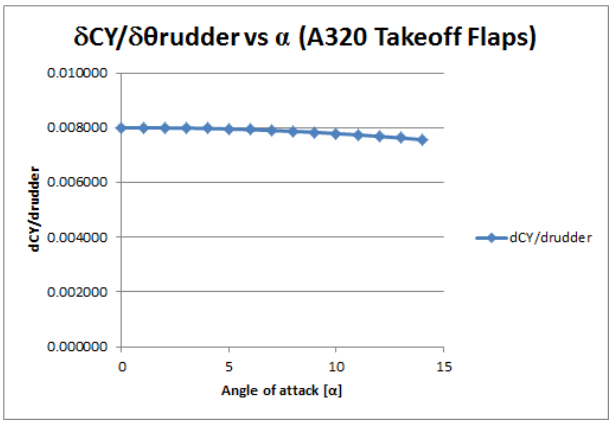

Figure 33. δCY/δθrudder Vs Angle of Attack (α) for A320

According to the Airbus A320 manual, these performance parameters and stability derivatives appear to match the actual parameters. This shows that the input files generated and VORLAX output values are accurate enough. Therefore we can move on to calculating and comparing VMCG and VMCA.

The Airbus manual only gives a single value for a VMCG equivalent speed named V1, recorded at the "worst case" temperature and a range of altitudes. 14 CFR § 25.107 (a.2)[17] states that V1 is calculated as VMCG plus a few extra Knots to allow the pilot to react in time to the engine failure. As in all engineering applications that involve human interaction, there is a delay in reaction time and action taken to correct any error. Figure 34 is a table of the V1 values mentioned earlier. For purposed of comparison to VMCG values calculated by the algorithm we will refer to Figure 35, a plot of "Comparable VMCG" values vs altitude. "Comparable VMCG" values are found by subtracting 2 Knots from the posted V1 values found in Figure 34.

A319/A320/A321 VIETNAM AIRLINES FLIGHT CREW OPERATING MANUAL	TAKEOFF	2.02.25	P 1
	MINIMUM SPEEDS	SEQ 160	REV 38

SPEEDS LIMITED BY VMC

Takeoff speeds all have a minimum value limited by control. These minimum values are given in the tables down below.

R

MINIMUM V1												
CONF	PRESSURE ALTITUDE (FT)											
	-1000	0	1000	2000	3000	4000	5000	6000	8000	9200	12000	14100
1+F	115	115	114	112	110	109	107	105	101	100	100	100
2	115	115	114	112	110	109	107	105	101	100	100	100
3	113	113	112	110	109	107	105	103	100	100	100	100

R

MINIMUM VR												
CONF	PRESSURE ALTITUDE (FT)											
	-1000	0	1000	2000	3000	4000	5000	6000	8000	9200	12000	14100
1+F	121	121	119	118	116	113	111	109	106	103	100	100
2	121	121	119	118	116	113	111	109	106	103	100	100
3	119	119	117	116	114	112	110	108	104	102	100	100

R

MINIMUM V2												
CONF	PRESSURE ALTITUDE (FT)											
	-1000	0	1000	2000	3000	4000	5000	6000	8000	9200	12000	14100
1+F	126	126	124	122	120	117	115	113	109	106	100	100
2	125	125	123	121	119	117	114	112	108	106	100	100
3	125	125	123	121	119	117	115	112	108	106	100	100

V2 LIMITED BY VMU/VMCA

The following tables, one per configuration, provide the V2 limited by minimum unstick speed and minimum control speed in the air.

Figure 34. Vietnam Airline A320 Performance Book Values for V2 and V1[18]

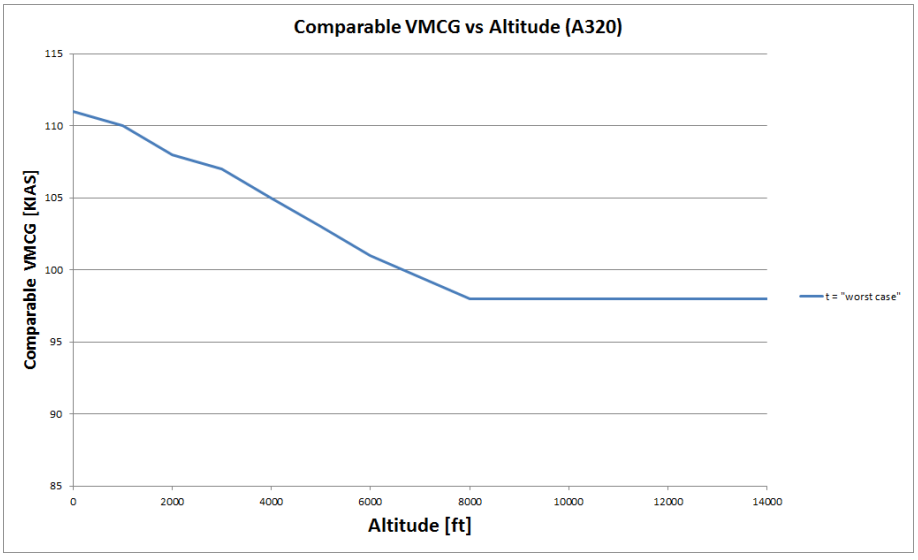

Figure 35. Vietnam Airline A320 "Comparable VMCG" Vs Altitude of A320

On the other hand, we have developed an algorithm to loop through temperatures and altitudes. Figure 36 is a plot of VMCG vs Altitude at five different temperatures; whereas Figure 37 is a plot of VMCG vs Temperature at six different altitudes. The values we will be comparing are the "t = ISA -20" values from Figure 36, this is because this is the "worst case" temperature of the algorithm and the values form Figure 35 are at the "worst case" temperature.

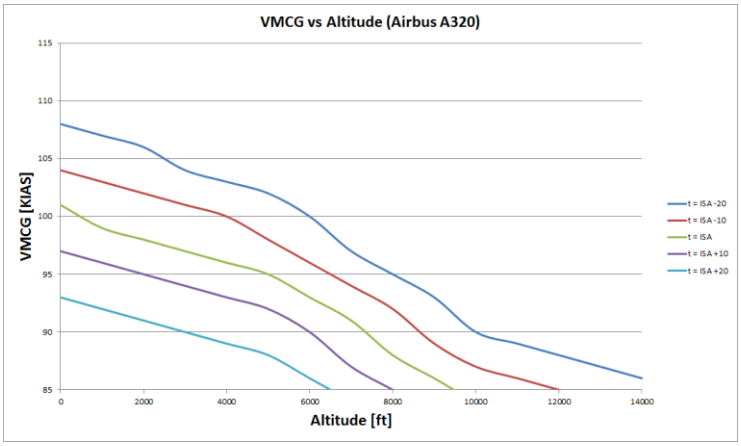

Figure 36. VMCG Vs Altitude at Five Different Temperatures for A320

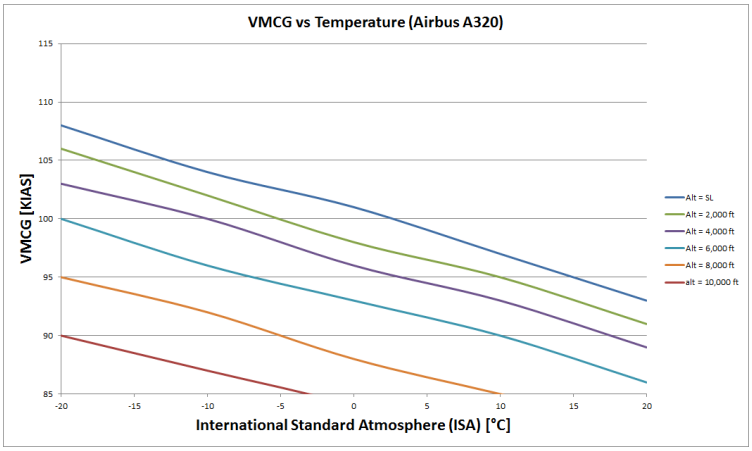

Figure 37. VMCG Vs Temperature at Six Different Altitudes for A320

We can see from Figure 36 that the calculation of VMCG that we have done is very close to the given values for the Airbus A320 at the appropriate altitude and temperature. This means that the calibration for VMCG is verified for the Airbus A320. Now we need to see if the VMCA portion of the algorithm can predict the flight manual values of VMCA for the Airbus A320.

Once again the Airbus A320 manual only gives a single chart for a speed dependent on VMCA, called V2. 14 CFR § 25.107[19] states that V2 is calculated as 1.10 times VMCA. This means by looking at Figure 34 we can calculate the VMCA by dividing the values of V2 by 1.10. Figure 38 is a plot of the VMCA values posted and derived from the provided A320 data, whereas Figure 39 is the calculated VMCA values fond by this algorithm.

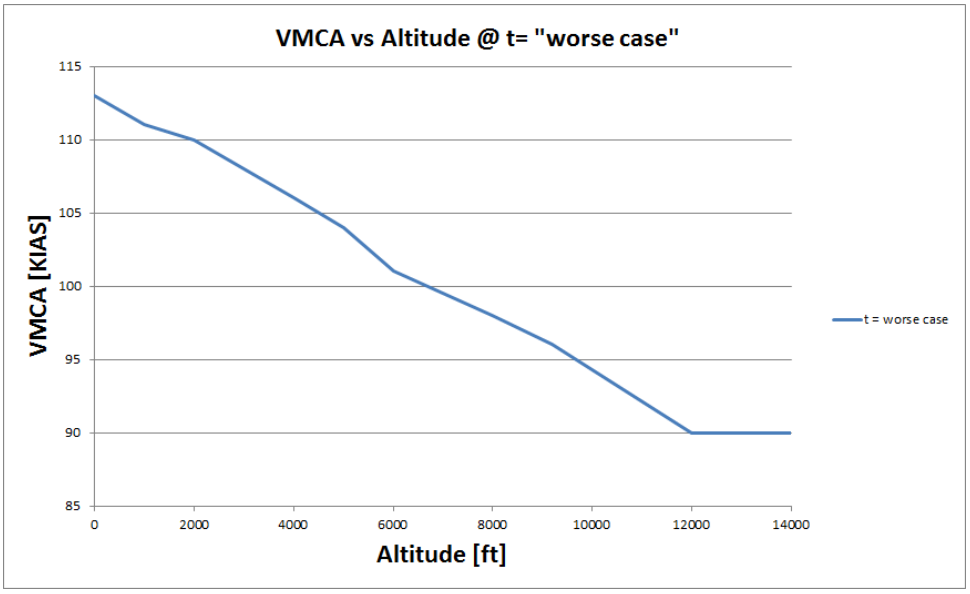

Figure 38. VMCA Vs Weight at “Worse Case” Temperature”

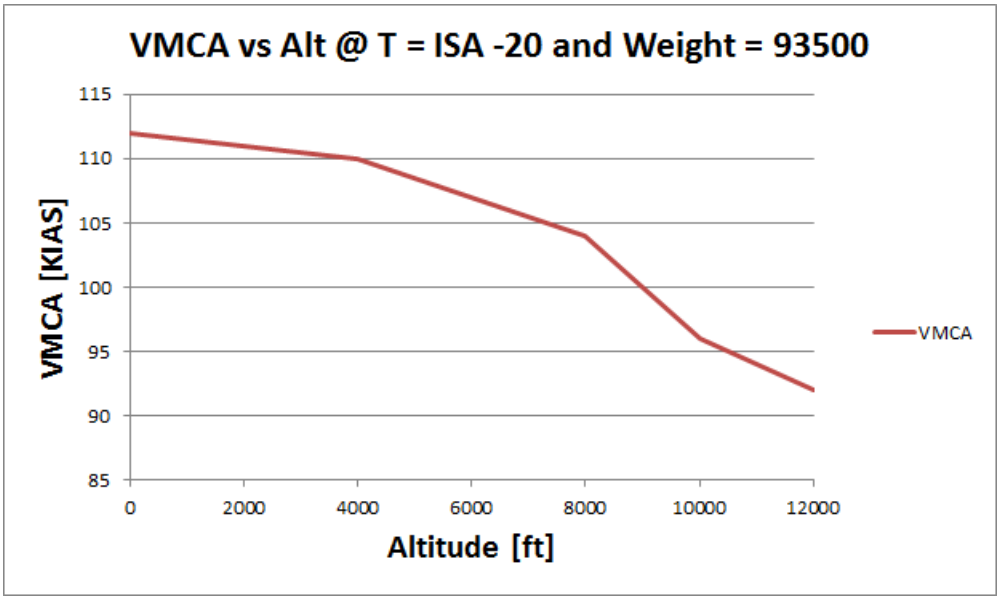

Figure 39. VMCA Vs Weight at T = ISA -20 for A320

The values found from the algorithm are close to those that are found in the Airbus A320 flight manual. The values differ very little at sea level and high altitudes, but deviate from each other at intermediate altitudes. This is most likely due to the fact that the stability derivatives are linearized from maximum deflection to no deflection.

Now that we have validated the algorithm using the Airbus A320, we will check to see if we can also validate the code using another airplane, specifically the Lockheed C130J-30. Obviously there are many things that could of "coincidently" lead to the values of the algorithm matching the Airbus A320, therefor having a second validation is crucial if we are going to state that this algorithm applies to all airplanes. We have chosen the C130J-30 because it has some distinct differences from the Airbus A320. The Lockheed C130J-30 has very little to no dihedral (upwards bend in the wings), turbofan

engines, and has no sweep in the wings; whereas the Airbus A320 has significant dihedral, wing sweep, and turbojet engines.

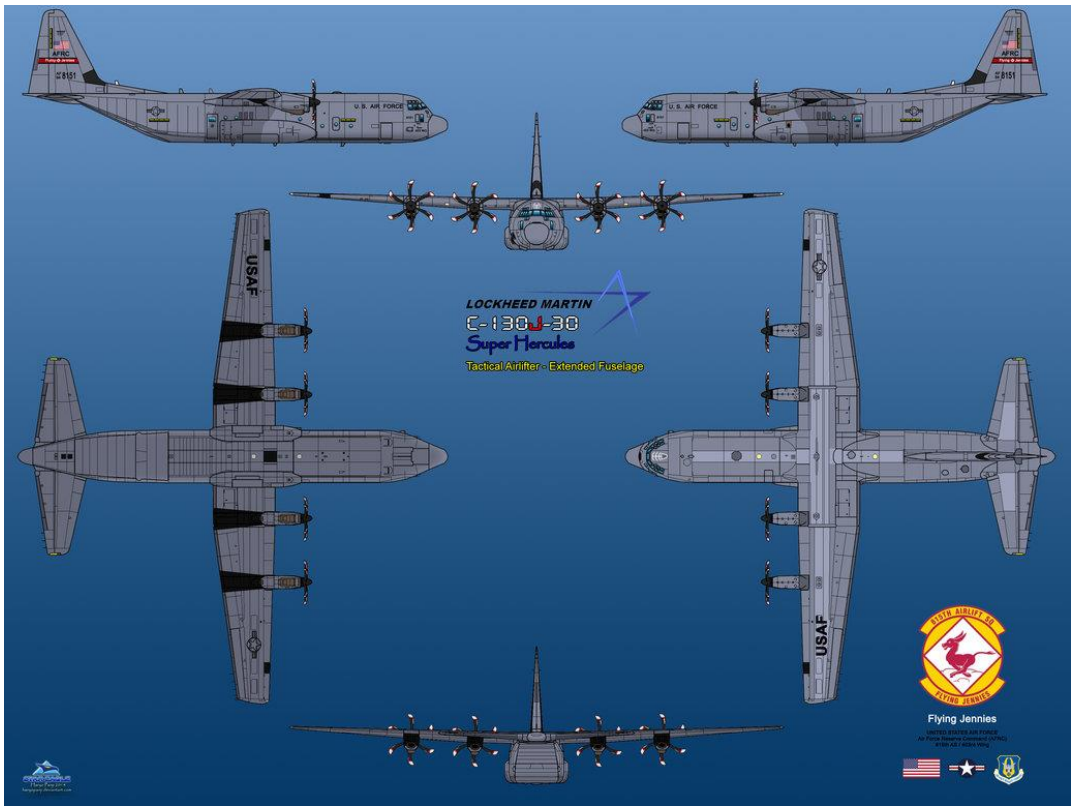

Figure 40. Line Art of Lockheed Martin C130J-30 Super Hercules[20]

Just as we did for the Airbus A320, the first thing we did was gather line art and geometric values for the Lockheed Martin C130J-30 Super Hercules. Figure 40 is some line art found from an archive of airplane posters. From this line art and easily accessible information found on the internet about the C130J-30[21], the inputs used for the Lockheed Martin C130J-30 Super Hercules that were inputted into the master EXCEL Inputs sheet (Figure 6) are:

Asymmetric Engine location (ye) = 33.3 ft

Reference Wing Area (S_{ref}) = 251280 in^2

Reference Chord (CBAR) = 149 in

Longitudinal Center of Gravity (XBAR) = 610 in

Vertical Center of Gravity (ZBAR) = 0

Reference Span (WSPAN) = 1560 in

14 geometrical panels “glued” together to represent the line art (Figure 41).

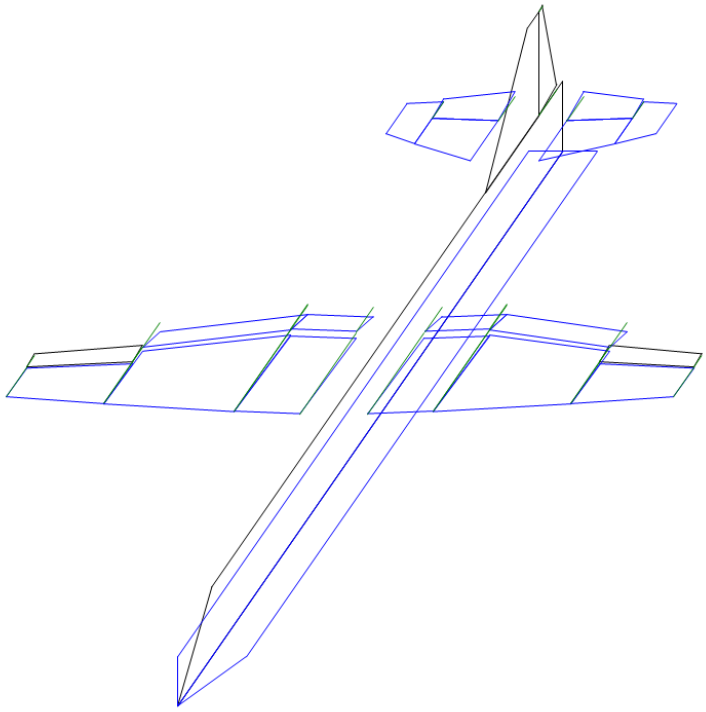

Figure 41. Isometric View of the C130J-30 Represented by 14 Geometric Panels

Once again, after the algorithm generates the five individual input files, the algorithm passes them through VORLAX to obtain the basic performance parameters, as well as the stability derivatives. The same three plots used to represent the airplane performance used in the A320 will also be used to show the performance of the C130J-30, namely CL vs α (Figure 22), CD vs CL (Figure 23) and Cm vs CL (Figure 24).

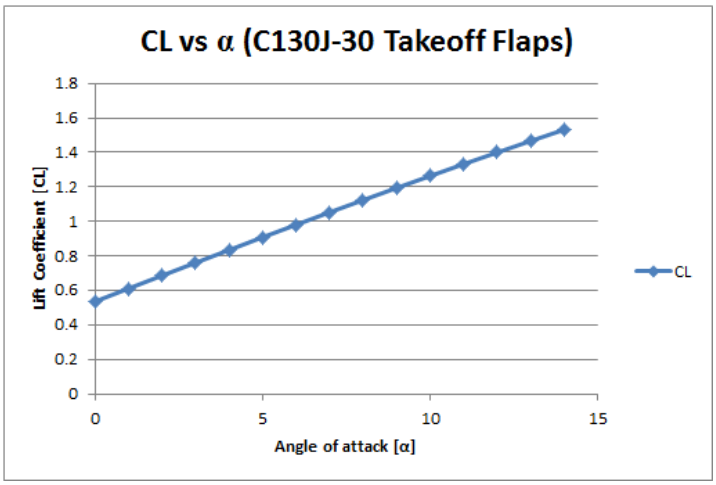

Figure 42. Coefficient of Lift (CL) Vs Angle of Attack (α) for C130J-30 (Takeoff Flaps)

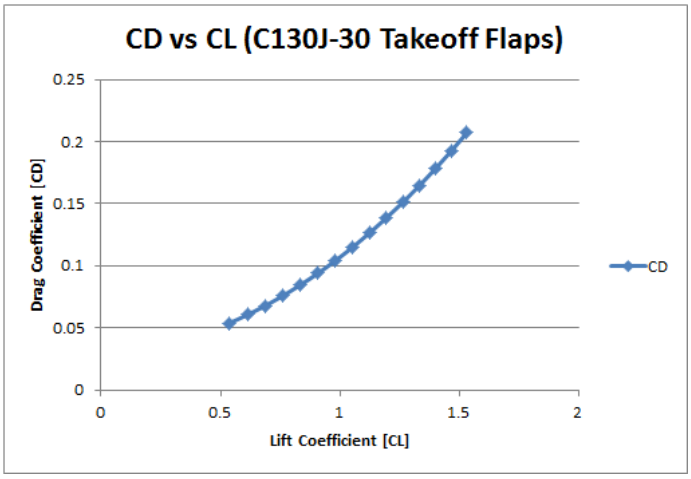

Figure 43. Coefficient of Drag (CD) Vs Coefficient of Lift (CL) for C130J-30 (Takeoff Flaps)

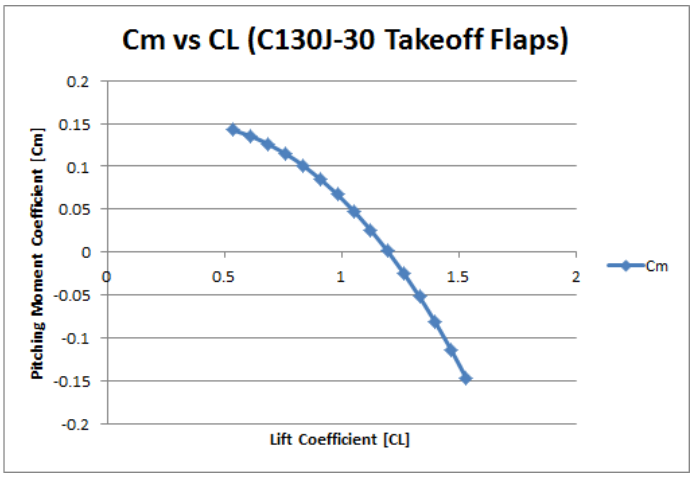

Figure 44. Pitching Moment Coefficient (Cm) Vs Coefficient of Lift (CL) for C130J-30 (Takeoff Flaps)

Additionally to the performance plots above, we have also plotted the stability derivatives as a function of angle of attack (α). Same as for the case of the A320, we found that the elevator actually gives no contribution to the trim equations developed earlier (Equations 18-20), thus the plots of the elevator stability derivatives will not be represented here, for it is extraneous information that does not help us in solving for VMCG or VMCA, nor calibrating the algorithm. Therefore the stability derivatives presented here are: $\delta Cn/\delta\beta$ vs α (Figure 45), $\delta Cl/\delta\beta$ vs α (Figure 46), $\delta CY/\delta\beta$ vs α (Figure 47), $\delta Cn/\delta\theta$aileron vs α (Figure 48), $\delta Cl/\delta\theta$aileron vs α (Figure 49), $\delta CY/\delta\theta$daileron vs α (Figure 50), $\delta Cn/\delta\theta$rudder vs α (Figure 51), $\delta Cl/\delta\theta$rudder vs α (Figure 52) and $\delta CY/\delta\theta$rudder vs α (Figure 53).

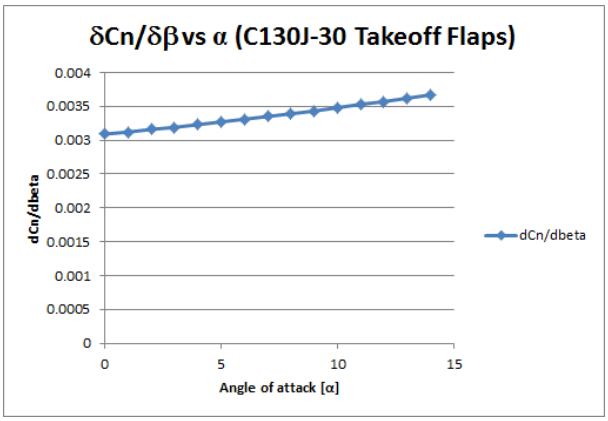

Figure 45. δCn/δβ Vs Angle of Attack (α) for C130J-30

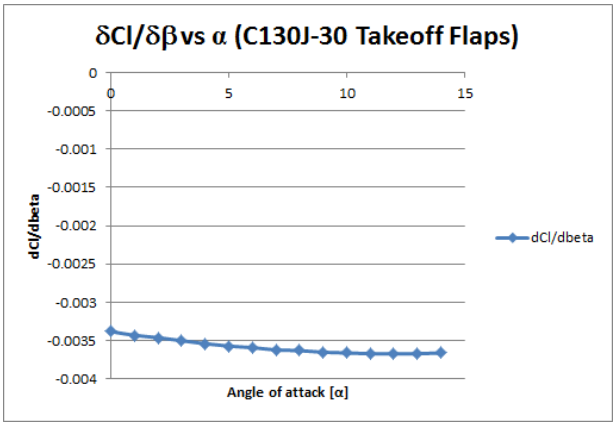

Figure 46. δCl/δβ Vs Angle of Attack (α) for C130J-30

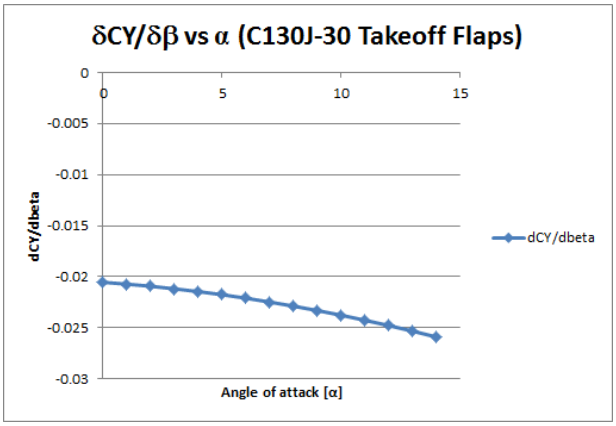

Figure 47. δCY/δβ Vs Angle of Attack (α) for C130J-30

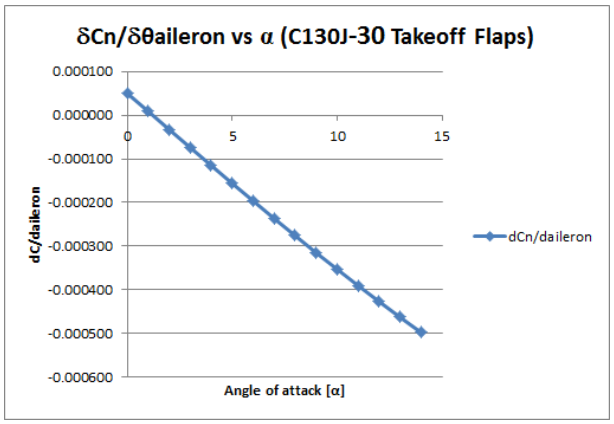

Figure 48. δCn/δθaileron Vs Angle of Attack (α) for C130J-30

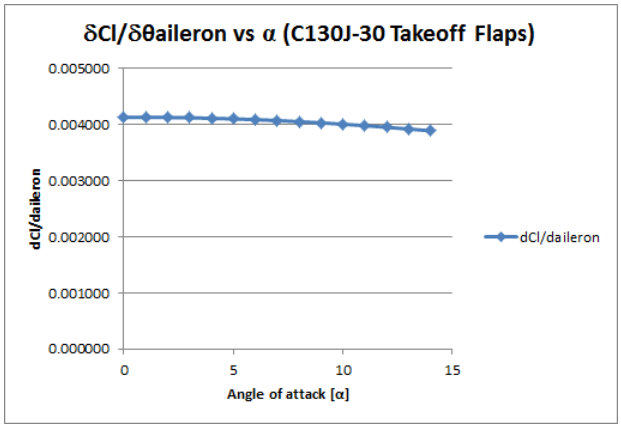

Figure 49. δCl/δθaileron Vs Angle of Attack (α) for C130J-30

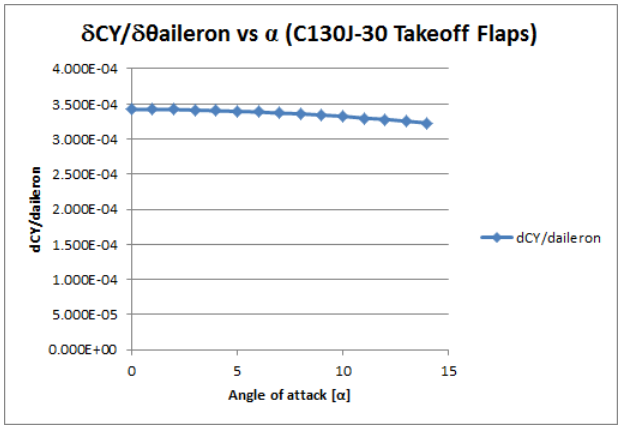

Figure 50. δCY/δθaileron Vs Angle of Attack (α) for C130J-30

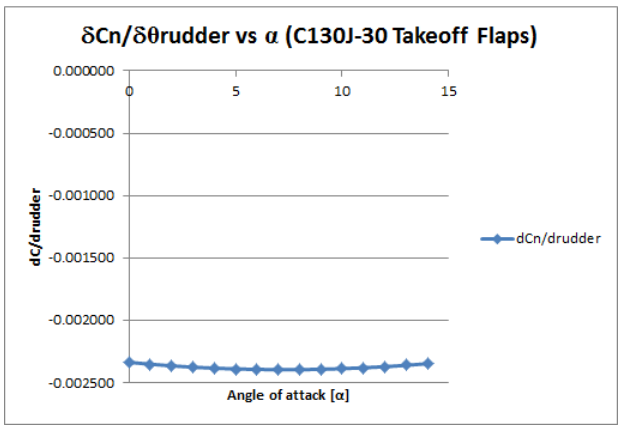

Figure 51. δCn/δθrudder Vs Angle of Attack (α) for C130J-30

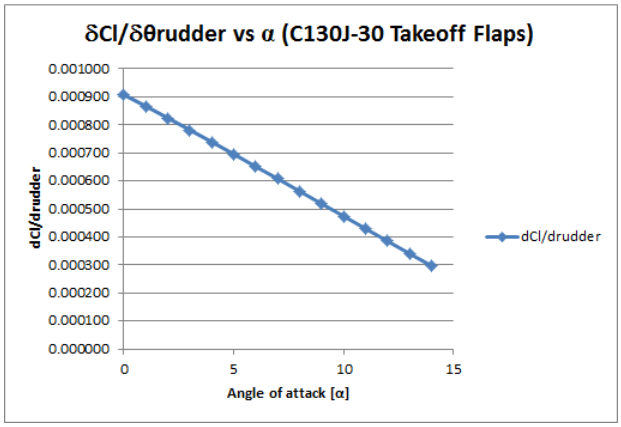

Figure 52. δCl/δθrudder Vs Angle of Attack (α) for C130J-30

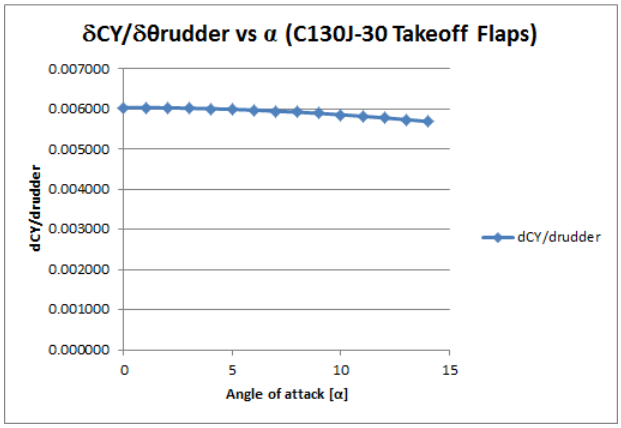

Figure 53. δCY/δθrudder Vs Angle of Attack (α) for C130J-30

These performance parameters and stability derivatives match the actual Lockheed Martin C130J-30 Super Hercules parameters. This shows that the input files generated and VORLAX output values are accurate, thus allowing us to move on to calculating and comparing VMCG and VMCA.

The C130J-30 manual only gives a multiple values of VMCG, recorded at a range of altitudes and temperature. However, unlike the A320, the C130J-30 is used for military transportation. This means that performance information on the C130J-30 are protected by The International Traffic in Arms Regulations (ITAR). "ITAR is a set of United States Government regulations on the export and import of defense related articles and services."[22] Therefore, due to ITAR, we cannot post any official figures showing the performance of the C130J-30, however we can state that the information we found using this algorithm matches closely to the performance parameters of the C130J-30.

Another reason why the C130J-30 was chosen in this work is because after the C130J-30 was manufactured and tested, it was concluded that the minimal control speeds were much higher than desired by the military. Therefore, in order to improve the minimal control speeds of the airplane, the engineers developed an "Automatic Thrust Control System (ATCS) [to] optimize the balance of power on the engines, allowing lower values of minimum control speeds and superior short-airfield performance."[23] To create the effects of the ATCS, we decided to dial back the thrust of the engine to two-thirds the full thrust.

Just as for the A320, the VMCG of the C130J-30 was found at a range of altitudes and temperatures. Figure 54 is a plot of VMCG vs Altitude at five different temperatures; whereas Figure 55 is a plot of VMCG vs Temperature at six different altitudes.

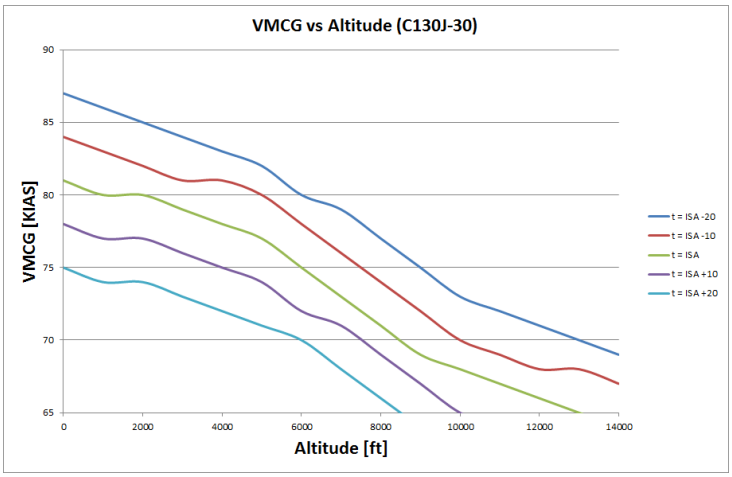

Figure 54. VMCG Vs Altitude at Five Different Temperatures for C130J-30

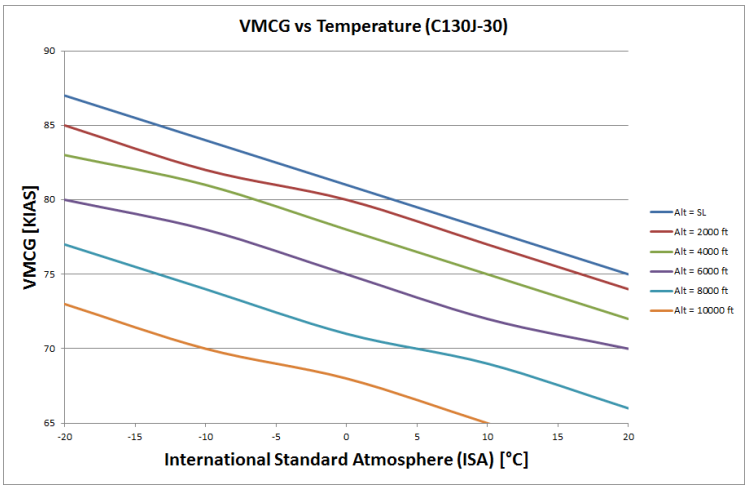

Figure 55. VMCG Vs Temperature at Six Different Altitudes for C130J-30

As previously mentioned, Figure 54 and Figure 55 closely represents the values given value for the Lockheed Martin C130J-30 Super Hercules at the appropriate altitude and temperature. This means that the calibration for VMCG is also verified for the C130J-30. Finally we have to verify the VMCA portion of the code, just as we did with the A320.

The C130J-30 manual only gives a much more complicated chart for VMCA, than that of the A320. However for the purposes of keeping the validation check consistent, we will show a plot like the one for the A320, namely at low weight, "worst temperature" and different altitudes. Figure 56 shows how the VMCA changes as a function of altitude at the temperature of ISA -20°C and low weight.

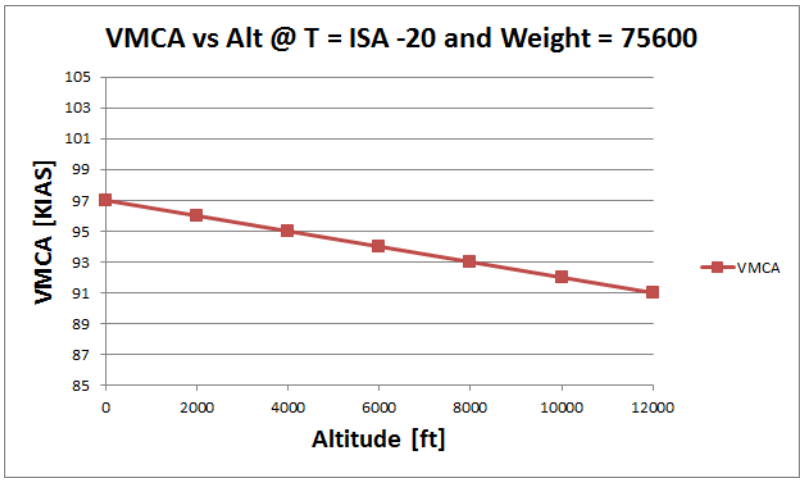

Figure 56. VMCA Vs Weight at T = ISA -20 for C130J-30

The values found from the algorithm are close to those that are found in the Lockheed Martin C130J-30 Super Hercules flight manual; therefore providing two

different validation cases for both VMCG and VMCA, using airplanes that are significantly different in geometry, design and functionality.

Now that the code has been verified for the calculation of VMCG and VMCA, we can look at patterns and trends as we discuss trade studies of simulated flight. Figure 15 shows that VMCA varies upon different parameters, it would be wise to run trade studies with these different parameters to be able to discover and trends in minimum control speed calculations.

Chapter 7: More Sophisticated Trades

In this Chapter, we will be conducting three different trade studies to show use what is happening and this will allow us to find any patterns or discover any trends. All of these trades that will be highlighted in this chapter will be conducted at a sideslip angle (β) of -3°. This sideslip angle was chosen to show the reader the vast differences in performance from one airplane to the other; implying that every individual airplane will also likely have different effects due to sideslip angle (β).

The first trade study that we conducted is one where we held the temperature the constant (15°C) and cycled through altitude and altitude. For the both the Airbus A320 and the Lockheed Martin C130J-30 Super Hercules, the altitude ranges from 0 to 12,000 ft in increments of 2,000 ft. The weight ranges from 93,500 lbm to 173,500 lbm in increments of 5,000 lbm for the A320 and from 75,600 lbm to 165,600 lbm in increments of 5,000 lbm for the C130J-30.

For this first trade we show each of the seven different altitudes in individual plots at the International Standard Atmosphere (ISA) temperature, as well as them all together one a single plot. We will show the information like this for the first trade study for the purposes of completeness. For the A320 case, Figure 57 through Figure 63 is each of the altitudes plotted in individual plots, and Figure 64 is all of them on a single plot.

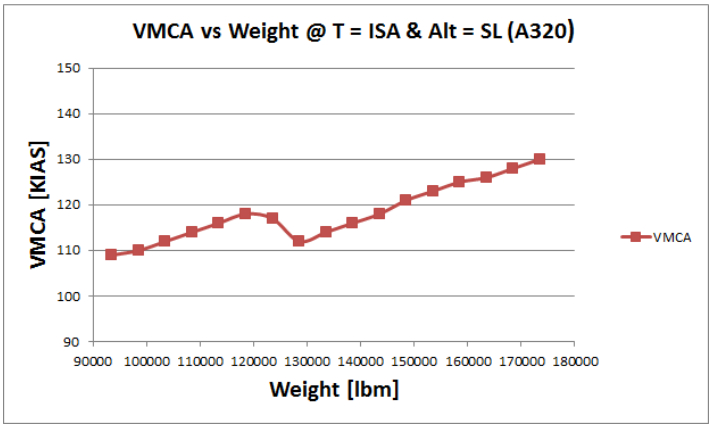

Figure 57. VMCA Vs Weight at T = ISA and Altitude = Sea Level for A320

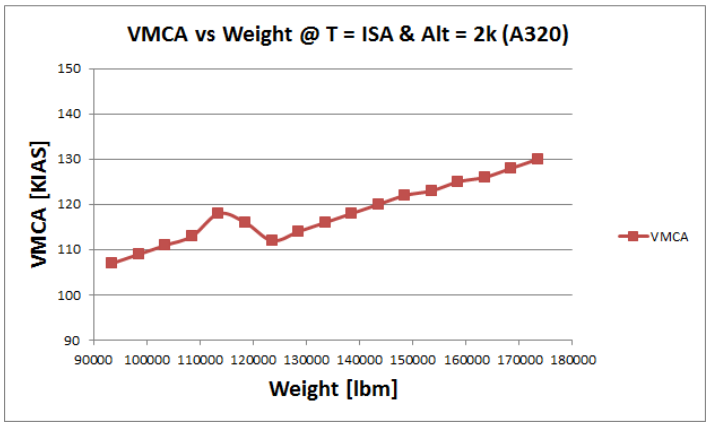

Figure 58. VMCA Vs Weight at T = ISA and Altitude = 2,000 Ft for A320

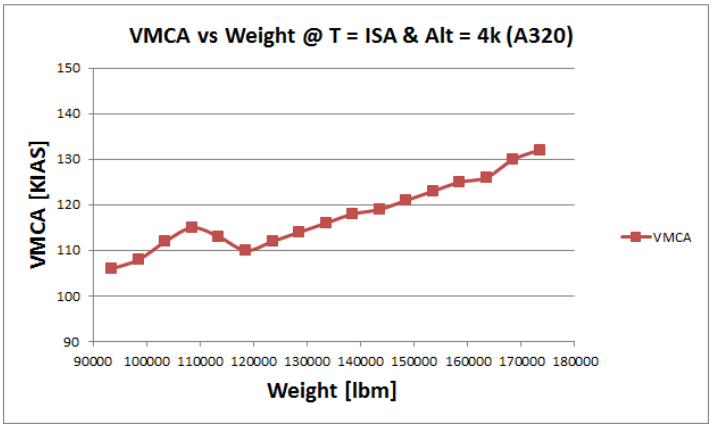

Figure 59. VMCA Vs Weight at T = ISA and Altitude = 4,000 Ft for A320

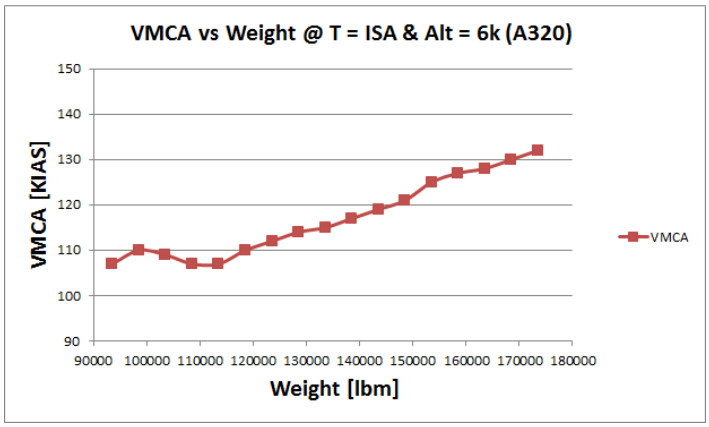

Figure 60. VMCA Vs Weight at T = ISA and Altitude = 6,000 Ft for A320

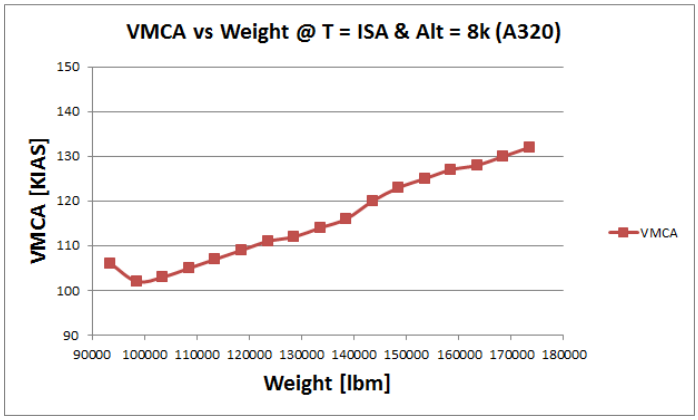

Figure 61. VMCA Vs Weight at T = ISA and Altitude = 8,000 Ft for A320

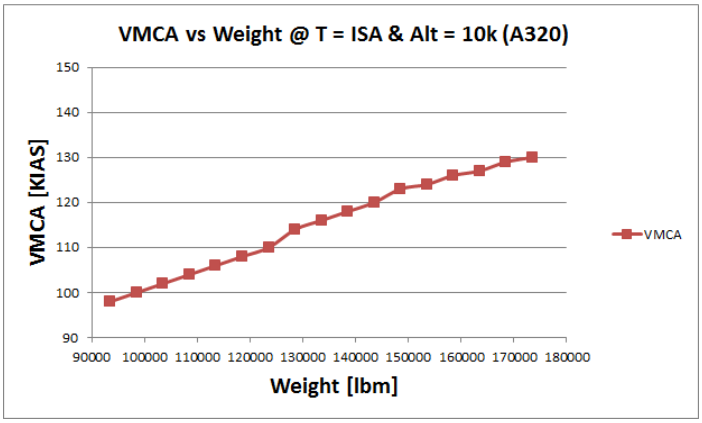

Figure 62. VMCA Vs Weight at T = ISA and Altitude = 10,000 Ft for A320

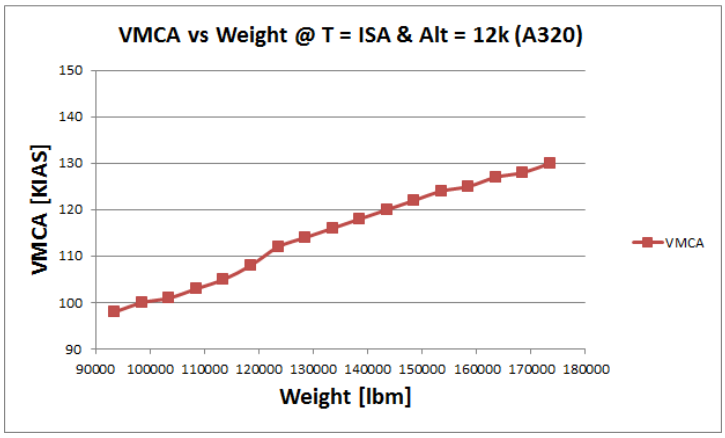

Figure 63 . VMCA Vs Weight at T = ISA and Altitude = 12,000 Ft for A320

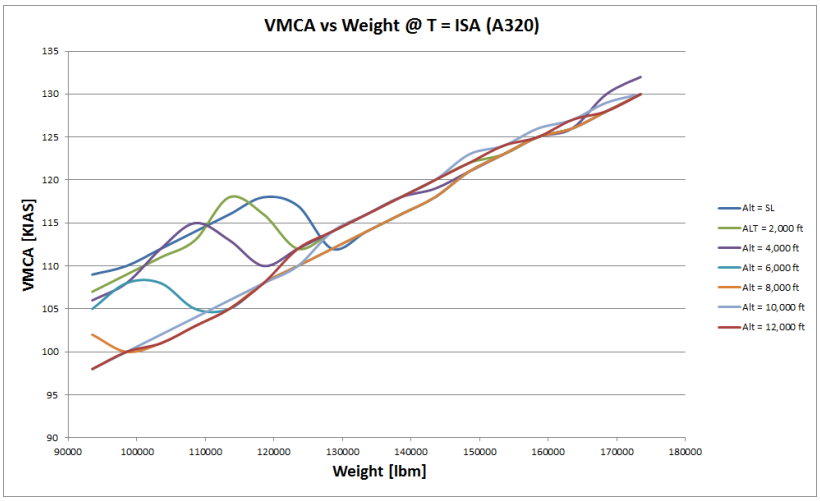

Figure 64. VMCA Vs Weight at T = ISA for A320

Before we discuss and trends or observations, we will first see how VMCA behaves for the C130J-30 airplane. This will allow us to discuss the trends between the two airplanes, and thus come up with general statements that could be applied to any airplane.

For the C130J-30 airplane, Figure 65 through Figure 71 is each of the altitudes plotted in individual plots, and Figure 72 is all of them on a single plot.

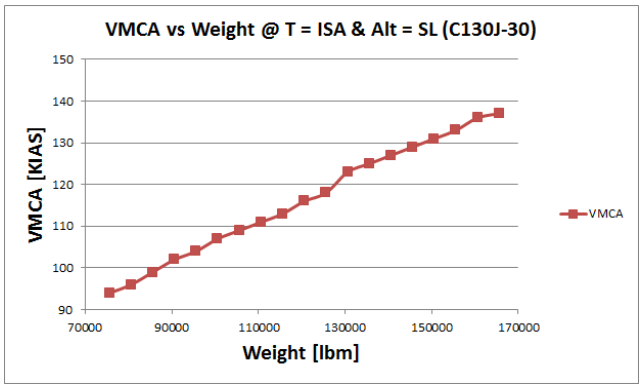

Figure 65. VMCA Vs Weight at T = ISA and Altitude = Sea Level for C130J-30

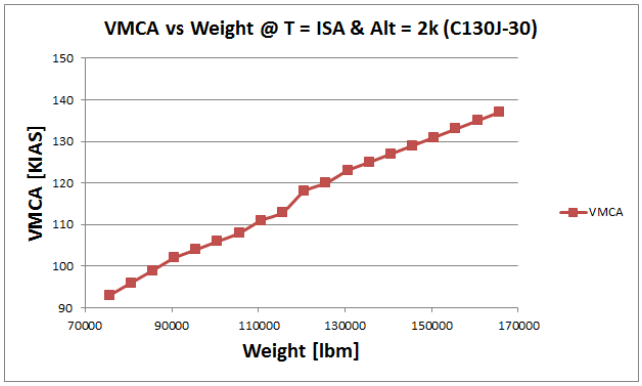

Figure 66. VMCA Vs Weight at T = ISA and Altitude = 2,000 Ft for C130J-30

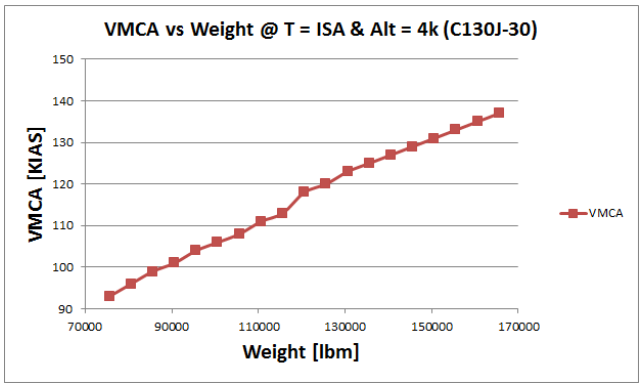

Figure 67. VMCA Vs Weight at T = ISA and Altitude = 4,000 Ft for C130J-30

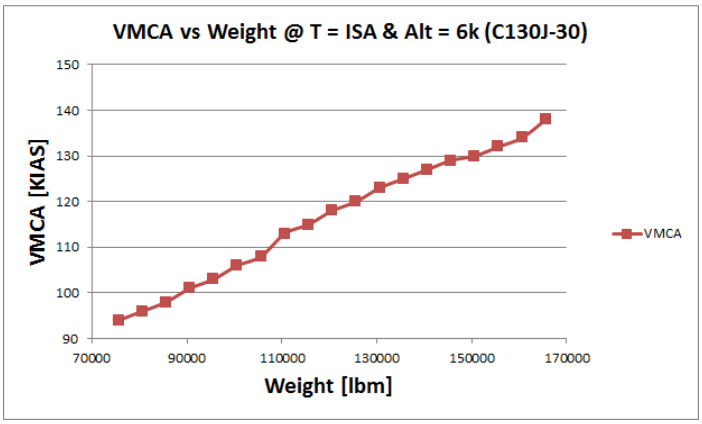

Figure 68. VMCA Vs Weight at T = ISA and Altitude = 6,000 Ft for C130J-30

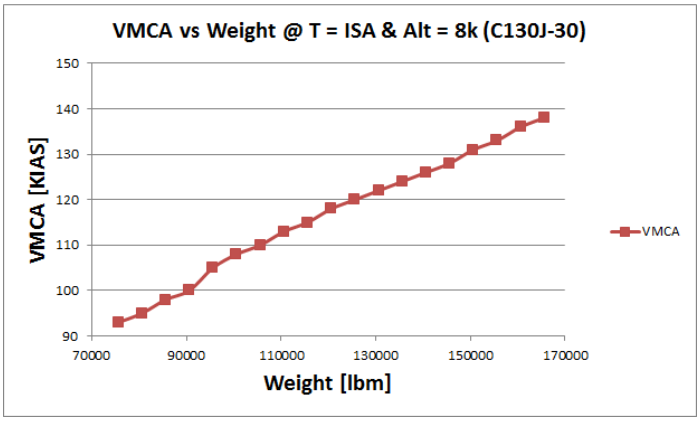

Figure 69. VMCA Vs Weight at T = ISA and Altitude = 8,000 Ft for C130J-30

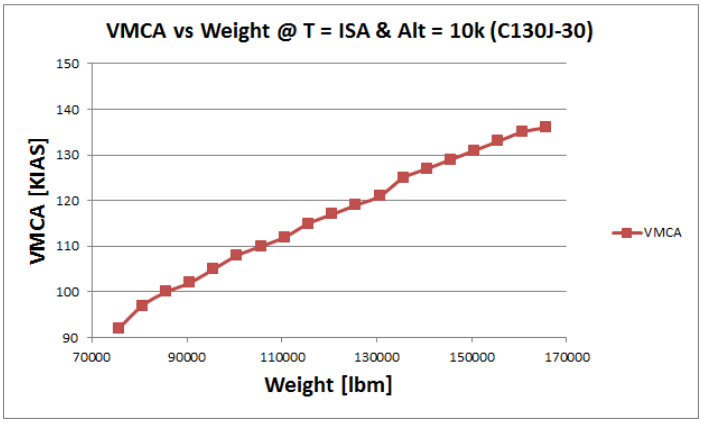

Figure 70. VMCA Vs Weight at T = ISA and Altitude = 10,000 Ft for C130J-30

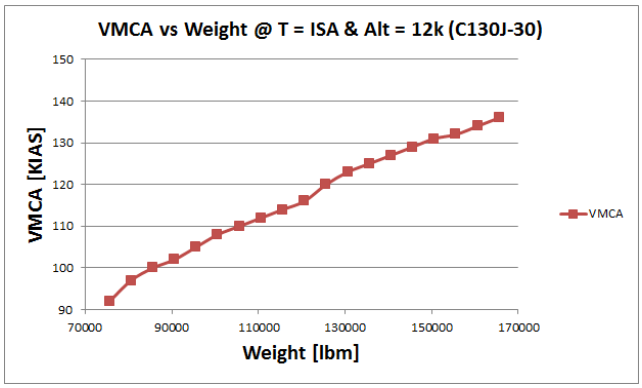

Figure 71. VMCA Vs Weight at T = ISA and Altitude = 12,000 Ft for C130J-30

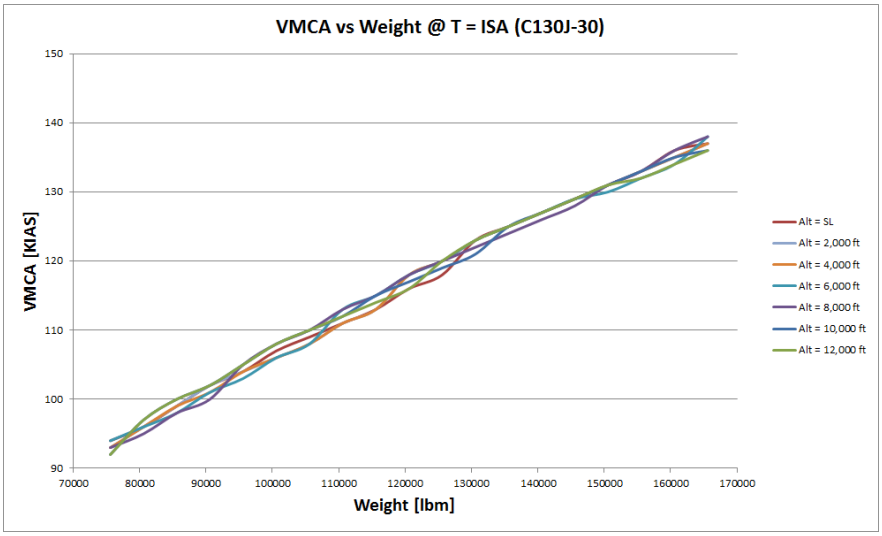

Figure 72 .VMCA Vs Weight at T = ISA for C130J-30

The first major observation that is seen is that at the maximum weight, all of the seven different altitudes produce a VMCA that are very close to each other, suggesting that at some point the weight of the airplane does not influence the calculation of VMCA. This is a very interesting observation, because at the lowest weight setting it is seen for the A320 that VMCA varies a lot. This means that there is a weight and altitude dependent term in the calculation of VMCA that affects the calculation of VMCA at a

low weight, but this influence falls off when the weight reaches some point. Furthermore, this fall off point changes as a function of altitude.

At sea level, this fall off point of the weight dependency is at a higher weight than that of the 12,000 ft altitude scenario. For both the A320 airplane at 12,000 ft, VMCA is a semi-straight linear line as weight increases, showing that at this altitude and weight dependent term is purely weight dependent term, yet this trend is seen for the C130J-30 regardless of the altitude. One suggestion that would explain this observation is found by looking at the angle of attack (α) of the VMCA solution as a function of altitude and weight.

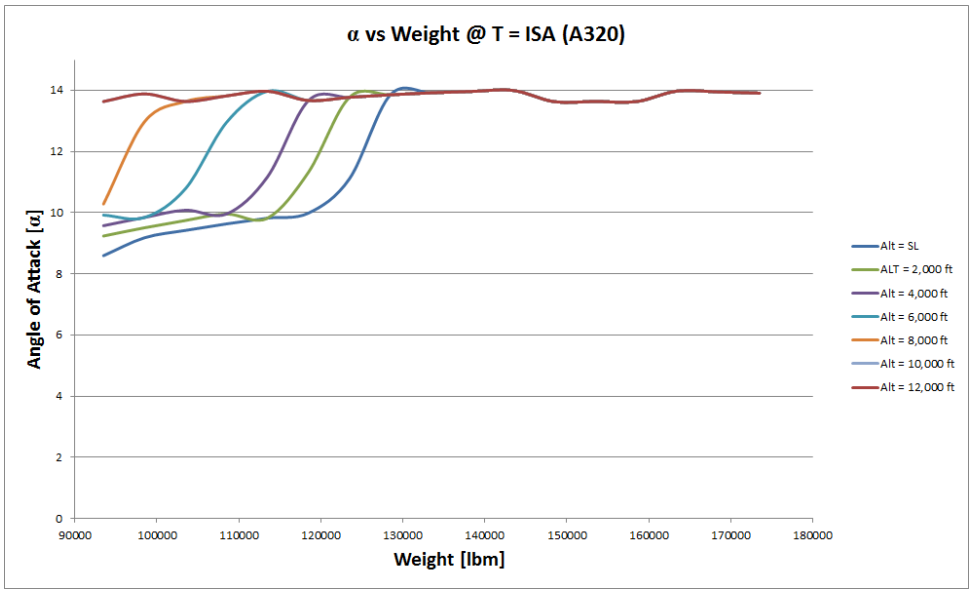

Figure 73. Angle of Attack (α) Vs Weight for A320

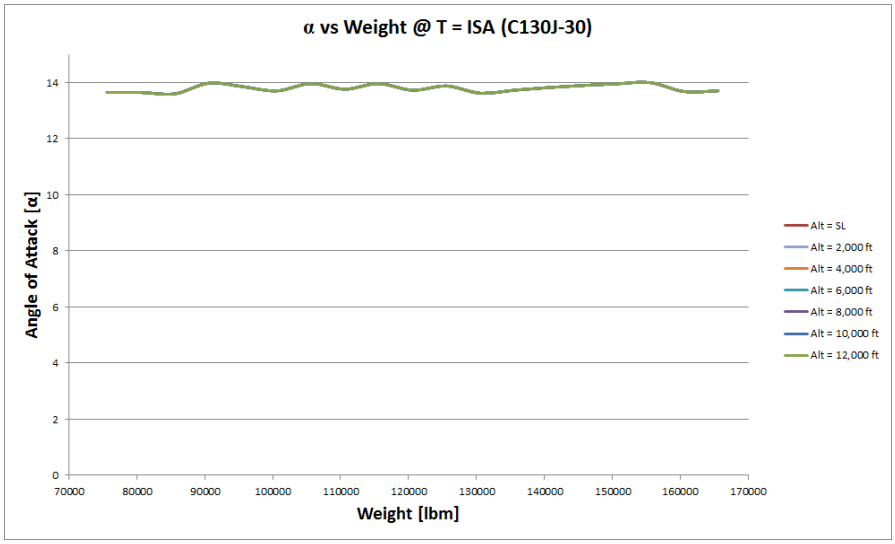

Figure 74. Angle of Attack (α) Vs Weight for C130J-30

Figure 73 and Figure 74 are plots of angle of attack (α) vs weight at the same altitudes as were used in the VMCA plots of Figure 64 and Figure 72 respectively. We observe that the fall off point that we mentioned earlier seems to coincide exactly when the angle of attack (α) become steady and is no longer changing. Just like how VMCA becomes dependent on weight only at 12,000 ft, the angle of attack (α) seems to linear at this altitude for the A320. Therefore we can make the statement that at low altitudes and weights, the limiting factor in solving for VMCA is the angle of attack (α).

If the angle of attack (α) is the limiting factor, this means that the airplane stalls out at higher angles of attack (α); therefore VMCA is limited by stall characteristics of the airplane. Figure 73 shows that the A320 is stall limited for a small range of altitudes and weights. Whereas Figure 74 shows that the C130J-30 is not stall limited at any range of altitudes and weights, most likely due to the ATCS installed.

On the other hand, VMCA still increases as a function of weight even after the airplane is at its maximum angle of attack (α), thus suggesting that there is yet another limit to VMCA that takes over once the maximum angle of attack (α) is reached. We suspect that this other limitation is a lateral-directional control power limitation.

Earlier on we discussed the three trim equations (Equations 18-20) used to solve for VMCA. Of these three equations, Equation 19 is the only one that is a function of weight. Equation 19 is the equation developed to balance the side forces acting on the airplane. The lateral-directional control power is the summation of the side forces acting on the airplane due to the control surfaces. At higher weights, the amount of side force needed to balance Equation 19 also increases, thus requiring higher airspeeds.

From this first trade study we have concluded that in reality VMCA is both stall limited and lateral-directional control power limited. The 12,000 ft altitude plot could be looked at as the underline slope of the lateral-directional control power limitation, and as the altitude decreases, the stall limitation supersedes this underline limitation.

The next trade study we conducted was one were the weight was held constant at a light weight, medium weight and heavy weight. Unlike for the constant temperature trade study, we will be showing all of the altitudes on a single plot for the three different weight configurations. This is done because it is quite fascinating what happens to VMCA as a function of altitude and temperature when the weight increases. Figure 75 is

the light weight configuration, Figure 76 is the medium weight configuration and finally Figure 77 is the heavy weight configuration for the Airbus A320.

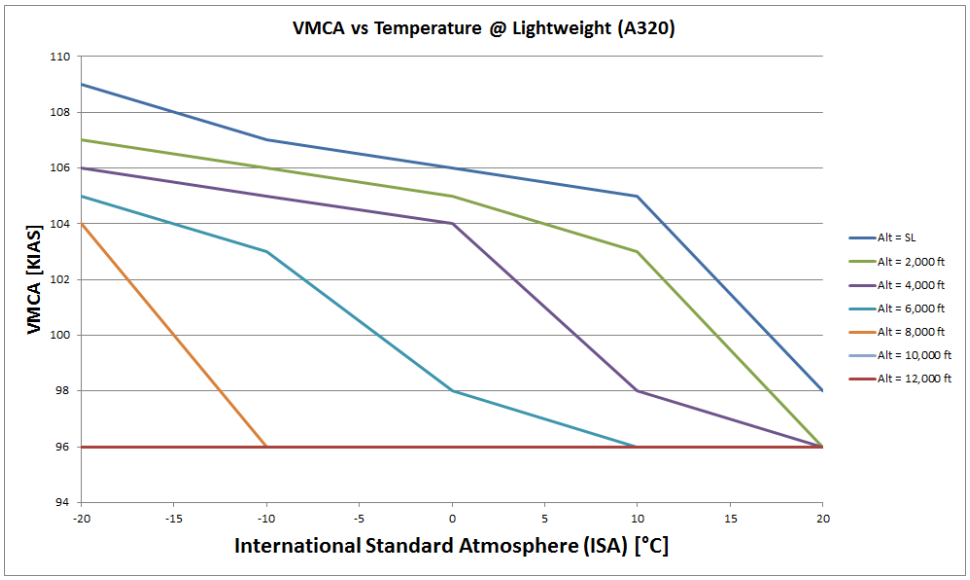

Figure 75. VMCA Vs Temperature at Light Weight for A320

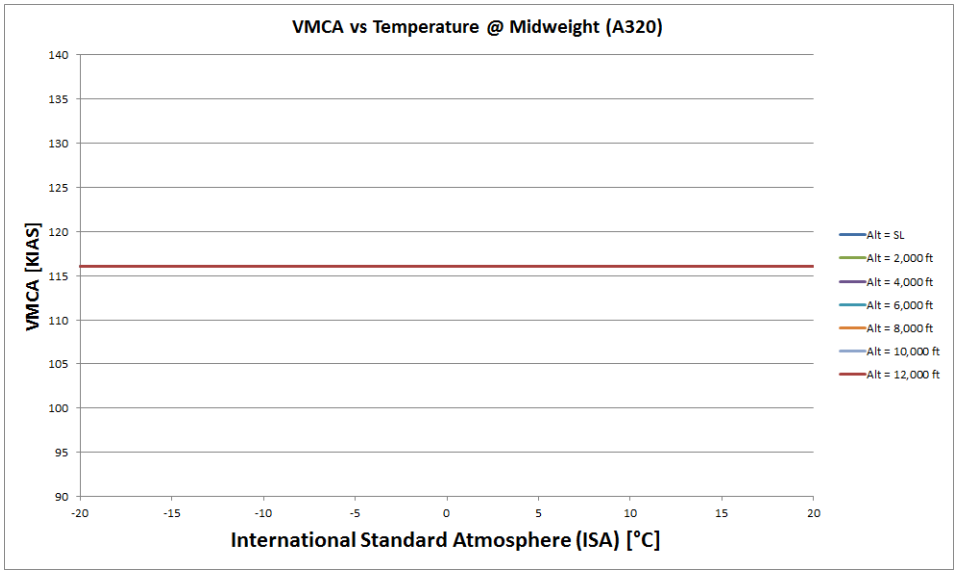

Figure 76. VMCA Vs Temperature at Medium Weight for A320

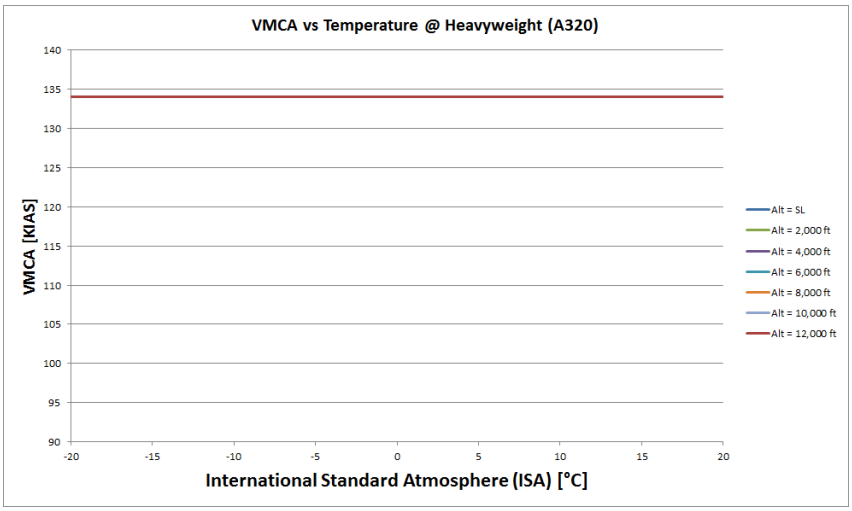

Figure 77. VMCA Vs Temperature at Heavy Weight for A320

Figure 78 is the light weight configuration, Figure 79 is the medium weight configuration and finally Figure 80 is the heavy weight configuration for the Lockheed Martin C130J-30 Super Hercules.

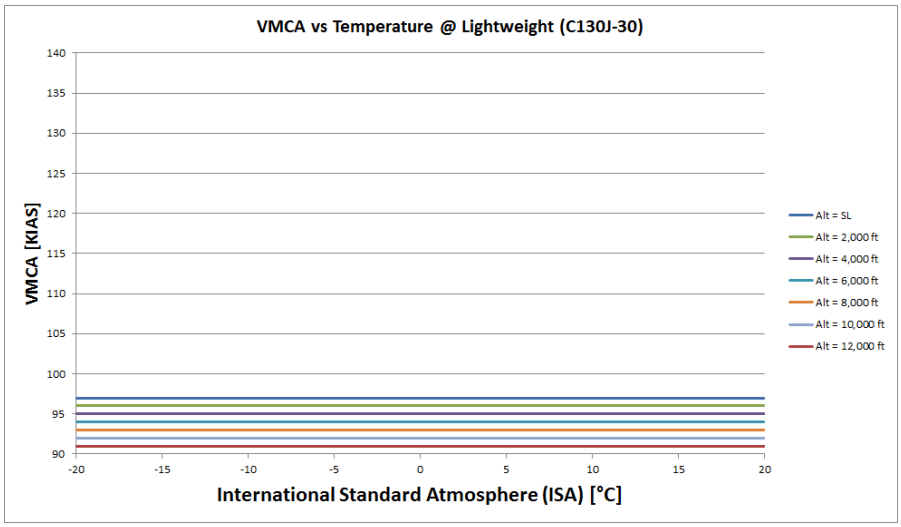

Figure 78. VMCA Vs Temperature at Light Weight for C130J-30

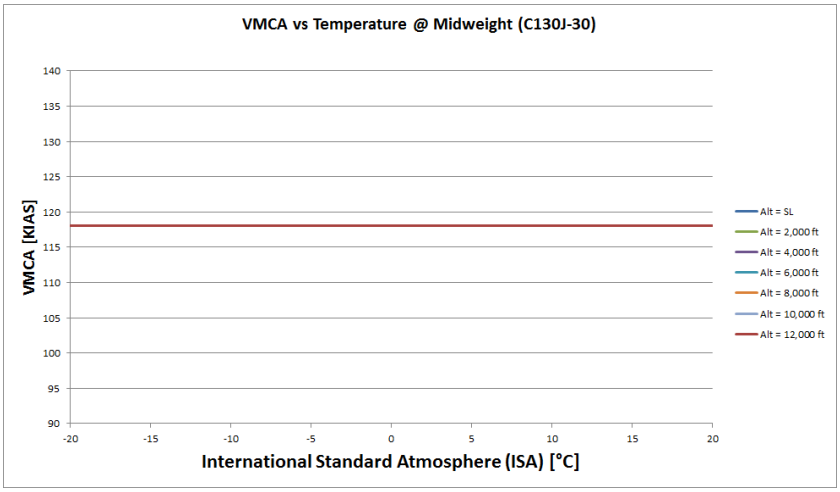

Figure 79. VMCA Vs Temperature at Medium Weight for C130J-30

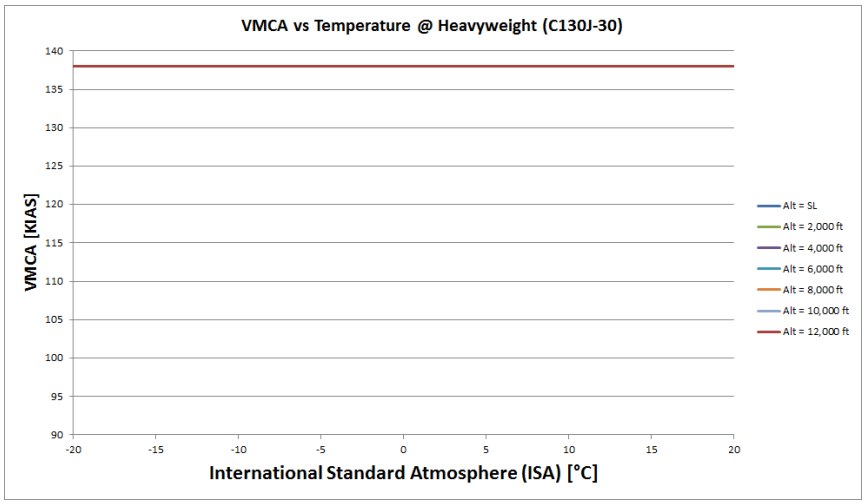

Figure 80. VMCA Vs Temperature at Heavy Weight for C130J-30

In the first trade study, we observed that there seemed to be two different major limitations to VMCA. It appears this is also the case in the second trade study. It also appears that these limitations hold for both the A320 and the C130J-30, therefore letting us make general statements about the limitations of VMCA for all airplanes.

As we did in the first trade study we will look at the plot of angle of attack (α) vs temperature at the VMCA solutions found in Figure 75 through Figure 80 for both the A320 and the C130J-30 airplanes.

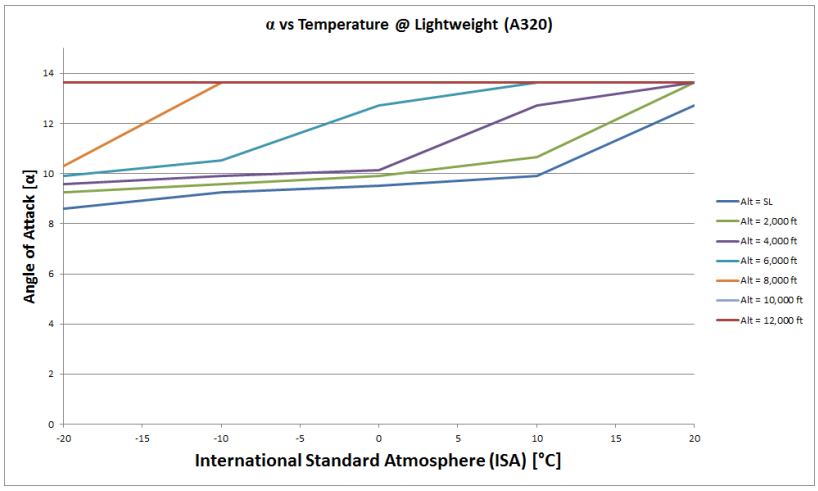

Figure 81. Angle of Attack (α) Vs Temperature at Light Weight for A320

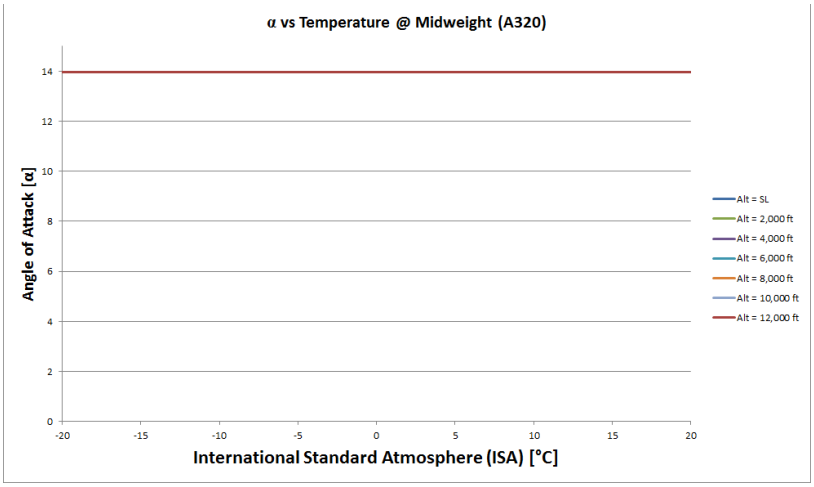

Figure 82. Angle of Attack (α) Vs Temperature at Medium Weight for A320

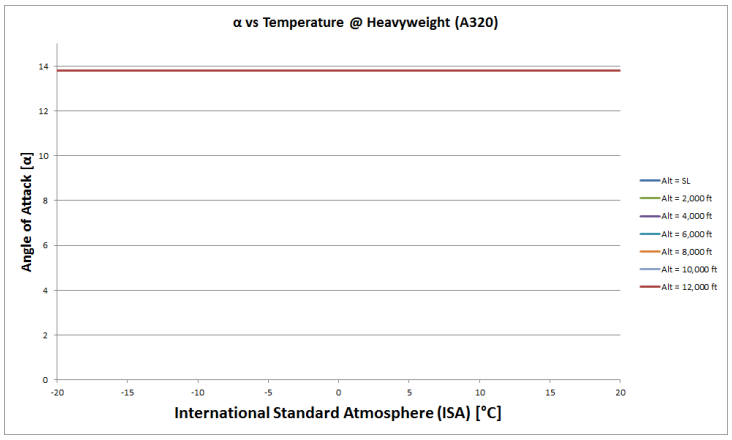

Figure 83. Angle of Attack (α) Vs Temperature at Heavy Weight for A320

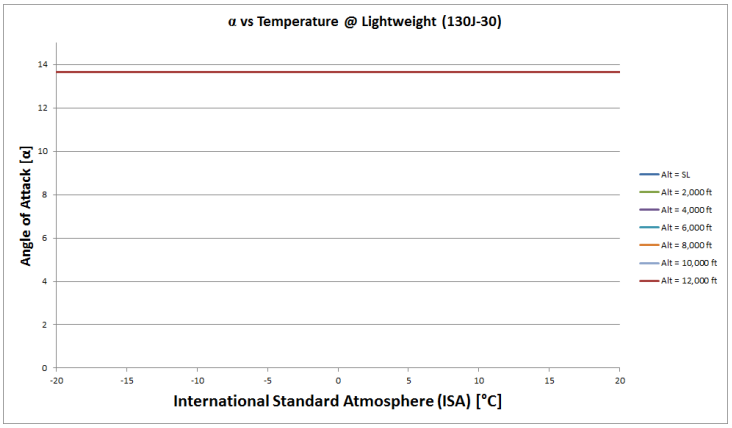

Figure 84. Angle of Attack (α) Vs Temperature at Light Weight for C130J-30

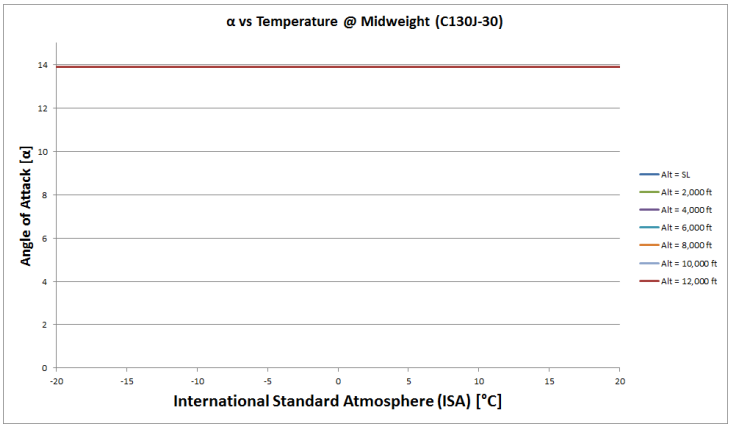

Figure 85. Angle of Attack (α) Vs Temperature at Medium Weight for C130J-30

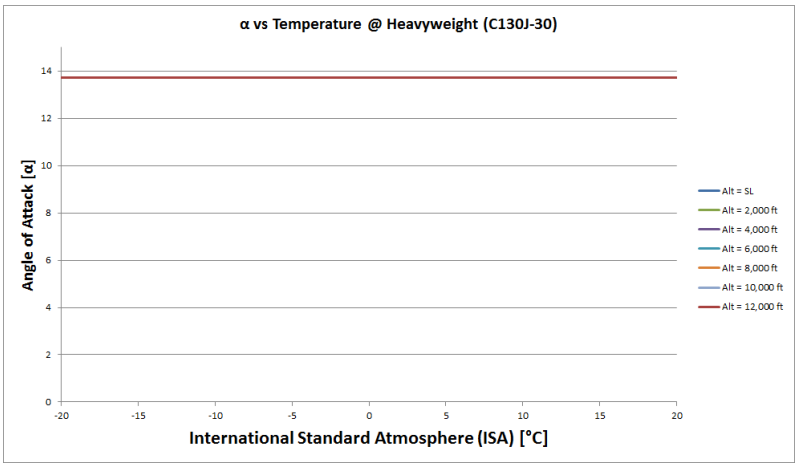

Figure 86. Angle of Attack (α) Vs Temperature at Heavy Weight for C130J-30

Right off the bat, we notice that at medium and heavy weight the angle of attack (α) remains constant, however at a lightweight the angle of attack (α) varies dramatically as a function of the temperature for the A320. Just as in the first trade study, it appears that the VMCA is stall limited at a lightweight, confirming the previous observation. Once again we can see the effects of the ATCS on the C130J-30, for a lightweight C130J-30 may fly at maximum angle of attack (α) thus allowing for the airplane to avoid the unpredictability seen in the A320 case (Figure 81).

Now that we have identified one of the limitations, we will isolate the other limitation. Looking at just the 12,000 ft altitude line we see that there is a floor, or minimal VMCA that is calculated regardless of the temperature. The lightweight scenario has the lowest floor VMCA and the heavy weight scenario has the highest floor VMCA, with an intermediate floor VMCA at the medium weight scenario. This limitation is a Thrust dependent lift limitation. In order to calculate VMCA the total amount of lift must

be equal to the weight of the airplane. Therefore there is a floor airspeed that the airplane must fly at to generate enough lift to even maintain constant altitude flight.

The third trade study that was conducted was one were the altitude was held constant at sea level, 6,000 ft and 12,000 ft and cycling through the temperature and weight to find any trends in this last configuration.

Figure 87 is the altitude of sea level configuration, Figure 88 is the altitude of 6,000 ft configuration and finally Figure 89 is the altitude of 12,000 ft configuration for the Airbus A320.

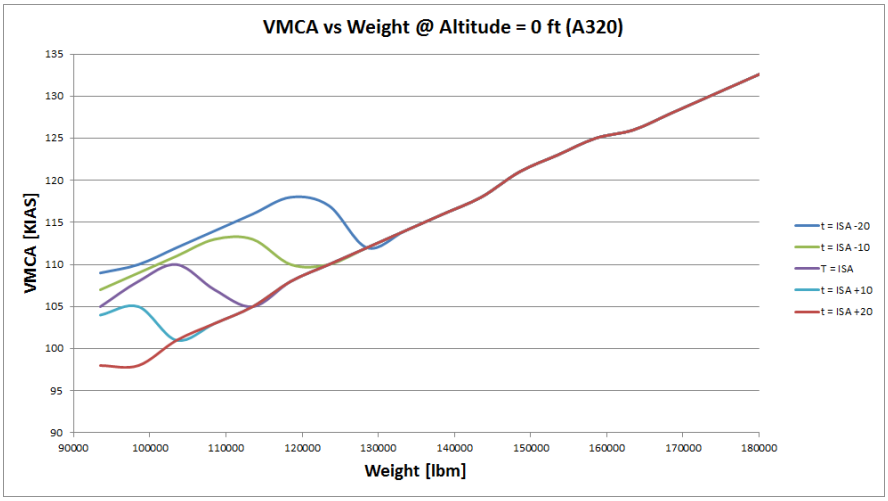

Figure 87. VMCA Vs Weight at Altitude of Sea Level for A320

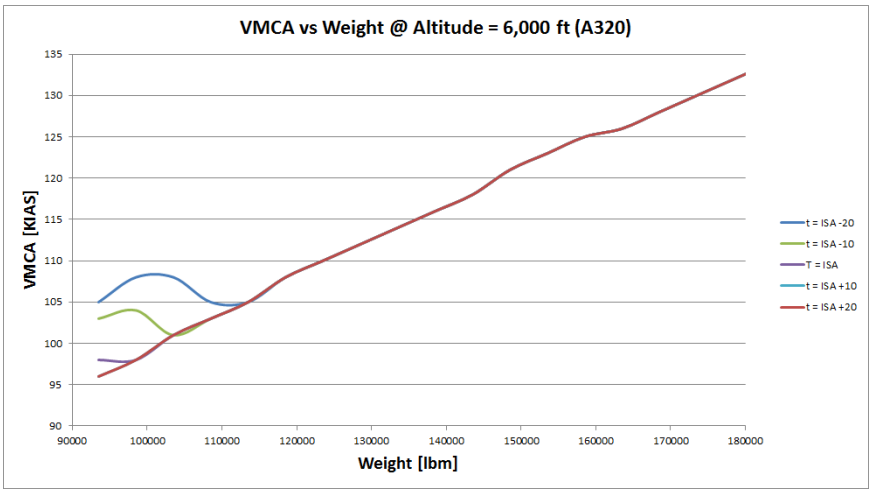

Figure 88. VMCA Vs Weight at Altitude of 6,000 Ft for A320

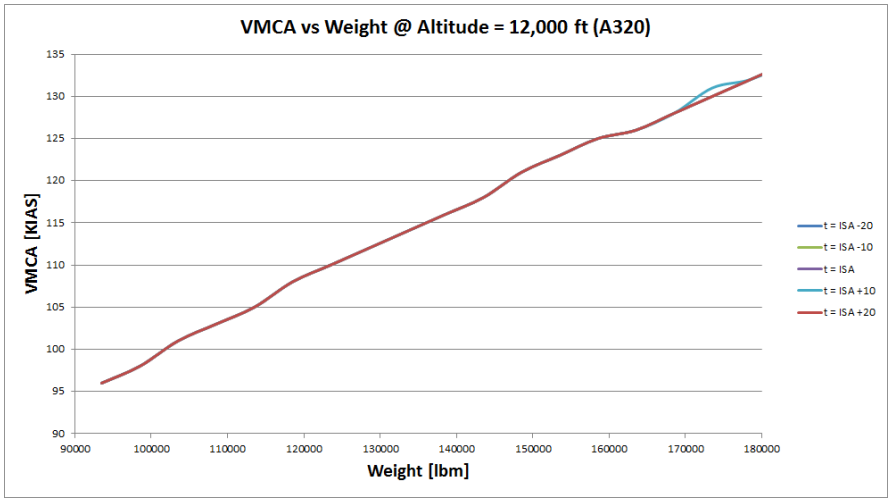

Figure 89. VMCA Vs Weight at Altitude of 12,000 Ft for A320

Figure 90 is the altitude of sea level configuration, Figure 91 is the altitude of 6,000 ft configuration and finally Figure 92 is the altitude of 12,000 ft configuration for the Lockheed Martin C130J-30 Super Hercules.

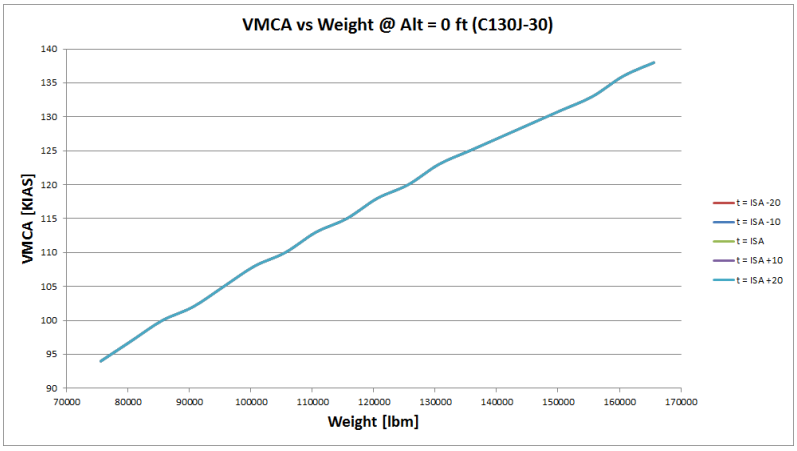

Figure 90. VMCA Vs Weight at Altitude of Sea Level for C130J-30

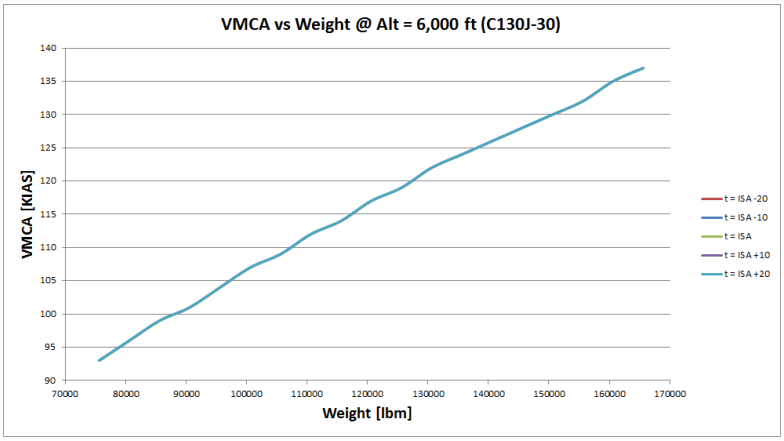

Figure 91. VMCA Vs Weight at Altitude of 6,000 Ft for C130J-30

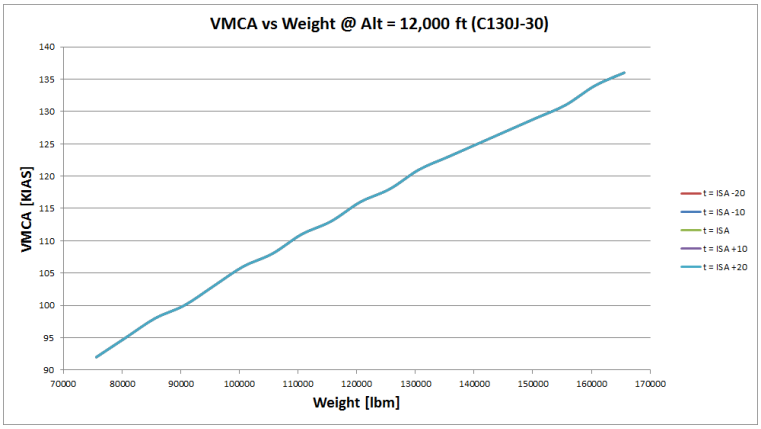

Figure 92. VMCA Vs Weight at Altitude of 12,000 Ft for C130J-30

As could be predicted, there seems to be two different limitations to VMCA that are observed in this third and final trade study. This trade study looks a lot like the first trade study, were there seems to be some underline slope of VMCA limitation, with some deviations at low weight, temperature, and altitude at least for the full thrust A320 airplane.

As we have for the first trade study, we will observe the angle of attack (α) as a function of weight at the three different altitude settings for both the A320 and the C130J-30 (Figure 93 through Figure 98).

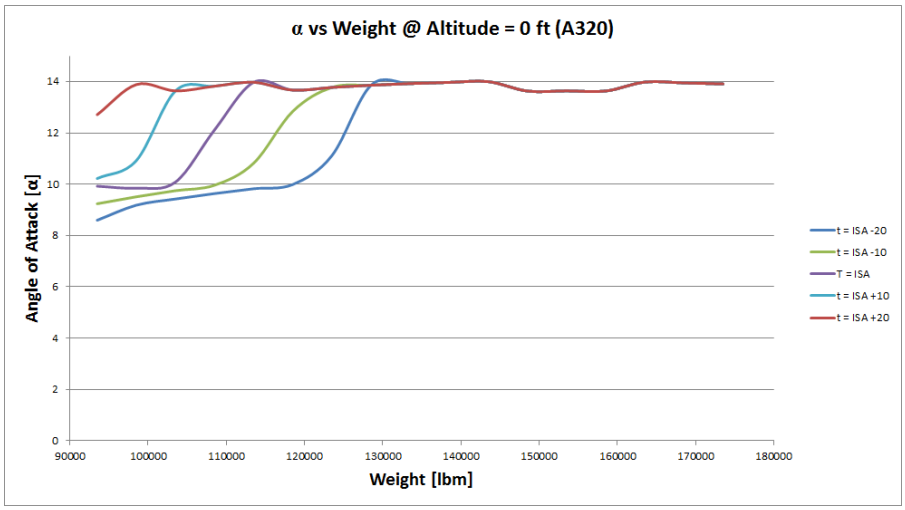

Figure 93. Angle of Attack (α) vs Weight at Altitude of Sea Level for A320

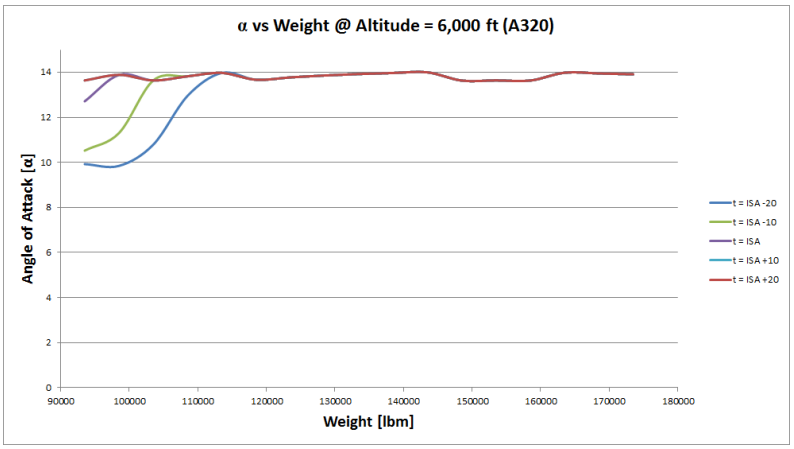

Figure 94. Angle of Attack (α) Vs Weight at Altitude of 6,000 Ft for A320

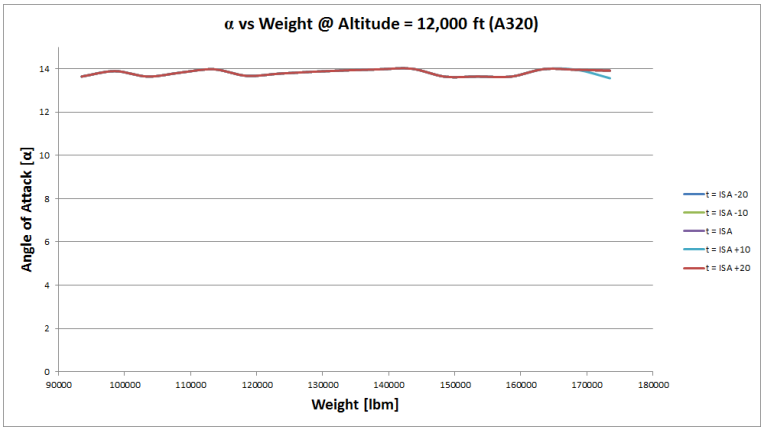

Figure 95. Angle of Attack (α) Vs Weight at Altitude of 12,000 Ft for A320

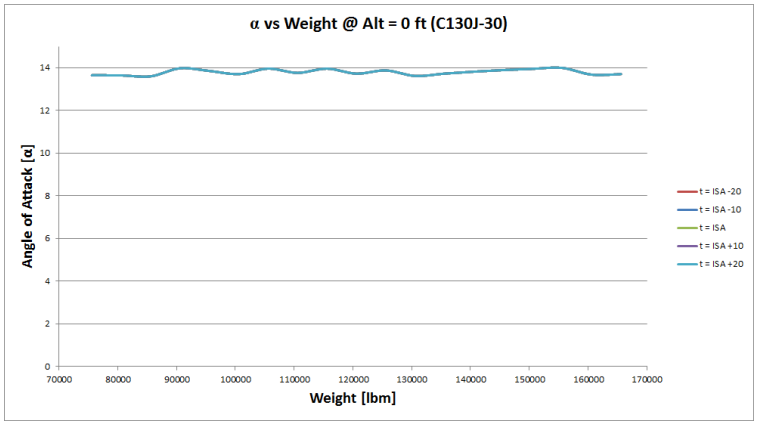

Figure 96. Angle of Attack (α) Vs Weight at Altitude of Sea Level for C130J-30

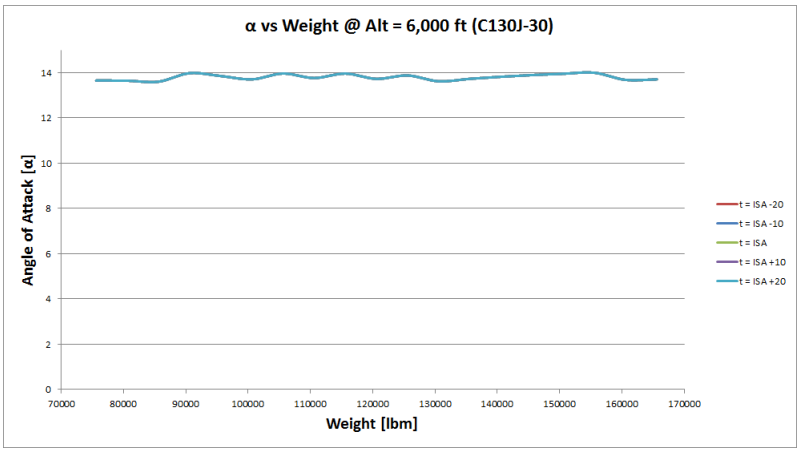

Figure 97. Angle of Attack (α) Cs Weight at Altitude of 6,000 Ft for C130J-30

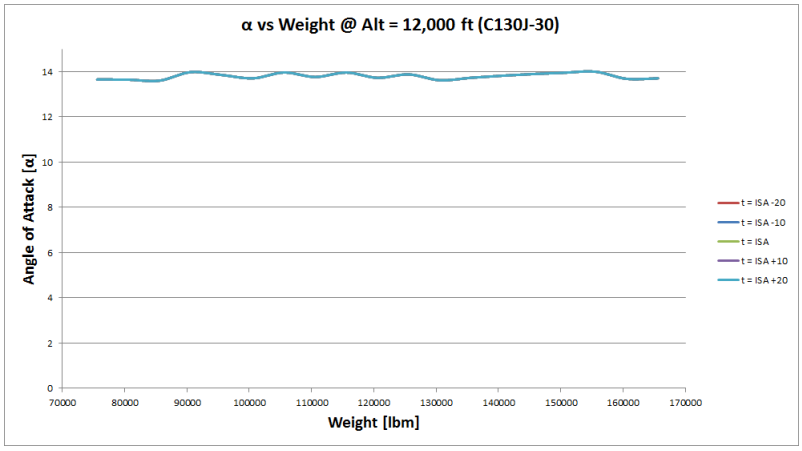

Figure 98. Angle of Attack (α) Vs Temperature at Heavy Weight for C130J-30

Once again we see that the angle of attack (α) plays a major role in calculating VMCA. At low altitudes, the A320 airplane stalls at low weight and low temperatures much more than in the high altitude scenario. Further confirming the statement that VMCA is stall limited at low temperature, weight and altitude. It is important to see that this trade study shows that there is some stall for the A320 still occurring at a medium altitude and low temperatures, whereas at medium temperature there was no stall at

medium altitudes. This shows that stall factors are greatly influenced by the outside temperature, whereas the altitude's influence falls off quicker.

Just as we discussed in the first trade study, Equation 19 is the only trim equation that is a function of weight. Therefore we suggest that the lateral-directional control power is the other limiting factor in this trade study. At higher weights the amount of side force needed to balance Equation 19 increases, thus requiring higher airspeeds to counter the side forces developed by the weight of the airplane. This is the underline slope of VMCA seen in the VMCA vs weight plots for the constant altitudes.

It is important to understand all of these limitations to calculating VMCA so that we can understand how an airplane behaves in an engine inoperative scenario. At low weight, altitude and temperature VMCA is driven by the stall characteristics of the airplane. This VMCA limit is greater than that of the lateral-directional control power limit; therefore the stall limitation is the driving limitation, and a pilot can be assured that if they are fling the airplane at an airspeed higher than the stall speed at low weight, temperature and altitude that they will have enough airspeed to generated sufficient lateral-directional control power.

This assumption is no longer valid once the airplane reaches the maximum angle of attack (α), the VMCA limitation then is driven by the lateral-directional control power of the control surfaces. To help us better understand what drives the lateral-directional power limitation, the last discussion in this paper will be about what flight configurations

of bank angle (φ), rudder deflection (θ_{rudder}) and aileron deflection ($\theta_{aileron}$) satisfy the three trim equations (Equations 18-20).

Chapter 8: Minimum Control Airspeed Flight Configuration Observations

The trade studies above were all conducted at a sideslip angle (β) of -3°. A negative sideslip angle (β) means that the pilot is to "crab" into the dead engine. This sideslip angle (β) was highlighted because it provided the most amount of discussion. However we will say that at a positive sideslip angle (β) of say 2°, the stall limitations that were discussed above are no longer limitations for the constant temperature and altitude cases. This means that there is another whole database of plots and figures that could be placed in this paper at each sideslip angle (β), however this would triple the size of this paper and therefore congest the paper. With that being said however, we will still discuss the general effects of sideslip angle (β) on the flight configurations of VMCA.

Starting with a constant sideslip angle (β) of -3° there are a few main observations that can be made about the flight configurations of bank angle (φ), rudder deflection (θrudder) and aileron deflection (θaileron). The engine that was producing the asymmetric propulsion force is along the positive y axis, therefore a sideslip angle (β) of -3° means that there is a cross wind that helps the rudder counter the unbalanced force. This is a sideslip angle (β) in which there is significant stall limitations at low weight, altitude and temperatures.

There are very many ways that we could discuss and show the flight configuration trends, for purposes of this discussion we will be looking at a constant temperature of 15°C, while varying altitude and weight. Below are several tables that show the flight

configurations of the Airbus A320 at different altitudes and weights. These tables are snap shots of the full database, with the purpose of showing trends and observations.

Table 1. Flight Configurations for the VMCA Solutions Found at Altitude of 0 Ft, Weight of 93,500 Lbm and Sideslip Angle (β) of -3° for A320

Airplane: A320			
Altitude: 0 ft			
Weight: 93,500 lbm			
Sideslip Angle (β): -3°			
VMCA	φ	θrudder	θaileron
109	2	-20	-8
109	2	-20	-7
109	2	-20	-6
110	2	-20	-9
110	2	-20	-8
110	2	-20	-7
110	2	-20	-6
110	2	-20	-5
110	2	-20	-4
111	2	-20	-9
111	2	-20	-8
111	2	-20	-7
111	2	-20	-6
111	2	-20	-5
111	2	-20	-4
111	2	-20	-3

Table 2. Flight Configurations for the VMCA Solutions Found at Altitude of 0 Ft, Weight of 128,500 Lbm and Sideslip Angle (β) of -3° for A320

Airplane: A320			
Altitude: 0 ft			
Weight: 128,500 lbm			
Sideslip Angle (β): -3°			
VMCA	φ	θrudder	θaileron
112	1	-20	-14
112	1	-20	-13
112	1	-20	-12
113	1	-20	-13
113	1	-20	-12
113	1	-20	-11
114	1	-19	-13
114	1	-19	-12

Table 3. Flight Configurations for the VMCA Solutions Found at Altitude of 0 Ft, Weight of 173,500 Lbm and Sideslip Angle (β) of -3° for A320

Airplane: A320			
Altitude: 0 ft			
Weight: 173,500 lbm			
Sideslip Angle (β): -3°			
VMCA	φ	θrudder	θaileron
130	1	-19	-16
130	1	-19	-15
130	1	-19	-14
130	1	-19	-13
130	1	-19	-12
130	1	-19	-11
130	1	-19	-10
131	1	-19	-15
131	1	-19	-14
131	1	-19	-13
131	1	-19	-12
131	1	-19	-11
131	1	-19	-10
131	1	-19	-9
131	1	-18	-14
131	1	-18	-13
131	1	-18	-12
132	1	-19	-14
132	1	-19	-13
132	1	-19	-12
132	1	-19	-11
132	1	-19	-10
132	1	-19	-9
132	1	-18	-15
132	1	-18	-14

Table 4. Flight Configurations for the VMCA Solutions Found at Altitude of 6,000 Ft, Weight of 93,500 Lbm and Sideslip Angle (β) of -3° for A320

Airplane: A320			
Altitude: 6,000 ft			
Weight: 93,500 lbm			
Sideslip Angle (β): -3°			
VMCA	φ	θrudder	θaileron
106	2	-20	-9
106	2	-20	-8
106	2	-20	-7
107	2	-20	-11
107	2	-20	-10
107	2	-20	-9
107	2	-20	-8
107	2	-20	-7
107	2	-20	-6
107	2	-20	-5
108	2	-20	-11
108	2	-20	-10
108	2	-20	-9
108	2	-20	-8
108	2	-20	-7

Table 5. Flight Configurations for the VMCA Solutions Found at Altitude of 6,000 Ft, Weight of 128,500 Lbm and Sideslip Angle (β) of -3° for A320

Airplane: A320			
Altitude: 6,000 ft			
Weight: 128,500 lbm			
Sideslip Angle (β): -3°			
VMCA	φ	θrudder	θaileron
112	1	-20	-16
112	1	-20	-15
112	1	-20	-14
112	1	-20	-13
112	1	-20	-12
112	1	-20	-11
112	1	-20	-10
113	1	-20	-15
113	1	-20	-14
113	1	-20	-13
113	1	-20	-12
113	1	-20	-11
113	1	-20	-10
113	1	-20	-9
114	1	-20	-13
114	1	-20	-12
114	1	-20	-11
114	1	-20	-10
114	1	-19	-16
114	1	-19	-15

Table 6. Flight Configurations for the VMCA Solutions Found at Altitude of 6,000 Ft, Weight of 173,500 Lbm and Sideslip Angle (β) of -3° for A320

Airplane: A320			
Altitude: 6,000 ft			
Weight: 173,500 lbm			
Sideslip Angle (β): -3°			
VMCA	φ	θrudder	θaileron
130	0	-15	-16
130	0	-15	-15
130	0	-15	-14
130	0	-15	-13
130	0	-15	-12
130	0	-15	-11
131	0	-15	-15
131	0	-15	-14
131	0	-15	-13
131	0	-15	-12
131	0	-15	-11
131	0	-14	-15
131	0	-14	-14
131	0	-14	-13
131	0	-14	-12

At higher altitudes, the data shows that the flight configurations are practically the same as the 6,000 ft case, thus these six tables are sufficient to see what is happening to the A320 under these parameters.

The first observation is that at low weight and altitude, the limiting factor is the rudder control surface. This is observed in Table 1 because the θrudder is at its maximum deflection of -20°. This means that the control power needed to trim the airplane was being restricted by the rudder, for the bank angle (φ) and aileron deflection (θaileron) were not at their maximum limits.

At higher weights the rudder deflection (θrudder) no longer at its maximum deflection. It is observed that the bank angle (φ) goes to zero and there is more deflection in the aileron (θaileron) than in the lower weight scenarios. Also at higher weights there are much more flight configuration combinations that satisfy the trim equations, suggesting that at higher weight there is more "wiggle room" for trimmed flight than there is at low weights.

We will now look at the flight configurations of trim for the C130J-30 airplane VMCA solutions. Just like for the A320 case, we will attempts to give the reader a snapshot of the database generated, for purposes of discussing and observations.

Table 7. Flight Configurations for the VMCA Solutions Found at Altitude of 0 Ft, Weight of 75,600 Lbm and Sideslip Angle (β) of -3° for C130J-30-30

Airplane: C130J-30			
Altitude: 0 ft			
Weight: 75,600 lbm			
Sideslip Angle (β): -3°			
VMCA	φ	θrudder	θaileron
94	2	-24	-2
94	2	-24	-1
94	2	-24	0
94	2	-23	-3
94	2	-23	-2
95	2	-23	-3
95	2	-23	-2
95	2	-23	-1
95	2	-23	0
95	2	-23	1
95	2	-22	-3
96	3	-25	-1
96	3	-25	0
96	2	-23	-2
96	2	-23	-1
96	2	-23	0

Table 8. Flight Configurations for the VMCA Solutions Found at Altitude of 0 Ft, Weight of 120,600 Lbm and Sideslip Angle (β) of -3° for C130J-30-30

Airplane: C130J-30			
Altitude: 0 ft			
Weight: 120,600 lbm			
Sideslip Angle (β): -3°			
VMCA	φ	θrudder	θaileron
116	1	-19	-2
116	1	-19	-1
116	1	-19	0
116	1	-18	-3
116	1	-18	-2
116	1	-18	-1
116	1	-18	0
117	1	-18	-3
117	1	-18	-2
117	1	-18	-1
117	1	-18	0
117	1	-17	-3
117	1	-17	-2
117	1	-17	-1
118	1	-18	-2
118	1	-18	-1
118	1	-18	0
118	1	-17	-3
118	1	-17	-2
118	1	-17	-1

Table 9. Flight Configurations for the VMCA Solutions Found at Altitude of 0 Ft, Weight of 165,600 Lbm and Sideslip Angle (β) of -3° for C130J-30

Airplane: C130J-30			
Altitude: 0 ft			
Weight: 165,600 lbm			
Sideslip Angle (β): -3°			
VMCA	φ	θrudder	θaileron
136	0	-14	-3
136	0	-14	-2
136	0	-14	-1
136	0	-14	0
136	0	-13	-4
136	0	-13	-3
136	0	-13	-2
137	0	-14	-3
137	0	-14	-2
137	0	-14	-1
137	0	-14	0
137	0	-13	-4
137	0	-13	-3
137	0	-13	-2
138	0	-14	-3
138	0	-14	-2
138	0	-14	-1
138	0	-14	0
138	0	-13	-4
138	0	-13	-3

Table 10. Flight Configurations for the VMCA Solutions Found at Altitude of 6,000 Ft, Weight of 75,600 Lbm and Sideslip Angle (β) of -3° for C130J-30-30

Airplane: C130J-30			
Altitude: 6,000 ft			
Weight: 75,600 lbm			
Sideslip Angle (β): -3°			
VMCA	φ	θrudder	θaileron
92	2	-23	-2
92	2	-23	-1
92	2	-23	0
92	2	-23	1
92	2	-22	-3
92	2	-22	-2
92	2	-22	-1
93	2	-23	-1
93	2	-23	0
93	2	-22	-2
93	2	-22	-1
93	2	-22	0
94	2	-22	-2
94	2	-22	-1
94	2	-22	0
94	2	-22	1
94	2	-21	-2

Table 11. Flight Configurations for the VMCA Solutions Found at Altitude of 6,000 Ft, Weight of 120,600 Lbm and Sideslip Angle (β) of -3° for C130J-30-30

Airplane: C130J-30			
Altitude: 6,000 ft			
Weight: 120,600 lbm			
Sideslip Angle (β): -3°			
VMCA	φ	θrudder	θaileron
116	1	-18	-1
116	1	-17	-2
116	1	-17	-1
116	0	-15	-2
116	0	-15	-1
116	0	-14	-4
116	0	-14	-3
116	0	-14	-2
117	1	-18	-1
117	1	-17	-2
117	1	-17	-1
117	0	-14	-3
117	0	-14	-2
118	1	-17	-2
118	1	-17	-1
118	1	-17	0
118	0	-14	-3
118	0	-14	-2

Table 12. Flight Configurations for the VMCA Solutions Found at Altitude of 6,000 Ft, Weight of 165,600 Lbm and Sideslip Angle (β) of -3° for C130J-30

Airplane: C130J-30			
Altitude: 6,000 ft			
Weight: 165,600 lbm			
Sideslip Angle (β): -3°			
VMCA	φ	θrudder	θaileron
136	0	-14	-3
136	0	-14	-2
136	0	-14	-1
136	0	-14	0
136	0	-13	-3
136	0	-13	-2
137	0	-14	-2
137	0	-14	-1
137	0	-14	0
137	0	-13	-3
137	0	-13	-2
137	0	-13	-1
137	0	-13	0
137	0	-12	-3
138	0	-14	-2
138	0	-14	-1
138	0	-13	-3
138	0	-13	-2
138	0	-13	-1
138	0	-13	0

At higher altitudes, the data shows that the flight configurations are practically the same as the 6,000 ft case, thus these six tables are sufficient to see what is happening to the C130J-30 under these parameters.

For the C130J-30 the maximum rudder deflection is about plus or minus 25°. The tables that show the C130J-30 flight configurations are very close to those of the A320 tables. They both are rudder control power limited, highlighted by the -25° θrudder. They

both are also at a small bank angle (φ) that gradually goes to zero as the weight increases. However, a difference is the range of aileron deflection (θaileron) needed to trim the airplane.

The fact that the rudder deflection is the same between the two airplanes shows us that the rudder plays a significant role in trimmed engine inoperative flight. The fact that the aileron deflections are different shows us that the trimmed flight conditions depend on the geometry and design of the airplane. However as the weight increases, both of the airplanes seem to go to a similar flight condition for trimmed flight.

The last step is to highlight a different sideslip angle (β) and compare the differences between the flight configurations needed to trim the airplane. As stated earlier, VMCA is dependent on sideslip angle (β) and there are corresponding plots to show all of these changes, however we will just be highlighting the differences in the flight configurations to discuss the effects of sideslip angle (β) on the trim conditions.

Just as before, the tables presented below are just snapshots of the overall database generated by the algorithm. The purpose of the tables is to help us understand and look for trends in flight configurations that manifest trimmed engine inoperative flight. We will first start with the A320 airplane at a sideslip angle (β) of 2°.

Table 13. Flight Configurations for the VMCA Solutions Found at Altitude of 0 Ft, Weight of 93,500 Lbm and Sideslip Angle (β) of 2° for A320

Airplane: A320			
Altitude: 0 ft			
Weight: 93,500 lbm			
Sideslip Angle (β): 2°			
VMCA	φ	θrudder	θaileron
97	5	-17	12
97	5	-17	13
97	5	-17	14
98	5	-16	13
99	5	-16	12
99	5	-16	13
99	5	-16	14

Table 14. Flight Configurations for the VMCA Solutions Found at Altitude of 0 Ft, Weight of 128,500 Lbm and Sideslip Angle (β) of 2° for A320

Airplane: A320			
Altitude: 0 ft			
Weight: 128,500 lbm			
Sideslip Angle (β): 2°			
VMCA	φ	θrudder	θaileron
112	4	-13	13
112	4	-12	8
112	4	-12	9
112	4	-12	10
112	4	-12	11
112	4	-12	12
112	4	-12	13
113	4	-12	9
113	4	-12	10
113	4	-12	11
113	4	-12	12
113	4	-12	13
113	4	-12	14
113	4	-12	15
114	4	-12	10
114	4	-12	11
114	4	-12	12
114	4	-12	13
114	4	-12	14
114	4	-12	15

Table 15. Flight Configurations for the VMCA Solutions Found at Altitude of 0 Ft, Weight of 173,500 Lbm and Sideslip Angle (β) of 2° for A320

Airplane: A320			
Altitude: 0 ft			
Weight: 173,500 lbm			
Sideslip Angle (β): 2°			
VMCA	φ	θrudder	θaileron
130	3	-7	8
130	3	-7	9
130	3	-7	10
130	3	-7	11
130	3	-7	12
131	3	-7	9
131	3	-7	10
131	3	-7	11
131	3	-7	12
131	3	-7	13
132	3	-7	9
132	3	-7	10
132	3	-7	11
132	3	-7	12
132	3	-7	13
132	3	-7	9
132	3	-7	10
132	3	-7	11
132	3	-7	12
132	3	-7	13

Table 16. Flight Configurations for the VMCA Solutions Found at Altitude of 6,000 Ft, Weight of 93,500 Lbm and Sideslip Angle (β) of 2° for A320

Airplane: A320			
Altitude: 6,000 ft			
Weight: 93,500 lbm			
Sideslip Angle (β): 2°			
VMCA	φ	θrudder	θaileron
96	5	-17	10
96	5	-17	11
96	5	-17	12
96	5	-17	13
96	5	-17	14
96	5	-17	15
96	5	-17	16
97	5	-17	12
97	5	-17	13
97	5	-17	14
97	5	-17	15
97	5	-16	9
97	5	-16	10
98	5	-16	10
98	5	-16	11
98	5	-16	12
98	5	-16	13
98	5	-16	14
98	5	-16	15
98	5	-16	16

Table 17. Flight Configurations for the VMCA Solutions Found at Altitude of 6,000 Ft, Weight of 128,500 Lbm and Sideslip Angle (β) of 2° for A320

Airplane: A320			
Altitude: 6,000 ft			
Weight: 128,500 lbm			
Sideslip Angle (β): 2°			
VMCA	φ	θrudder	θaileron
112	4	-12	10
112	4	-12	11
112	4	-12	12
112	4	-12	13
112	4	-12	14
112	4	-12	15
113	4	-12	12
113	4	-12	13
113	4	-12	14
113	4	-11	8
113	4	-11	9
113	4	-11	10
113	4	-12	12
114	4	-11	9
114	4	-11	10
114	4	-11	11
114	4	-11	12
114	4	-11	13
114	4	-11	14

Table 18. Flight Configurations for the VMCA Solutions Found at Altitude of 6,000 Ft, Weight of 173,500 Lbm and Sideslip Angle (β) of 2° for A320

Airplane: A320			
Altitude: 6,000 ft			
Weight: 173,500 lbm			
Sideslip Angle (β): 2°			
VMCA	φ	θrudder	θaileron
130	3	-7	8
130	3	-7	9
130	3	-7	10
130	3	-7	11
130	3	-7	12
130	3	-7	13
131	3	-7	8
131	3	-7	9
131	3	-7	10
131	3	-7	11
131	3	-7	12
131	3	-7	13
132	3	-7	9
132	3	-7	10
132	3	-7	11
132	3	-7	12
132	3	-7	13
132	3	-7	14

Now that there is a positive sideslip angle (β) it seems that the rudder control power is no longer the limiting factor in calculating VMCA. Table 13 indicated that the bank angle (φ) is the limiting parameter. The airplane is limited to 5 degrees of bank angle (β) per regulation, which we have previously discussed. It is also interesting to see that the aileron deflection (θaileron) also reaches a higher deflection than in the sideslip angle (β) of -3° case.

We will now compare these values to the ones for the C130J-30 at a 2° sideslip angle (β) to see if this trend is specific to the airplane, or if it is a general trend that can be assumed for all airplanes. The values that we get at a positive sideslip angle (β) do not even provide a solution if the ATCS is not installed, thus further showing the need and purpose behind the need of the ATCS for the C130J-30. However, for this work we still applied the modified thrust in the VMCA calculations.

Table 19: Flight Configurations for the VMCA Solutions Found at Altitude of 0 Ft, Weight of 75,600 lLbm and Sideslip Angle (β) of 2° for C130J-30

Airplane: C130J-30			
Altitude: 0 ft			
Weight: 75,600 lbm			
Sideslip Angle (β): 2°			
VMCA	φ	θrudder	θaileron
92	5	-15	1
92	5	-15	2
92	5	-15	3
92	5	-15	4
93	5	-15	2
93	5	-15	3
93	5	-15	4
93	5	-14	1
94	5	-15	3
94	5	-15	4
94	5	-14	1

Table 20: Flight Configurations for the VMCA Solutions Found at Altitude of 0 Ft, Weight of 120,600 Lbm and Sideslip Angle (β) of 2° for C130J-30

Airplane: C130J-30			
Altitude: 0 ft			
Weight: 120,600 lbm			
Sideslip Angle (β): 2°			
VMCA	φ	θrudder	θaileron
116	4	-11	3
116	4	-11	4
116	4	-10	1
116	4	-10	2
116	4	-10	3
116	4	-10	4
117	4	-10	1
117	4	-10	2
117	4	-10	3
117	4	-10	4
117	4	-10	5
118	4	-10	1
118	4	-10	2
118	4	-10	3
118	4	-10	4
118	4	-9	1
118	4	-9	2
118	4	-9	3

Table 21: Flight Configurations for the VMCA Solutions Found at Altitude of 0 Ft, Weight of 165,600 Lbm and Sideslip Angle (β) of 2° for C130J-30

Airplane: C130J-30			
Altitude: 0 ft			
Weight: 165,600 lbm			
Sideslip Angle (β): 2°			
VMCA	φ	θrudder	θaileron
136	4	-9	2
136	4	-9	3
136	3	-6	1
136	3	-6	2
136	3	-6	3
136	3	-6	4
137	4	-9	2
137	4	-9	3
137	4	-9	4
137	3	-6	1
137	3	-6	2
137	3	-6	3
138	4	-9	2
138	4	-9	3
138	4	-9	4
138	4	-8	2
138	4	-8	3
138	3	-6	1
138	3	-6	2

Table 22: Flight Configurations for the VMCA Solutions Found at Altitude of 6,000 Ft, Weight of 75,600 Lbm and Sideslip Angle (β) of 2° for C130J-30

Airplane: C130J-30			
Altitude: 6,000 ft			
Weight: 75,600 lbm			
Sideslip Angle (β): 2°			
VMCA	φ	θrudder	θaileron
92	5	-15	2
92	5	-15	3
92	5	-15	4
92	5	-15	5
92	5	-14	1
92	5	-14	2
92	5	-14	3
93	5	-15	3
93	5	-15	4
93	5	-14	1
93	5	-14	2
93	5	-14	3
94	5	-14	2
94	5	-14	3
94	5	-14	4
94	5	-14	5
94	5	-13	1

Table 23: Flight Configurations for the VMCA Solutions Found at Altitude of 6,000 Ft, Weight of 120,600 Lbm and Sideslip Angle (β) of 2° for C130J-30

Airplane: C130J-30			
Altitude: 6,000 ft			
Weight: 120,600 lbm			
Sideslip Angle (β): 2°			
VMCA	φ	θrudder	θaileron
116	4	-10	2
116	4	-10	3
116	4	-10	4
116	4	-9	1
116	4	-9	2
116	4	-9	3
116	4	-9	4
117	4	-10	2
117	4	-10	3
117	4	-10	4
117	4	-9	1
117	4	-9	2
117	4	-9	3
117	4	-9	4
118	4	-10	3
118	4	-10	4
118	4	-9	1
118	4	-9	2
118	4	-9	3
118	4	-9	4
118	4	-8	1

Table 24: Flight Configurations for the VMCA Solutions Found at Altitude of 6,000 Ft, Weight of 165,600 Lbm and Sideslip Angle (β) of 2° for C130J-30

Airplane: C130J-30			
Altitude: 6,000 ft			
Weight: 165,600 lbm			
Sideslip Angle (β): 2°			
VMCA	φ	θrudder	θaileron
136	3	-6	1
136	3	-6	2
136	3	-6	3
136	3	-6	4
136	3	-5	0
136	3	-5	1
136	3	-5	2
137	3	-6	2
137	3	-6	3
137	3	-6	4
137	3	-5	0
137	3	-5	1
137	3	-5	2
138	3	-6	2
138	3	-6	3
138	3	-5	1
138	3	-5	2
138	3	-5	3
138	3	-5	4

As mentioned for the A320, these tables show that VMCA is limited by bank angle (φ). It is also interesting to see that in the case of the C130J-30, VMCA is also more limited by the rudder deflection (θrudder) than aileron deflection (θaileron). Table 19 and Table 22 have values of maximum bank angle (φ) and greater values of rudder deflection (θrudder) than aileron deflection (θaileron). This is an interesting observation, because this is different than the A320 tables. For the case of the A320 at a 2° sideslip angle (β), VMCA was limited by bank angle (β) and aileron deflection (θaileron).

Due to these observations we can state that as the sideslip angle (β) increases, VMCA is bank angle (φ) limited as well as a control surface limited. For the A320 it is more aileron deflection (θaileron) limited, for the C130J-30 it is more rudder deflection (θrudder) limited at positive sideslip angles (β). Whereas both the A320 and C130J-30 share the rudder deflection (θrudder) limitation at negative sideslip angles (β). This means that the limitations on VMCA depend on the geometry of each individual airplane.

Chapter 9: Conclusion

It appears that the algorithm used to calculate VMCG and VMCA produces values that are accurate compared against published values. Although the exact values of VMCG and VMCA for both the A320 and C130J-30 could not be found using the algorithm, the generated values of VMCG and VMCA were close enough to show general ideas and trends of the behavior of VMCG and VMCA.

There are many factors that go into calculating minimum control speeds, yet there are only a few equations that are used to numerically predict VMCG and VMCA. Thus generating a map of flight configurations needed to trim an airplane. We showed earlier that there are some general trends like rudder deflection (θ_{rudder}) limitations at negative sideslip angles (β), and bank angle (φ) limitations at positive sideslip angles (β). Yet we also showed that the A320 was more aileron deflection ($\theta_{aileron}$) limited at positive sideslip angles (β), whereas the C130J-30 was more rudder deflection (θ_{rudder}) limited at positive sideslip angles (β).

Each individual airplane has its own specific VMCG and VMCA characteristics that make up its database of trimmed flight conditions. However, there may be several types of airplanes that have the same general trends depending on dihedral, wing style, wing sweep, length, number of engines, size of engines or other factors. Therefore with more research there may be general categories of airplanes that would have the same trends and limitations. This would be significant for an airliner to know which category

their airplanes are in to best develop and train their pilots in case of an engine inoperative scenario.

It is crucial to have a tool developed to be able to calculate the flight configuration options required to fly the airplane engine inoperative. There are so many factors involved in calculating minimal control airspeeds, and it goes to show that the current methods used are not sufficient in painting the picture on minimal control speeds. The airplane industry is also not consistent in calculating VMCG or VMCA. The A320 manual only provided one value for VMCA depending on altitude, whereas the C130J-30 has a chart of VMCA dependent on temperature and altitude, thus increasing confusion and inconsistency for pilots.

This work also showed that linearizing the effects of control surface deflection is an allowable strategy when trying to calculate VMCG and VMCA. As discussed earlier for the A320, the VMCA values calculated by the algorithm matched closely to the given values of VMCA provided by the A320 manual at sea level and high altitudes. However, at medium altitudes the values were less accurate. At sea level we showed that the rudder deflection is limiting the VMCA calculations, therefore the stability derivatives used to calculate the VMCA are the exact values found from VORLAX. However as the altitude increases, VMCA is no longer rudder deflection limited and the stability derivatives used to calculate VMCA are now linearized. This knowledge insinuates that if we were to make more VORLAX files at intermediate deflections of the control surfaces, we would most likely calculate a more accurate value of VMCA.

Although this work mainly focused on predicting the minimum control speeds of existing airplanes, this algorithm could be used to aid in the design process of a new airplane. For example, the C130J-30 has extremely high minimal control speeds without the ATCS. This algorithm would have been able to predict this and aid the designers in sizing the engine, rudder, aileron, elevator or wing. Due to the engine power being much higher than needed for the geometry of the airplane, the Automatic Thrust Control System (ATCS) was avoidably developed as a fix to overcome the poor control speeds. The C130J-30 was able to have the ATCS because of its military use. An Automatic Thrust Control System (ATCS) is available for use in non-military airplanes and can be certified under 14 CFR § 25.904[24]. This fact further increases the need to be able to accurately predict minimum control speeds early on in the design of an airplane. With an algorithm like the one described in this work, designers can run ATCS trades to evaluate the effectiveness of using such a system. Just as with other computer aided engineering tools, an airplane designer would be able to save a lot of time and money with the ability to predict and calculate the minimum control speeds of an airplane using this tool.

REFERENCES

[1] Anonymous. no date. *Lockheed C130 Low-Speed Handling Qualities.* Lockheed Aeronautical Systems Co.

[2] NASA. “Trimmed Aircraft”. Trimmed Aircraft. https://www.grc.nasa.gov/www/k-12/airplane/trim.html.

[3] Code770 Normals Abnormals. “Basic Aerodynamics”. Stability and Control. http://code7700.com/stability.html.

[4] 14 CFR § 25.149 “Minimum control speed.” (2015)

[5] Jane, Frederick, Paul Jackson. 2003. *Jane’s All the World's Aircraft*. London: Jane's Information Group.

[6] Haryopanji. “Lockheed Martin C-130J Super Hercules”. Deviant Art. http://www.deviantart.com/art/Lockheed-Martin-C-130J-Super-Hercules-464814110.

[7] NASA. “A Generalized Vortex Lattice Method for Subsonic and Supersonic Flow Applications”. VORLAX. http://ntrs.nasa.gov/archive/nasa/casi.ntrs.nasa.gov/19780008059.pdf.

[8] NPSS, Numerical Propulsion System Simulation, Software Package, Ver. 2.3.0.1, Ohio Aerospace Institute,Cleveland, OH, 2010.

[9] Garnica, I., and Takahashi, T. T., “A Study of Engine Parameters and Shaft Configuration on Transport Aircraft Performance,” AIAA 2017-#### (TBD), 2017 AIAA SciTech Conference, January 2017.

[10] Federal Aviation Administration, Flight Test Guide for Certification of Transport Category Airplanes, Advisory Circular AC-25-7C, U.S. Department of Transportation, Washington, D.C., Oct 16, 2012.

[11] Takahashi, T.T. 2016. *Aircraft Performance and Sizing: Vol II: Applied Aerodynamic Design*. New York: Momentum Press.

[12] W.H. Mason. “Standard atmosphere routines”. Software for Aerodynamics and Aircraft Design. http://www.dept.aoe.vt.edu/~mason/Mason_f/MRsoft.html#StdAtm.

[13] 14 CFR § 25.121 “Climb: One-engine-inoperative.” (2015)

[14] Takahashi, T.T. 2016. *Aircraft Performance and Sizing: Vol II: Applied Aerodynamic Design*. New York: Momentum Press.

[15] Jane, Frederick, Paul Jackson. 2003. *Jane's All the World's Aircraft*. London: Jane's Information Group.

[16] Anonymous. "Airbus A320 family". Wikipedia. https://en.wikipedia.org/wiki/Airbus_A320_family.

[17] 14 CFR § 25.107 "Takeoff speeds." (2015)

[18] Vietnam Airlines. 2008. *A319/A320/A321 Flight Crew Operating Manual*

[19] 14 CFR § 25.107 "Takeoff speeds." (2015)

[20] Haryopanji. "Lockheed Martin C-130J Super Hercules". Deviant Art. http://www.deviantart.com/art/Lockheed-Martin-C-130J-Super-Hercules-464814110.

[21] Anonymous. "Lockheed Martin C-130J Super Hercules". Wikipedia. https://en.wikipedia.org/wiki/Lockheed_Martin_C-130J_Super_Hercules.

[22] U.S. Department of Commerce, Bureau of Industry and Security. "EXPORT LICENSING (ITAR & EAR)". US Department of Commerce. https://www.bis.doc.gov/index.php/forms-documents/doc_view/781-export-licensing.

[23] Anonymous. "C-130J Hercules Tactical Transport Aircraft, United States of America". airforce-technology. http://www.airforce-technology.com/projects/hercules/.

[24] 14 CFR § 25.904 "Automatic takeoff thrust control system (ATTCS)." (2015)